DOE/JPL-1024-77/1
Distribution Category UC-59a

A Fixed Tilt Solar Collector Employing Reversible Vee-Trough Reflectors and Vacuum Tube Receivers for Solar Heating and Cooling Systems

Final Report

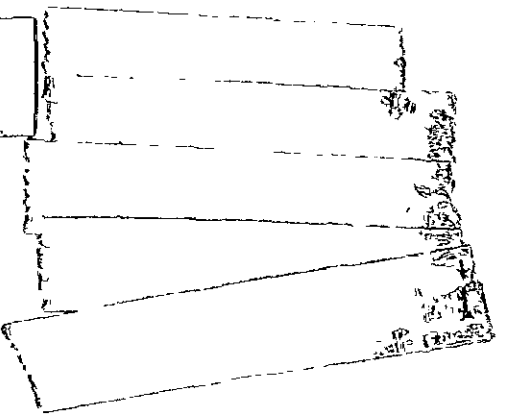

Prepared for
Department of Energy
by
Jet Propulsion Laboratory
California Institute of Technology
Pasadena, California

(JPL PUBLICATION 77-78)

Printed in the United States of America
Available from
National Technical Information Service
U.S. Department of Commerce
5285 Port Royal Road
Springfield, VA 22161
Price: Printed Copy $7.25: Microfiche $3.00

N78-15567

TECHNICAL REPORT STANDARD TITLE PAGE

1. Report No. JPL Pub. 77-78	2. Government Accession No.	3. Recipient's Catalog No.
4. Title and Subtitle A Fixed Tilt Solar Collector Employing Reversible Vee-Trough Refelectors and Vacuum Tube Receivers for Solar Heating and Cooling Systems		5. Report Date December 1977 6. Performing Organization Code
7. Author(s) M. Kudret Selcuk		8. Performing Organization Report No.
9. Performing Organization Name and Address JET PROPULSION LABORATORY California Institute of Technology 4800 Oak Grove Drive Pasadena, California 91103		10. Work Unit No. 11. Contract or Grant No. NAS 7-100 13. Type of Report and Period Covered JPL Publication
12. Sponsoring Agency Name and Address NATIONAL AERONAUTICS AND SPACE ADMINISTRATION Washington, D.C. 20546		14. Sponsoring Agency Code

15. Supplementary Notes

16. Abstract

The objective of the Vee-Trough/Vacuum Tube Collector (VTVTC) Project undertaken for the DOE Solar Heating and Cooling Branch was to prove the usefulness of vee-trough concentratos in improving the efficincy and reducing the cost of collectors assembled form evacuated tube receivers.

The VTVTC was analyzed rigorously and various mathematical models were developed to calculate the optical performance of the vee-trough concentrator and the thermal performance of the evacuated tube receiver. A test bed was constructed to verify the matematical analyses and compare reflectors made out of glass, Alzak and aluminized FEP Teflon. Tests were run at termperatures ranging from 95 to 180°C during the months of April, May, June, July and August 1977. Vee-trough collector efficiencies of 35 to 40% were observed at an operating temperature of about 175°C. Test results compared well with the calculated values. Test data covering a complete day are presented for selected dates throughout the test season.

Predicted daily useful heat collection and efficiency values are presented for a year's duration of operation temperatures ranging from 65 to 230°C. Estimated collector costs and resulting thermal energy costs are presented. Analytical and experimental results are discussed along with a complete economic evaluation.

Recommendations for the continuation of the project are presented.

17. Key Words (Selected by Author(s))	18. Distribution Statement
Energy Production and Conversion	Unclassified - Unlimited

19. Security Classif. (of this report)	20. Security Classif. (of this page)	21. No. of Pages	22. Price
Unclassified	Unclassified	60	

HOW TO FILL OUT THE TECHNICAL REPORT STANDARD TITLE PAGE

Make items 1, 4, 5, 9, 12, and 13 agree with the corresponding information on the report cover. Use all capital letters for title (item 4). Leave items 2, 6, and 14 blank. Complete the remaining items as follows:

3. Recipient's Catalog No. Reserved for use by report recipients.
7. Author(s). Include corresponding information from the report cover. In addition, list the affiliation of an author if it differs from that of the performing organization.
8. Performing Organization Report No. Insert if performing organization wishes to assign this number.
10. Work Unit No. Use the agency-wide code (for example, 923-50-10-06-72), which uniquely identifies the work unit under which the work was authorized. Non-NASA performing organizations will leave this blank.
11. Insert the number of the contract or grant under which the report was prepared.
15. Supplementary Notes. Enter information not included elsewhere but useful, such as: Prepared in cooperation with... Translation of (or by)... Presented at conference of... To be published in...
16. Abstract. Include a brief (not to exceed 200 words) factual summary of the most significant information contained in the report. If possible, the abstract of a classified report should be unclassified. If the report contains a significant bibliography or literature survey, mention it here.
17. Key Words. Insert terms or short phrases selected by the author that identify the principal subjects covered in the report, and that are sufficiently specific and precise to be used for cataloging.
18. Distribution Statement. Enter one of the authorized statements used to denote releasability to the public or a limitation on dissemination for reasons other than security of defense information. Authorized statements are "Unclassified—Unlimited," "U. S. Government and Contractors only," "U. S. Government Agencies only," and "NASA and NASA Contractors only."
19. Security Classification (of report). NOTE: Reports carrying a security classification will require additional markings giving security and downgrading information as specified by the Security Requirements Checklist and the DoD Industrial Security Manual (DoD 5220.22-M).
20. Security Classification (of this page). NOTE: Because this page may be used in preparing announcements, bibliographies, and data banks, it should be unclassified if possible. If a classification is required, indicate separately the classification of the title and the abstract by following these items with either "(U)" for unclassified, or "(C)" or "(S)" as applicable for classified items.
21. No. of Pages. Insert the number of pages.
22. Price. Insert the price set by the Clearinghouse for Federal Scientific and Technical Information or the Government Printing Office, if known.

Printed in the United States of America
Available from
National Technical Information Service
U. S. Department of Commerce
5285 Port Royal Road
Springfield, VA 22161

DOE/JPL-1024-77/1
Distribution Category UC-59a

A Fixed Tilt Solar Collector Employing Reversible Vee-Trough Reflectors and Vacuum Tube Receivers for Solar Heating and Cooling Systems

Final Report

M. Kudret Selcuk
Principal Investigator

December 1977

Prepared for
Department of Energy
by
Jet Propulsion Laboratory
California Institute of Technology
Pasadena, California
(JPL PUBLICATION 77-78)

This document was prepared by the Jet Propulsion Laboratory, California Institute of Technology, for the Department of Energy, Division of Solar Energy under an Interagency Agreement with the National Aeronautics and Space Administration

FOREWORD

This report is submitted to the United States Department of Energy, Division of Solar Energy R&D Branch, and covers the work conducted by the Jet Propulsion Laboratory under Interagency Agreement No. E(49-26)-1024 by agreement with the National Aeronautics and Space Administration, Contract No. NAS7-100. The work was performed under the direction of Dr. Stephen Sargent, Program Manager from the DOE R&D Branch, Heating and Cooling Office, and Jo Perry, the Contract Monitor from the Los Alamos Scientific Laboratories.

ACKNOWLEDGMENTS

This project was undertaken by a team consisting of numerous members of the technical staff of JPL.

Mr. Eugene W. Noller designed the test bed. Mr. James A. Bryant was responsible for the instrumentation and data acquisition system. Mr. Donald C. Schneider constructed the test bed.

Early mathematical analysis of the vee-trough concentrator and vacuum tube receiver and computer programming was undertaken by Dr. Burton Zeldin. Later Mr. Nabil El Gabalawi extended the analysis and generated computer codes which examined the optical performance of the vee-trough/vacuum tube collector employing a "strips" approach. Mr. Edward (Larry) Noon was responsible for the data processing routines and provided the necessary interfaces for the IDAC data acquisition system and the Univac 1108 computer.

Dr. Kemal Onat, Professor at the Mechanical Engineering Faculty of Istanbul Technical University, contributed to the thermal analysis of the vacuum tube receiver and data evaluation of the test setup while serving as a NATO Research Fellow at JPL.

Dr. Ugur Ortabaşi and Dr. Francis P. Fehlner of Corning Glass Works (CGW) gave invaluable advice regarding the vacuum tube receiver developed by GGW and supplied those tubes used in the test setup.

The whole project was managed by Dr. V. C. Truscello, Supervisor of the Nuclear and Solar Thermal Conversion Group, who provided invaluable help at all phases of the study.

ABSTRACT

The objective of the Vee-Trough/Vacuum Tube Collector (VTVTC) Project undertaken for the DOE Solar Heating and Cooling Branch was to prove the usefulness of vee-trough concentrators in improving the efficiency and reducing the cost of collectors assembled from evacuated tube receivers.

The VTVTC was analyzed rigorously and various mathematical models were developed to calculate the optical performance of the vee-trough concentrator and the thermal performance of the evacuated tube receiver. A test bed was constructed to verify the mathematical analyses and compare reflectors made out of glass, Alzak and aluminized FEP Teflon. Tests were run at temperatures ranging from 95 to 180°C during the months of April, May, June, July and August 1977. Vee-trough collector efficiencies of 35 to 40% were observed at an operating temperature of about 175°C. Test results compared well with the calculated values. Test data covering a complete day are presented for selected dates throughout the test season.

Predicted daily useful heat collection and efficiency values are presented for a year's duration at operation temperatures ranging from 65 to 230°C. Estimated collector costs and resulting thermal energy costs are presented. Analytical and experimental results are discussed along with a complete economic evaluation.

Recommendations for the continuation of the project are presented.

CONTENTS

CONTENTS (Contd.)

CONTENTS (Contd.)

FIGURES

FIGURES (Contd.)

TABLES

NOMENCLATURE

Symbol	Item	Unit
A	area	m^2 (ft^2)
A_c	collector area	m^2 (ft^2)
A_p	absorber plate area	m^2 (ft^2)
C	cost of collector	dollars
c	energy cost	dollars
CR	concentration ratio	dimensionless
C_p	specific heat	dimensionless
d	density	kg/m^3 (lb/gal.)
F_R	heat removal factor	dimensionless
F_c	correction factor for manifold losses	dimensionless
I_B	beam radiation intensity	W/m^2 ($Btu/hr-ft^2$)
I_d	diffuse radiation intensity	W/m^2 ($Btu/hr-ft^2$)
I_R	reflected radiation intensity	W/m^2 ($Btu/hr-ft^2$)
I_t	total radiation intensity	W/m^2 ($Btu/hr-ft^2$)
i	angle of incidence	degrees
K	glass extinction coefficient	1/cm (1/inch)
k	thermal conductivity	W/m^oC ($Btu/hr-ft\ ^oF$)
L	length	m (ft)
m	air mass	dimensionless
$\dot{m}$	mass flow rate	kg/hr (lb/hr)
N	day number	dimensionless
n	index of refraction for glass	dimensionless
Q_t	total heat collected	KJ/hr (Btu/hr)
Q_{in}	incident heat	KJ/hr (Btu/hr)

NOMENCLATURE (contd.)

Symbol	Item	Unit
Q_u	useful heat	KJ/hr (Btu/hr)
Q_l	lost heat	KJ/hr (Btu/hr)
Q_s	stored heat	KJ/hr (Btu/hr)
T	temperature	^oC (^oF)
T_a	ambient temperature	^oC (^oF)
$T_{f,i}$	fluid inlet temperature	^oC (^oF)
ΔT	temperature difference	^oC (^oF)
$\Delta T_{f,i}$	fluid inlet temperature - ambient temperature	^oC (^oF)
U_L	heat loss coefficient	$W/m^{2o}C$ (Btu/hr-$ft^{2o}F$)
V	wind speed	m/sec
W	flap side width	m (ft)
X, Y, Z	coordinates of flap corner points and their reflections	m (ft)

Subscripts

a	ambient
b	bottom
B	beam
c	collector
d	diffuse
f	fluid
g	glass
i	inlet
o	outlet
p	plate

NOMENCLATURE (contd.)

Greek Symbols

Symbol	Item	Unit
α	absorptivity	dimensionless
δ	declination	degrees
ϵ	emissivity	dimensionless
η	vee trough aperture angle	degrees
η	efficiency	dimensionless
θ	flap side tilt	degrees
λ	wavelength	microns
ρ	reflectivity	dimensionless
$(\tau\alpha)_e$	effective transmissivity absoprtivity product	dimensionless
τ	transmissivity	dimensionless
σ_o	Stephan-Boltzmann constant	dimensionless
ϕ	latitude	degrees

SECTION I

INTRODUCTION

This report discusses the analyses and test experiments conducted on vee-trough concentrators to prove their usefulness in improving the efficiency and reducing the cost of collectors assembled from evacuated tube receivers. This work was performed at JPL during the contract period of June 1, 1976, to May 31, 1977, and its extension from June 1, 1977, until September 30, 1977, under the sponsorship of the ERDA (now DOE) Solar Heating and Cooling Branch.

Asymmetric vee-trough optical performance analyses were undertaken for various flap tilt and vee-trough aperture angles, and included cases with and without a cylindrical envelope. Thermal performance analysis of a vacuum tube receiver with a flat plate absorber was also carried out with and without a vee-trough concentrator.

Analytical results were verified with data acquired using an experimental arrangement designed to test evacuated tube receivers that were developed by the Corning Glass Works of Corning, New York. Test temperatures ranged from 95 to 180°C and were repeated during spring and summer of 1977 several times to determine the seasonal variations of the performance of the vee-trough concentrator and vacuum tube receiver. Studies were extended to find the optimum design parameters yielding the best thermal performance and/or minimum energy cost.

1.1 VEE-TROUGH COLLECTOR CONFIGURATION

An asymmetrical-reversible vee-trough reflector maintaining a year-round concentration factor of about 2 has been studied for use with evacuated receivers. This vee-trough collector configuration eliminates the complications of the tilt adjustments associated with a collector box assembly. Figure 1-1 illustrates the principle of operation of such a collector having a concentration ratio of about 3.

Although the likely applications of these collectors are for heating/cooling, they are also adaptable to both total energy systems and small-scale rural power supplies (especially in combination with an organic fluid turbine), such as solar pumping stations. The performance of a solar Rankine, mechanical compression, air conditioning system would also be enhanced by using the proposed collector assembly (Ref. 1).

Dimensions of vacuum tube receiver courtesy of Corning Glass Works, Corning, N.Y.

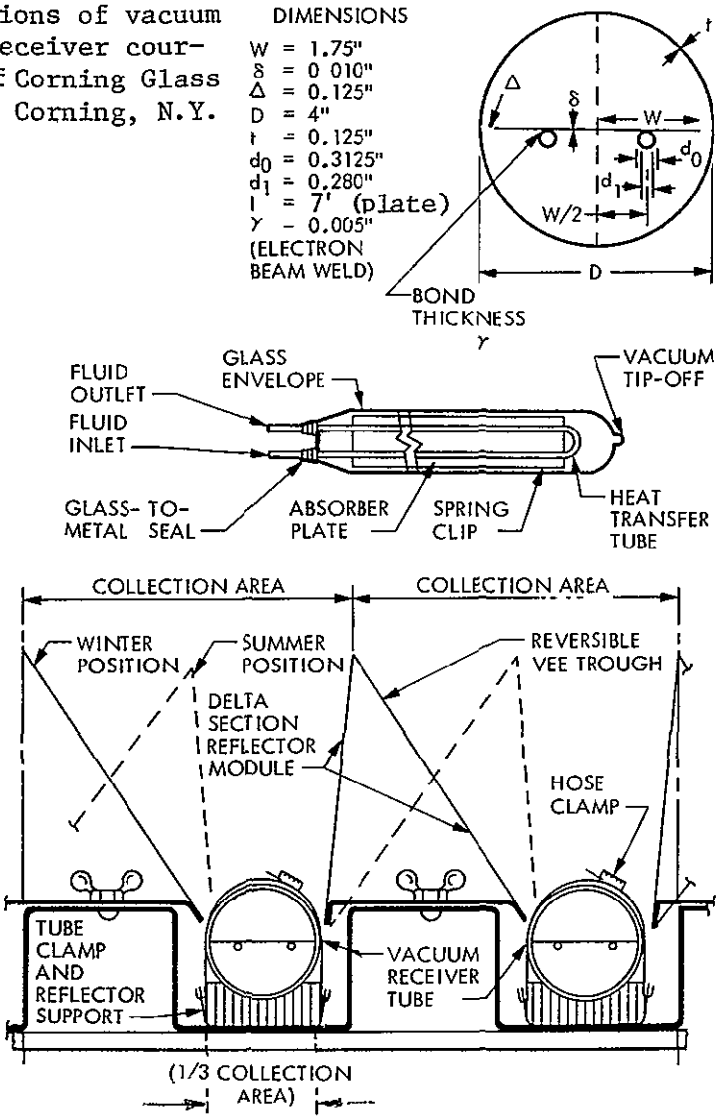

Figure 1-1. Reversible Asymmetric Vee-Trough Collector with Vacuum Tube

1.2 BACKGROUND/JUSTIFICATION

An efficient collector (especially for temperatures around 100-200°C) which is also reliable in performance, requires little maintenance, has low operating expenses, and has a relatively low initial cost is needed for economically viable absorption air conditioning and solar power systems.

The conventional flat plate collector has been studied and built in various forms for almost a hundred years. Present cost projections for these types of collectors will probably not reduce significantly since material requirements are substantially the same regardless of variation in structural design. Among attempts made to improve the fixed collector performance and to reduce its cost are the use of mirror boosters in the early 1960s (Ref. 2), the recent introduction of vacuum tube collectors (Refs. 3 and 4), and the use of vee-trough reflectors. Vee-trough reflectors to improve solar cell performance, as proposed by Hollands (Ref. 5) and by Durand (Ref. 6), have recently been used in a box-type flat plate collector by Bannerot and Howell (Ref. 7). The compound parabolic concentrator is also being considered for use with a flat plate collector to enhance its output at high temperatures (Ref. 8). In addition to the use of a selective coating on the absorber with high α and low ϵ to reduce radiation losses, which is widely applied now, honeycomb cell convection suppressors (Ref. 9) or reduction of convective losses by partial evacuation of the space between the absorber plate and a transparent cover (Refs. 10 and 11) have also been attempted to assure high efficiencies. The former reduces the incoming flux by absorption and increases the backward conduction. Moreover, potential material problems exist with plastic honeycombs, and the glass honeycomb is expensive.

Evacuated flat plate collectors have numerous problems. Among them are stresses on the glass plates and difficulties of maintaining vacuum during lifetime (which requires either expensive vacuum seals or continuous operation of a vacuum pump). Plastic covers for evacuated flat plate collectors offer some advantages over glass from a stress standpoint; however, operational problems such as scratching, distortion and even melting under static conditions and degassing under vacuum must be considered. Recently, the design originally proposed by Speyer, et al. in the 1960s (Ref. 12), using evacuated tube collectors made of borosilicate glass tubes with a flat plate absorber, has been tested as a non-tracking solar heat collector (Ref. 3). Evacuated tubes of the thermos bottle type are also being offered (Ref. 4). The latter design employs a diffusely reflecting rear surface to boost the collector output. The effect is more pronounced at the off-noon periods, during which time the ratio of the heat collected to the daily total insolation available is not signifi-

cant (Ref. 13). Although the performance of a vacuum tube collector is superior to conventional flat plate designs, its cost is expected to be well above the simple flat plate; a single-glazed flat plate collector is estimated to cost $\$40/m^2$ compared to $\$150/m^2$ for the vacuum tube (in large volume production).

Recently the evacuated tube receivers have been examined both analytically and experimentally. Among these investigations are the original studies undertaken at Corning Glass Works by Dr. U. Ortabaşı and his colleagues (Ref. 14, 15), and more recently by Dr. S. Karaki, et al., at the Colorado State University, Fort Collins, Colorado (Ref. 16). Both investigators have examined vacuum tube collector tubes and modules without a concentrator. The latter, however, has examined reflections from a back sheet.

Use of vacuum tube receivers with moderately concentrating systems has also been considered by some investigators and research teams. Argonne National Laboratories (Refs. 17-19) is proposing to use a compound parabolic concentrator (CPC) in connection with a vacuum tube receiver for concentration ratios above 3. The tilt of a CPC with a concentration of 3 must be adjusted twice a year, unlike the asymmetrical vee-trough suggested in this project which requires only reversal of the reflector twice a year. Larger concentration ratios are unsafe for dry run operations unless special measures are taken for protection in case the fluid circulation stops. The General Electric Company has recently introduced a back-reflecting concentrator (a low concentrating parabolic cylinder) having an optical concentration ratio on the order of 2. It has a thermos bottle type of evacuated glass envelope (which is hermetically sealed) and a concentric cylindrical plane receiver (Ref. 20). Analysis and performance data for this concept are not yet available in the open literature. The evacuated glass envelope may, however, be fitted to the bottom of the asymmetric vee-trough concentrator developed in this project. However, the second layer of glass wall is heated by the concentrated solar flux. The heat then must pass through the glass wall and air gap, which should be traded off with the elimination of the glass-metal seal. Thus contact resistance and end losses are larger than the vacuum-protected absorber plate of Corning Glass Works design.

Because of these factors and the unavailability of the tubes during the project initiation period, in addition to its small size (2-inch OD only), we were led to select the single-walled, flat-surfaced selectively coated absorber plate type vacuum tube with a 4-inch OD and glass-metal seals, fabricated by Corning Glass Works.

Should more refined evacuated receiver designs become available, they could always be tested using the inexpensive, asymmetric vee-trough concentrator.

SECTION II

ANALYSIS OF THE VEE-TROUGH CONCENTRATOR AND VACUUM TUBE RECEIVER

2.1 METHODOLOGY

The analysis used in this project was based on a mathematical model of the vee-trough vacuum tube collector incorporating an optical model of the vee-trough concentrator and a thermal model of the vacuum tube receiver. Varying solar flux and ambient conditions were considered. Initially, it was planned to formulate a rigorous mathematical model and then compare the analytical solution with test data. During the progress of the project an alternative approach was followed. Instead of formulating the most rigorous model initially, it was decided to analyze each component of the collector by starting with a simple model and selectively introducing more complex models as deemed necessary. Thus, intermediate results defining the optical performance of the vee-trough and vacuum tube receiver alone could be obtained and tested for accuracy.

Figure 2-1 illustrates various versions of the mathematical models of the vee-trough and vacuum tube collector and its components. Major versions of the mathematical models are labeled for easy reference in the following discussions of analysis procedures and testing.

2.1.1 Optical Models

Three versions of the optical model were formulated. Initially, they considered first reflections only. Later a refined model including secondary reflections was developed. These models are briefly described below:

1) Total Mirrors Approach

   Predicts the optical performance of the vee-trough by determining the reflections from full mirrors. End effects are included.

2) Strips Approach

   Predicts the optical performance of the vee-trough collector by dividing the mirror surfaces into fine strips to obtain an accurate flux map at the bottom of the vee-trough. End effects are included, but the glass envelope surrounding the absorber plate is not considered.

3) Strips Approach With a Glass Envelope Over the Absorber Plate

   Flux map on the absorber plate is obtained considering the mod-

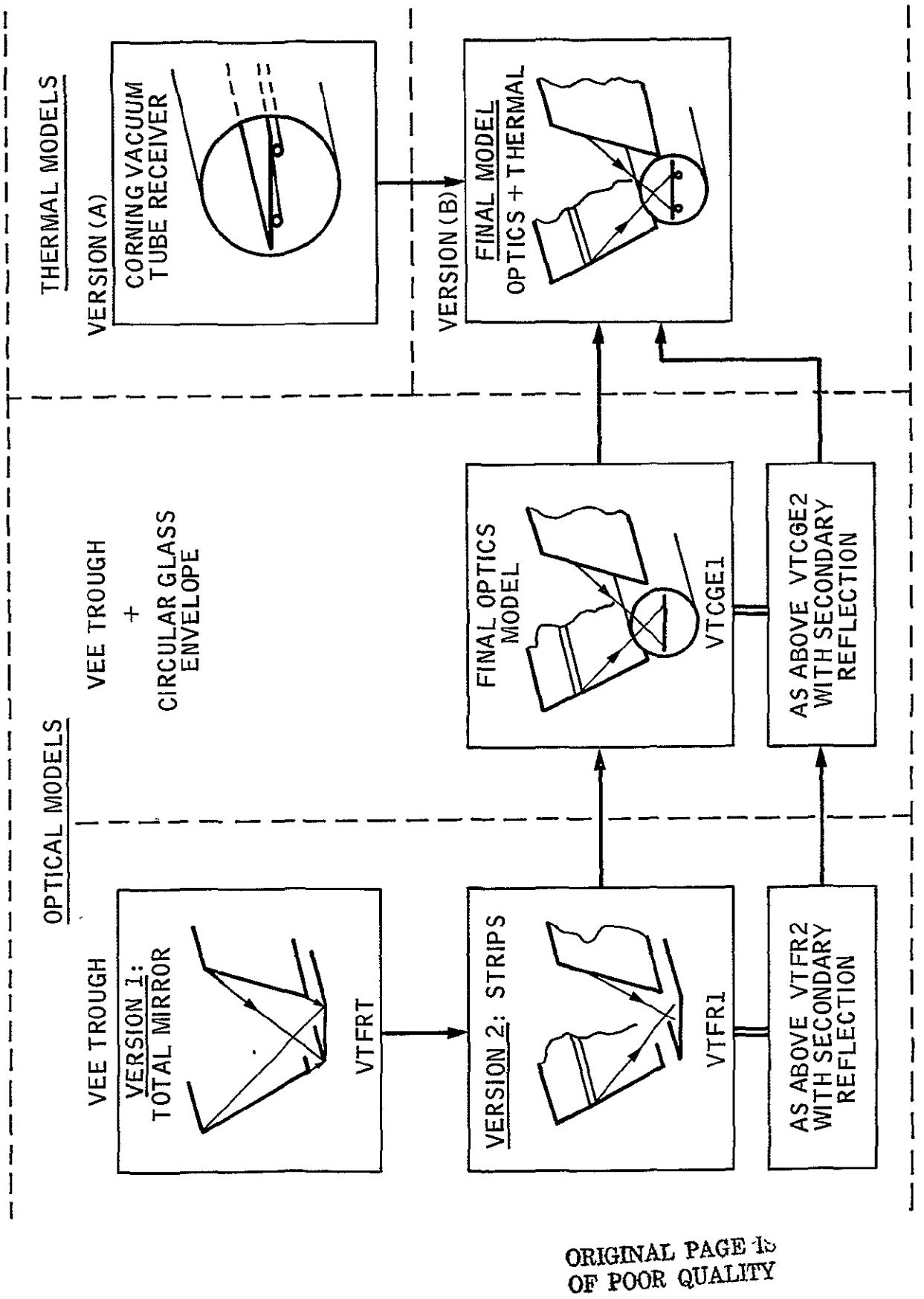

ORIGINAL PAGE IS
OF POOR QUALITY

Figure 2-1. Vee-Trough Vacuum Tube Collector Mathematical Models

ification effects of a glass envelope which attenuates the flux intensity and limits the absorbed radiation.

2.1.2 Thermal Models

The first model simulated only the thermal performance of the vacuum tube receiver. This version of the model is similar to the formulations in References 15 and 16. In this model the flux intensity on the absorber plate is considered to be uniform.

The final model, which defines the collector performance, combines the most comprehensive optical model with the vacuum tube receiver thermal model. Secondary reflections from the mirror are taken into consideration.

2.2 OPTICAL ANALYSIS OF THE VEE-TROUGH CONCENTRATOR

The incident solar flux intensity on the evacuated tube without a concentrator equals the total incident flux on the tilted collector plane. Losses due to the transmission of beam and diffuse components of the incident flux must be taken into account.

Calculation of the solar flux intensity on the total collector plane using the normal beam solar flux and diffuse solar flux data is straightforward. The incident total and diffuse solar flux intensity are measured by means of a pyranometer. However, the flux incident on the receiver tube and that part transmitted through the glass envelope and captured by the absorber plate has to be calculated. The following section discusses the method by which this calculation is performed.

2.2.1 Optical Model Using the Total Mirror Approach (VTFRT)

The simplest approach in formulating the configuration of a vee-trough without a circular receiver is the total mirror approach. The sides of the vee-trough (known as flaps) are examined as a single piece unit. Coordinates of the four corners of each flap are identified and the projection of these points on the absorber plane is determined via vector analysis for the incoming solar and reflected beam radiation. Figure 2-2 illustrates the vee-trough and solar ray geometry employed in version 1 of the optical math model (VTFRT).

The following assumptions were used in the formulation:

1) The solar beam is specularly reflected from the mirror surface having a reflectivity of ρ. Since the target size is about 1/3

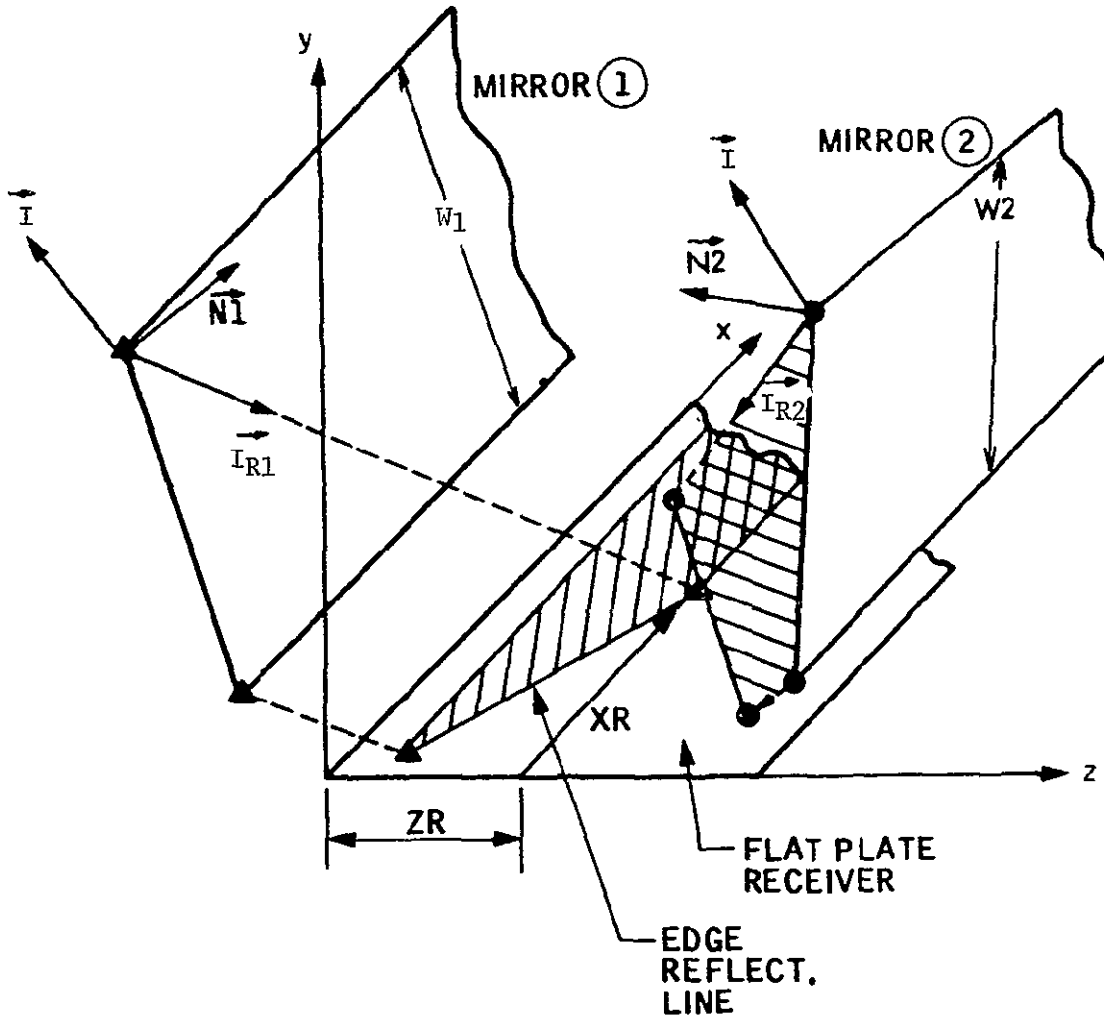

Figure 2-2. Vee-Trough Solar Ray Geometry for Total Mirror Model Version 1 (VTFRT)

of the aperture size and, for a practical design, the flap width is on the order of 30 cm (1 ft), the divergence of the reflected beam due to the parallax of solar rays and surface errors and roughness were ignored. In other words, the reflectance of the surface was taken as total reflectance which assumes that all of the reflected specular beam is captured by the receiver. Figure 2-3 (adapted from Ref. 21) indicates that the above assumption is valid for silvered surfaces (both smooth concentrators or heliostat systems). The mirror reflectivity is considerably lower at small divergences for Alzak than for highly specularly reflecting silvered surfaces.

2) The diffuse radiation intensity at the bottom of the vee-trough is assumed to be about 80 percent of the diffuse radiation incident on the aperture plane. This assumption, previously based on data in Reference 5, was later confirmed when the flux intensity on the aperture plane was compared to the flux intensity at vee-trough concentrator bottom during an overcast day.

3) Surface reflectivity is taken to be dependent upon the angle of incidence as given in Reference 22. However, change of reflectance with the wavelength was neglected.

4) Secondary reflection of the beam radiation was neglected.

5) End effects, namely changes of the position of the reflected beam along the tube axis and effects on the total energy incident on the absorber tube, were taken into consideration.

The total mirror approach model enables one to predict the concentration ratio using little computer time and yields reasonably accurate results for the receiver without a glass envelope. In determing the intensity of the solar flux on the absorber plate, the position of the sun is first determined for the specified time. Then both the beam and diffuse radiation intensities must be known. For the preliminary year-round performance predictions, the 1962 radiation data for Burbank, California, were used. Beam and diffuse radiation data processed from beam radiation measurements and cloud cover ratio were recorded onto weather tapes and preserved at the Tape Library of JPL's computer center. Referring to the beam and diffuse radiation intensities on the horizontal plane from the weather tape,

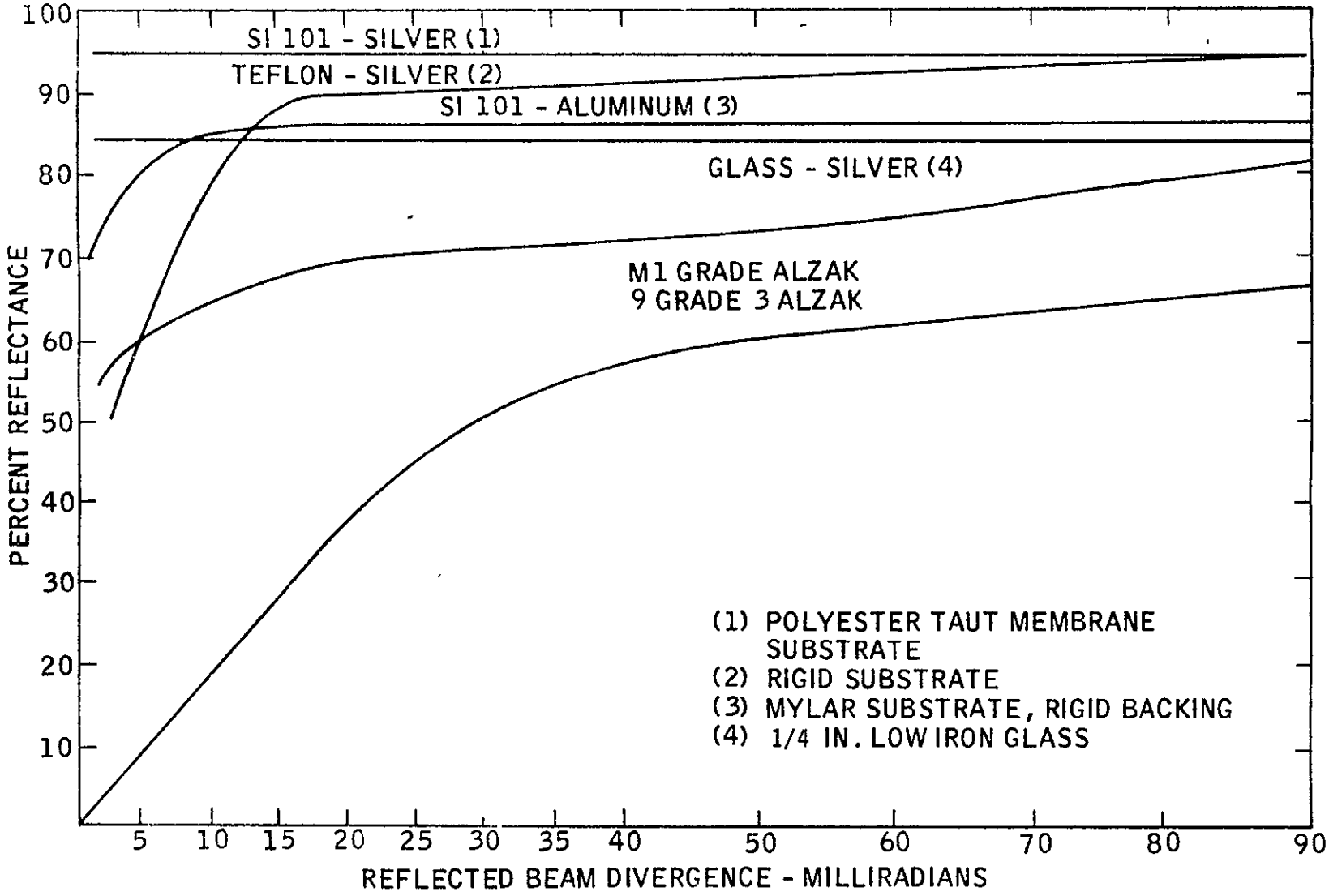

Figure 2-3. Specular Reflectance of Thin Films and Typical Mirror Surfaces (Ref. 21)

the concentrated solar flux on the absorber plate was calculated as shown in the logic diagram illustrated in Figure 2-4. The steps followed are:

1) Sun's position was determined for a particular hour and day of the year (N) with corrections to Pacific Standard (or Daylight Saving) time and using the approximate equation for the declination δ,

$$\delta = 23.45 \sin \left\{ \frac{360\ (284 + N)}{365} \right\} \tag{2.1}$$

2) Components of the solar beam vector I_{Bx}, I_{By} and I_{Bz} were determined.

3) Position of the four corner points where the reflected beam radiation intersects the absorber plane for each flap was determined.

4) Component of the reflected beam radiation normal to the absorber plane I_{Ry} was determined.

The total solar radiation Q_t on the absorber plate, having an area of A_p, with the vee-trough is the summation of the following terms:

$(I_{Ry}\ A_{image})$ for first flap
$(I_{Ry}\ A_{image})$ for second flap
} $A_{image} \leq A_p$ for both flaps

$(I_B A_p)$ beam radiation normal to the absorber

$(I_d A_p)$ diffuse radiation over the absorber plate

$$Q_t = (I_{Ry}\ A_{image})_1 + (I_{Ry}\ A_{image})_2 + (I_B + I_d)\ A_p \tag{2.2}$$

Subscripts 1 and 2 refer to the first and second flaps.

5) The actual concentration ratio was obtained from

$$CR = \frac{\text{Total energy incident on the absorber plate with vee-trough}}{\text{Total energy incident on the absorber plate without vee-trough}}$$

$$CR = \frac{(I_{Ry}\ A_{image})_1 + (I_{Ry}\ A_{image})_2 + I_B\ A_p + I_d\ A_p}{(I_B + I_d)\ A_p} \tag{2.3}$$

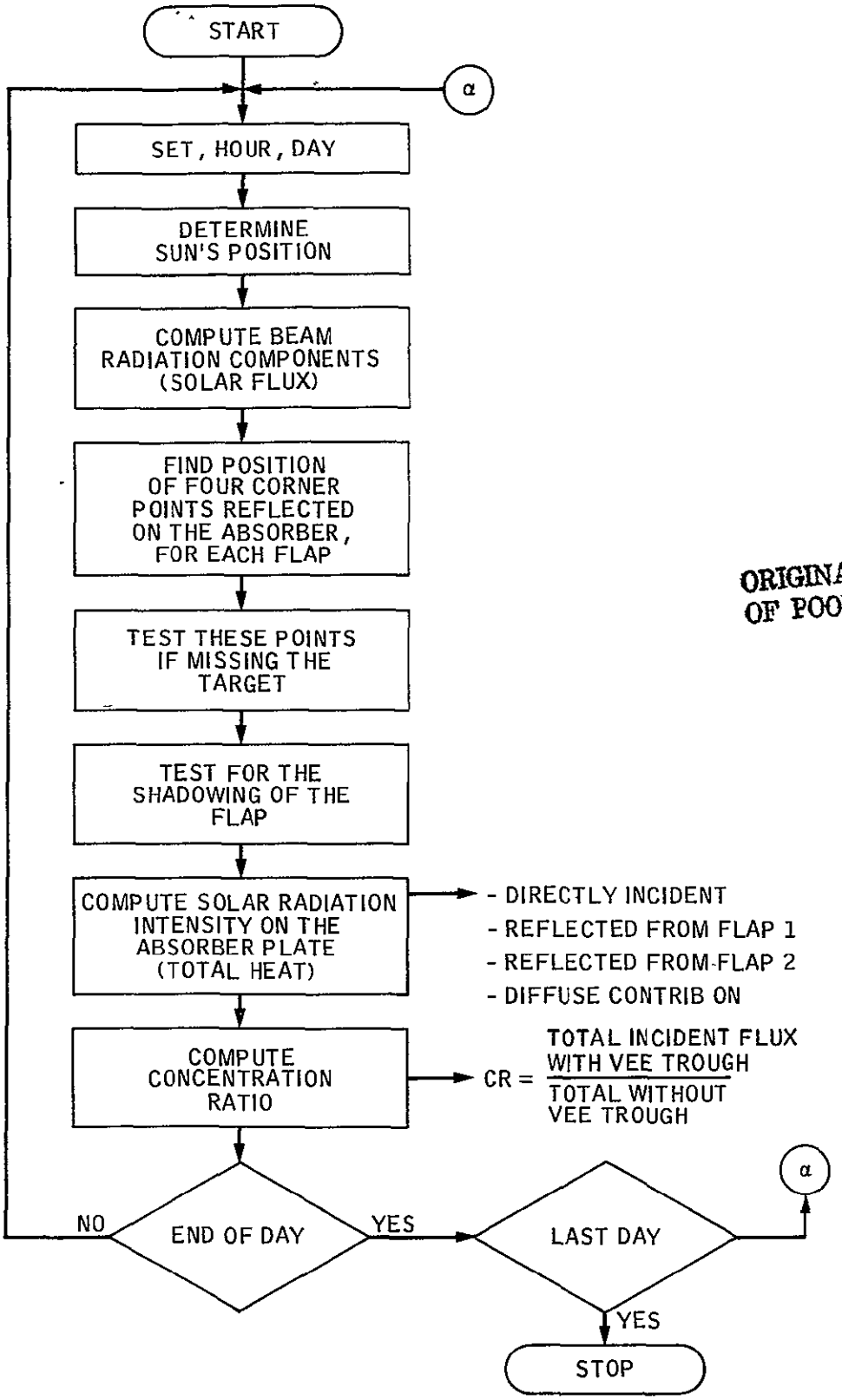

Figure 2-4. Logic Diagram for the Program (VTFRT) Total Mirror

The concentration ratio thus defined is obviously less than the optical concentration ratio based on the aperture to bottom opening ratio. Its value may be further reduced if the flap length is equal to or less than the absorber length. When sufficiently long flaps are used, the end losses are eliminated during early morning and late afternoon hours. The final choice of the flap length, of course, is a matter of compromise between the increase in flap cost and the increase in total thermal energy collected.

2.2.2 Optical Model Using the Strips Approach (VTFR)

The strips version of the optical model is labeled as VTFR1 for the analysis with first reflections only. First and second reflections are considered in the model labeled as VTFR2. Both models are applicable to the analysis of receivers with a glass envelope surrounding the absorber plate. The total mirror approach (VTFRT) is not applicable to the analysis of a receiver with a circular envelope surrounding the absorber. The basic assumptions in formulating the optical models VTFR1 and VTFR2 are the same as for VTFRT. The only difference is that the mirror flaps are divided into fine strips. Therefore, steps 1 through 5 (indicated earlier) are followed for each strip. The total radiation intensity can be calculated from

$$Q_t = \sum_{i=m}^{k} (I_{Ry}\,(dz)\,L_i)_1 + (I_{Ry}(dz)\,L_i)_2 + I_B A_p + I_d A_p \qquad (2.4)$$

where

L_i = length of the image of the strip

dz = width of the image of the strip

i = index for strip

m = first strip which reflects on the absorber plate

k = last strip which reflects on the absorber plate

A_p = absorber plate area

Subscripts 1 and 2 refer to the first and second flaps. Figure 2-5 illustrates the ray trace geometry used in formulating the optical model VTFR. Figure 2-6 is a logic diagram for the program VTFR.

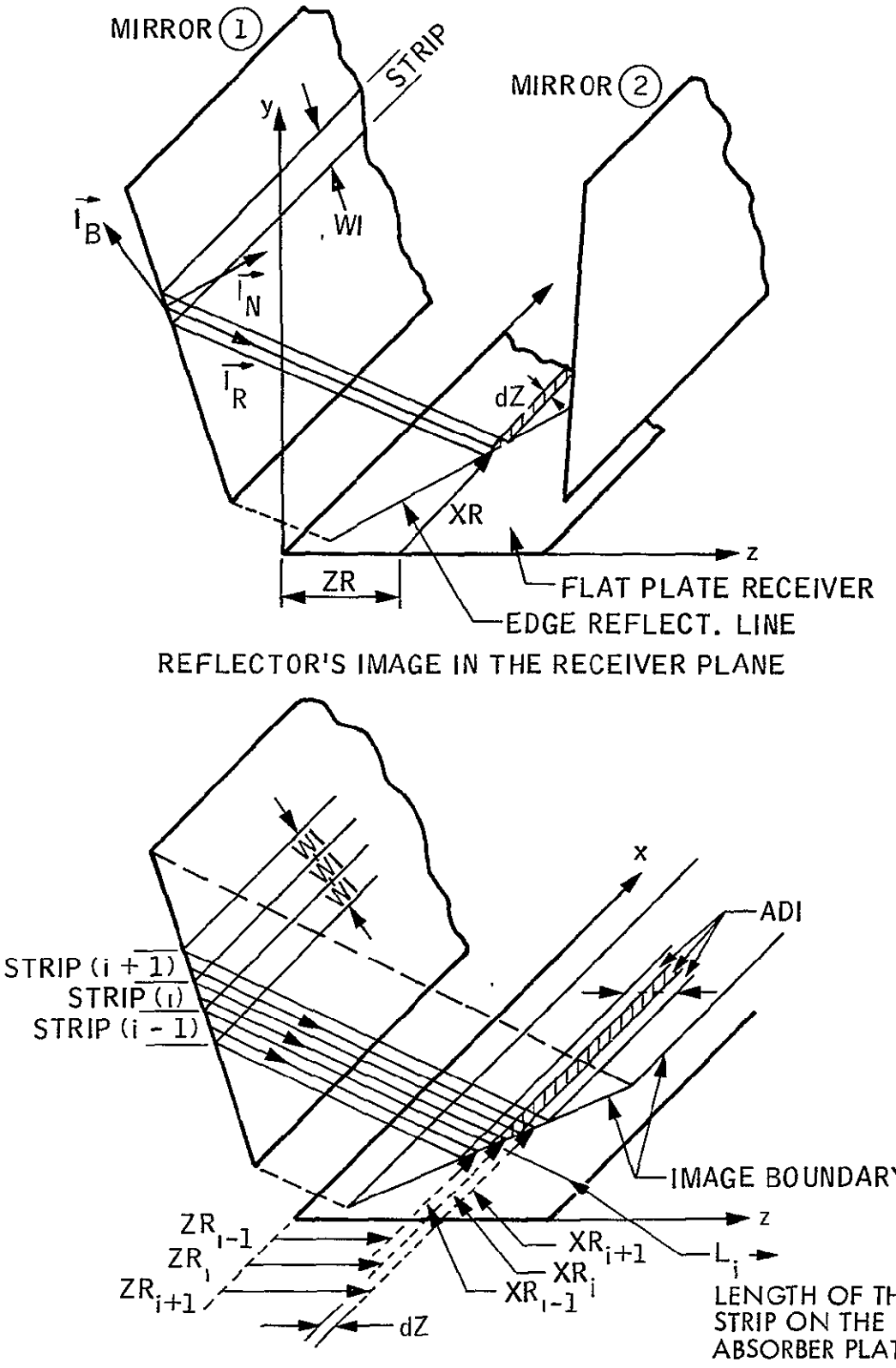

Figure 2-5. Strips Model for the Vee-Trough (VTFR)

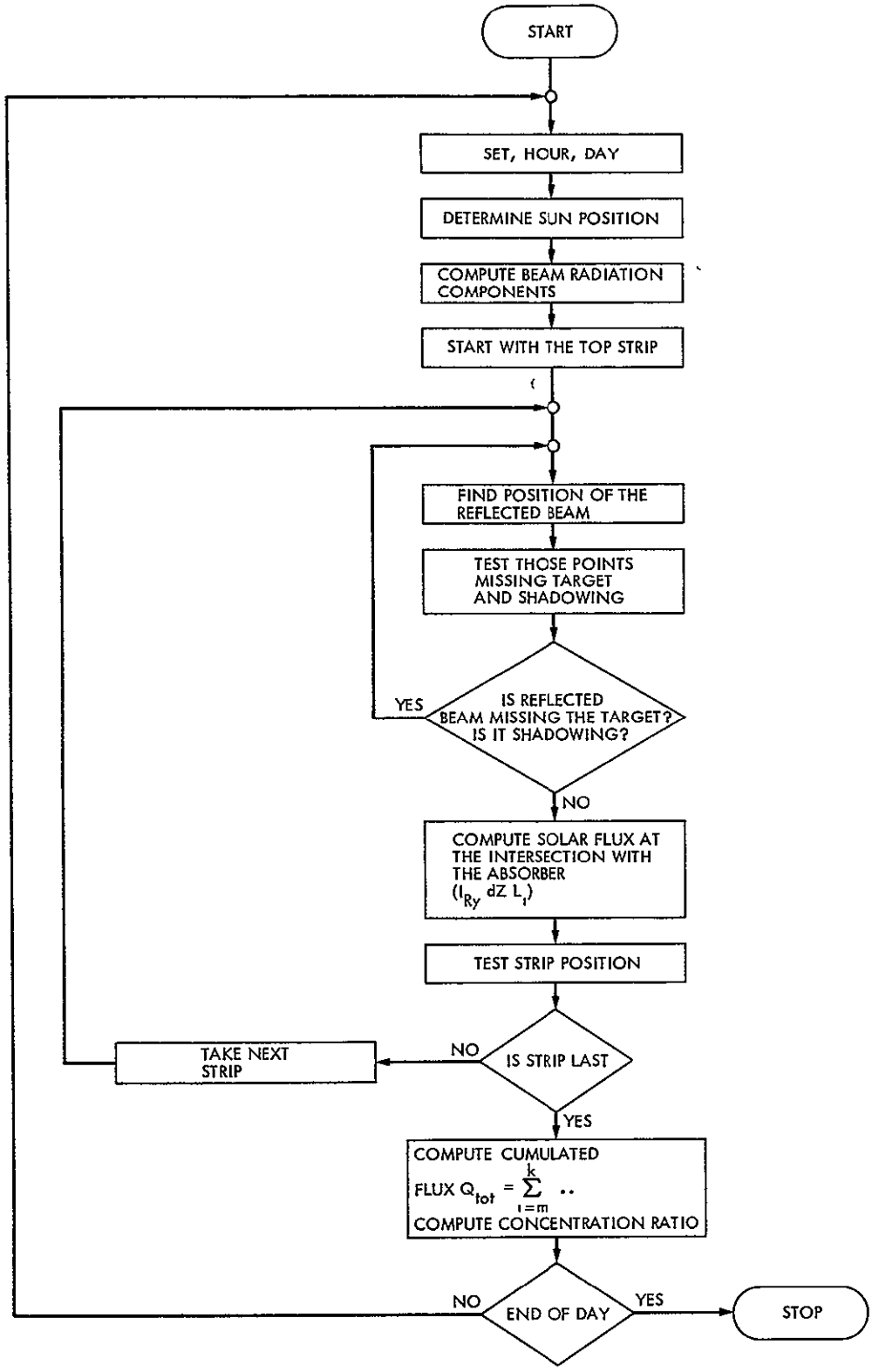

Figure 2-6. Logic Diagram for Strips Analysis

2.2.3 Optical Model for Vee-Trough With Circular Glass Envelope (VTCGE)

Steps 1, 2, 3, etc., described for the total mirror and strips analyses, are applicable to the VTCGE (vee-trough with circular glass envelope) model. VTCGE calculates the amount of reduction of the solar radiation intensity due to transmission losses through the glass envelope. Assumptions in VTFRT and VTFR1 or VTFR2 are also applicable to VTCGE. Additionally, the transmissivity of the glass envelope was taken to be dependent on the angle of incidence. The transmissivity of the glass envelope was, however, assumed to be constant for wavelengths less than $4\,\mu$. Pyrex tube has a sharp cutoff at $\lambda = 4\,\mu$. Since most of the solar radiation (more than 99%) lies within a band of $0.4\,\mu$ to $4\,\mu$ for an air mass of m = 1, the solar flux for $\lambda > 4\,\mu$ was neglected. This assumption, therefore, does not introduce any appreciable error.

Figure 2-7 identifies the definition angles of incidence on the glass envelope. The incident radiation intensity is calculated in a manner similar to that for VTFR1 and VTFR2. Beam radiation reflected both from flap 1 and flap 2 is transmitted through the circular glass envelope. In addition to the reflected radiation, beam solar radiation directly strikes the tube without being reflected from the mirrors. Diffuse radiation (directly incident from the sky and reflected from either flap) is also transmitted through the transparent cover. The diffuse flux density at the bottom of the vee-trough is greater than 80% of the intensity at the aperture plane.

2.3 THERMAL ANALYSIS OF THE VACUUM TUBE RECEIVER

This section outlines the thermal analysis of the vacuum tube receiver with and without the vee-trough concentrator. The thermal model of the vacuum tube receiver without the concentrator is almost identical to those developed by Karaki and Ortabasi. However, the configuration used in the models developed by these investigators has included the effect of neighboring vacuum tubes on the tube under study. These effects of shadowing and reflection as well as reflections from a rear plate do not apply in the configuration studied in this project. Since the centerlines of the tubes are about 3 diameters apart, and the space between the tubes is filled with the vee-trough reflectors, the tubes themselves are assumed to have no effect on each other.

2.3.1 Vacuum Tube Without Reflectors

The mathematical model of a single vacuum tube without any adjacent

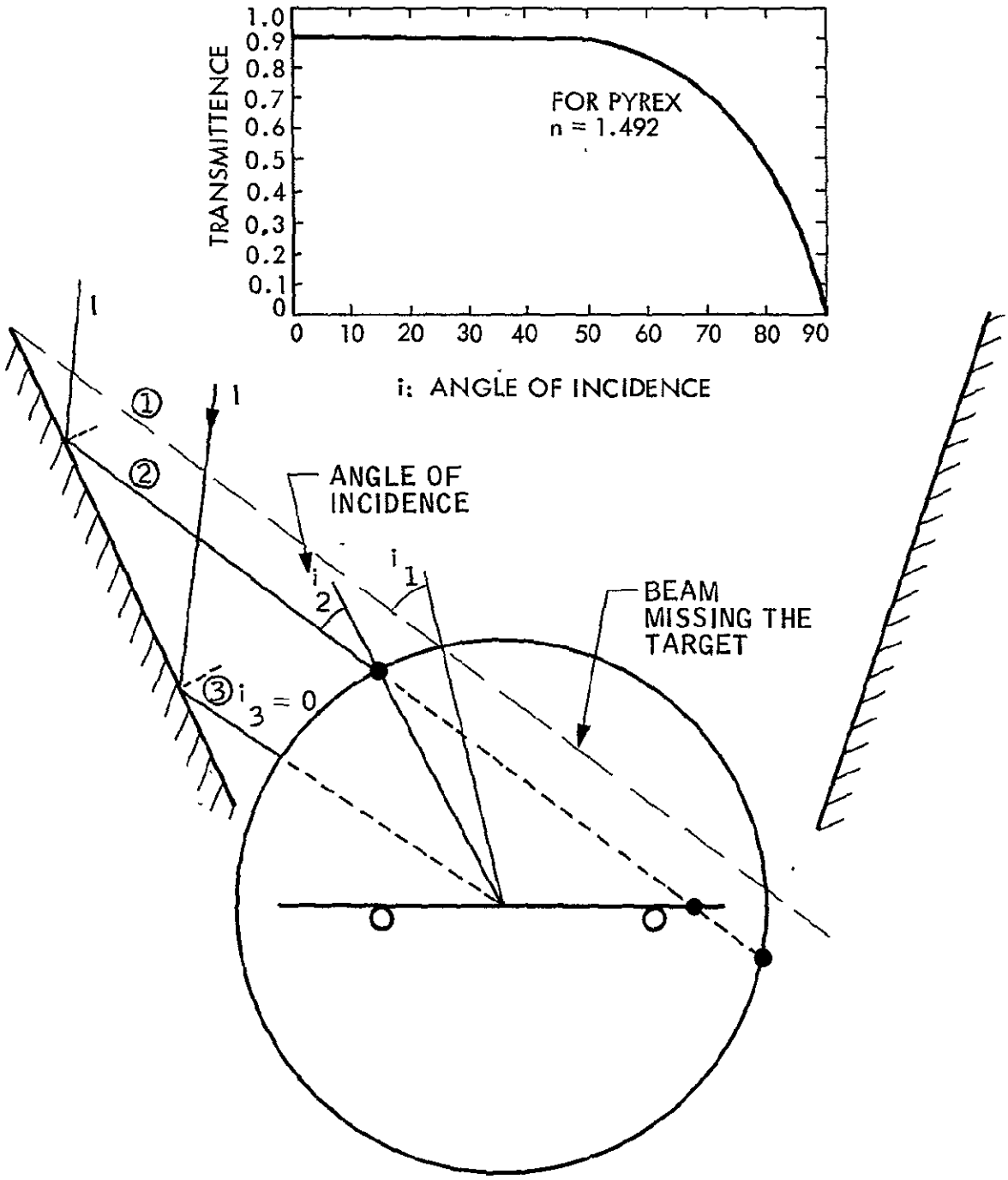

Figure 2-7. Vee-Trough Concentration with Circular Glass Envelope (Optical Model VTCGR)

tube effects was developed to obtain theoretical performance data. In addition, a vacuum tube without any reflectors was installed on a test stand (which will be described later) to identify the performance improvement by using vee-trough reflectors and to verify the thermal model of the vacuum tube.

The following assumptions were used in the formulation of the mathematical model of a single vacuum tube:

1) Convection inside the tube is completely eliminated since the pressure is $P < 0.4 \times 10^{-4}$ torr. Studies in Reference 23 reveal that under a vacuum level of $P < 10^{-4}$ torr, convection losses are reduced to a level so that effects inside the tube can be disregarded. For such low vacuum levels, conduction and radiation losses play a major role in the thermal energy balance of the absorber plate.

2) Conduction to the wall through the clips, attached to the absorber plate to center it in the glass tube, is neglected.

3) Conduction through the U tube and manifolding is significant. Its magnitude was on the order of 5 to 10 percent for temperatures around 200 and 300°F, respectively. A correction factor was applied, as will be explained later.

Details of the formulation of vacuum tube thermal performance are outlined below. Dimensions of the vacuum tube under study are given in Figure 1-1. Additional data are:

Absorber plate length	$L = 7$ ft
Selective coating absorptivity	$\alpha = 0.935$
Selective coating emissivity	$\epsilon_p = 0.08$
Emissivity of the uncoated side of the plate	$\epsilon_{pb} = 0.12$ (polished copper)
Glass surface emissivity	$\epsilon_g = 0.88$
Glass index of refraction	$n = 1.472$
Glass extinction coefficient	$K = 0.078$ cm^{-1} (0.198 in.$^{-4}$)
Thermal conductivity of the plate	$k = 385$ W/m °C (222.5 Btu/hr-°F)

2.3.2 Energy Balance of the Vacuum Tube Receiver

First Law of Thermodynamics can be applied to the vacuum tube receiver. The energy balance equation for the absorber plate considering thermal storage effects is

$$I_t (\tau\alpha)_e A_p = Q_u + Q_l + Q_s \tag{2.5}$$

where

I_t = rate of incidence of total flux on a unit area of the absorber plate

$(\tau\alpha)_e$ = effective transmittance-absorptance product of glass for beam and diffuse radiation

A_p = absorber plate surface area (collector area)

Q_u = rate of useful heat transfer to the working fluid

Q_l = rate of heat losses from the collector to the surroundings by reradiation, convection, and by conduction through supports

Q_s = rate of heat storage in the collector

Since the thermal capacity of the working fluid and the tubes is low, Q_s may be neglected. The total useful energy gain of the collector Q_u for quasi-steady-state operation can be expressed as

$$Q_u = \dot{m}C_p \Delta T = A_p F_R \left[I_t (\tau\alpha)_e - U_L (T_{f,i} - T_a) \right] \tag{2.6}$$

where

$\dot{m}$ = mass flow rate

C_p = average specific heat of the working fluid

ΔT = temperature increase of the working fluid

F_R = heat removal factor

U_L = overall heat transfer coefficient between the absorber plate and the ambient

$T_{f,i}$ = fluid inlet temperature

T_a = ambient temperature

Derivations of equations giving F_R, $(\tau\alpha)_e$ and U_L are given in Appendix B.

Based on derivations (given in Appendix B) the vacuum tube efficiency is obtained as

$$\eta = \frac{Q_u}{Q_{in}} = F_R \left[(\tau\alpha)_e - \frac{U_L}{I_t} (T_{f,i} - T_a) \right] \tag{2.7}$$

where the incident solar heat input is

$$Q_{in} = I_t A_p \tag{2.8}$$

2.3.3 Formulation of the Vacuum Tube Thermal Model with Concentrators

The useful heat and efficiency equations for tubes with concentrator can be derived in steps similar to that described for plain tubes. Without following those identical steps, the useful heat, the incident solar heat input and the hourly efficiency of the collector, respectively, are given below:

$$Q_u = F_R A_p \left[CRI_t (\tau\alpha)_e - U_L (T_{f,i} - T_a) \right] \tag{2.9}$$

$$Q_{in} = I_t A_c \tag{2.10}$$

$$\eta = F_R \frac{A_p}{A_c} \left[CR (\tau\alpha)_e - \frac{U_L}{I_t} (T_{f,i} - T_a) \right] \tag{2.11}$$

where CR show the concentration ratio and A_c the collector area. All other values are the same as in the previous section.

SECTION III

RESULTS OF THE MATHEMATICAL ANALYSES

Computer codes were generated to solve each mathematical model. Listing of these codes or the details of the analysis will not be given in this report due to space limitations. Instead, only the highlights of the solutions of each model will be presented.

3.1 OPTICAL MODELS RESULTS

The total mirror approach (VTFRT) has significance since it is simple and requires the least computer time compared to the more rigorous approaches. Deviation of results obtained through VTFRT from the ideal solution, however, is the largest among the approaches used. Besides, it does not apply to the optical analysis of the circular glass envelope. This particular model is almost identical to that used to generate curves of daily average concentration ratios during precontract conceptual studies and presented in Ref. 1.

The more elaborate model, which considers first and second reflections from mirrors, yields results closer to the actual case. Results of the computer code for this model (VTFR2) are given for selected days of the year in Figure 3-1. Day-long variation of the concentration ratio for a surface having a reflectivity of $\rho = 0.9$, a collector plane tilt of 34.10° (which is the latitude of Burbank, California), and flap angles of $\theta_1 = 55^{\circ}$ and $\theta_2 = 85^{\circ}$ are given. Flap widths are 1.105 ft and 0.94 ft for wide and narrow flaps, respectively.

Near the solstices the concentration ratio varies from a figure of about 1.15 to a peak of about 2.3, whereas during equinoxes it is constant around 1.4.

The daily average concentration ratio (which is defined as the ratio of the total incident concentrated flux on the absorber plate during the period from 8:00 am to 4:00 pm to the incident flux on the receiver without any concentrators) is given in Figure 3-2 for a period of one year. Results of VTFR2, which considers the secondary reflections, yield a concentration ratio, on the average, between 5 to 10% above the results of the first reflections model (VTFR1).

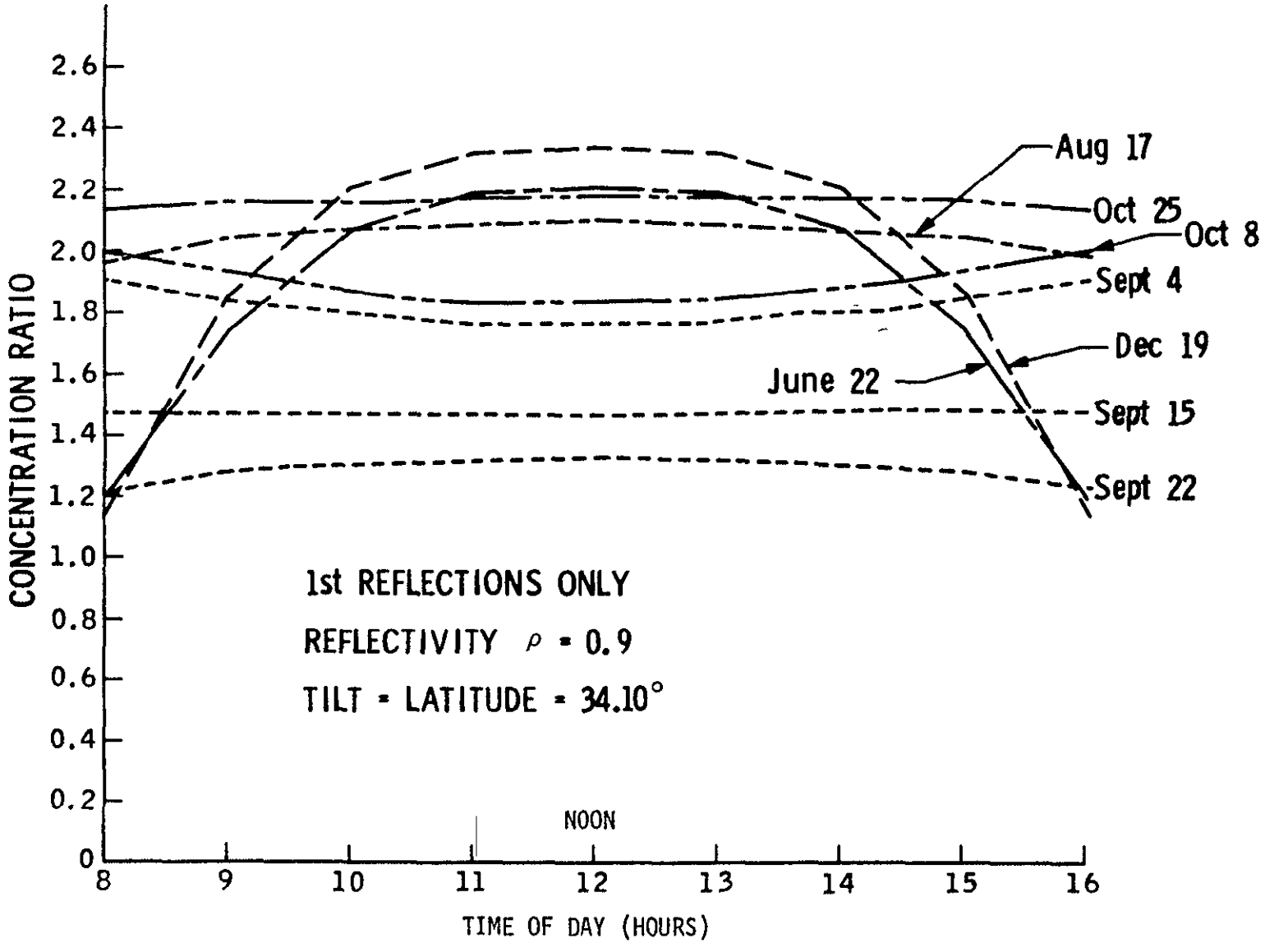

Figure 3-1. Daylong Variation of the Concentration Ratio for a Vee-Trough Concentrator

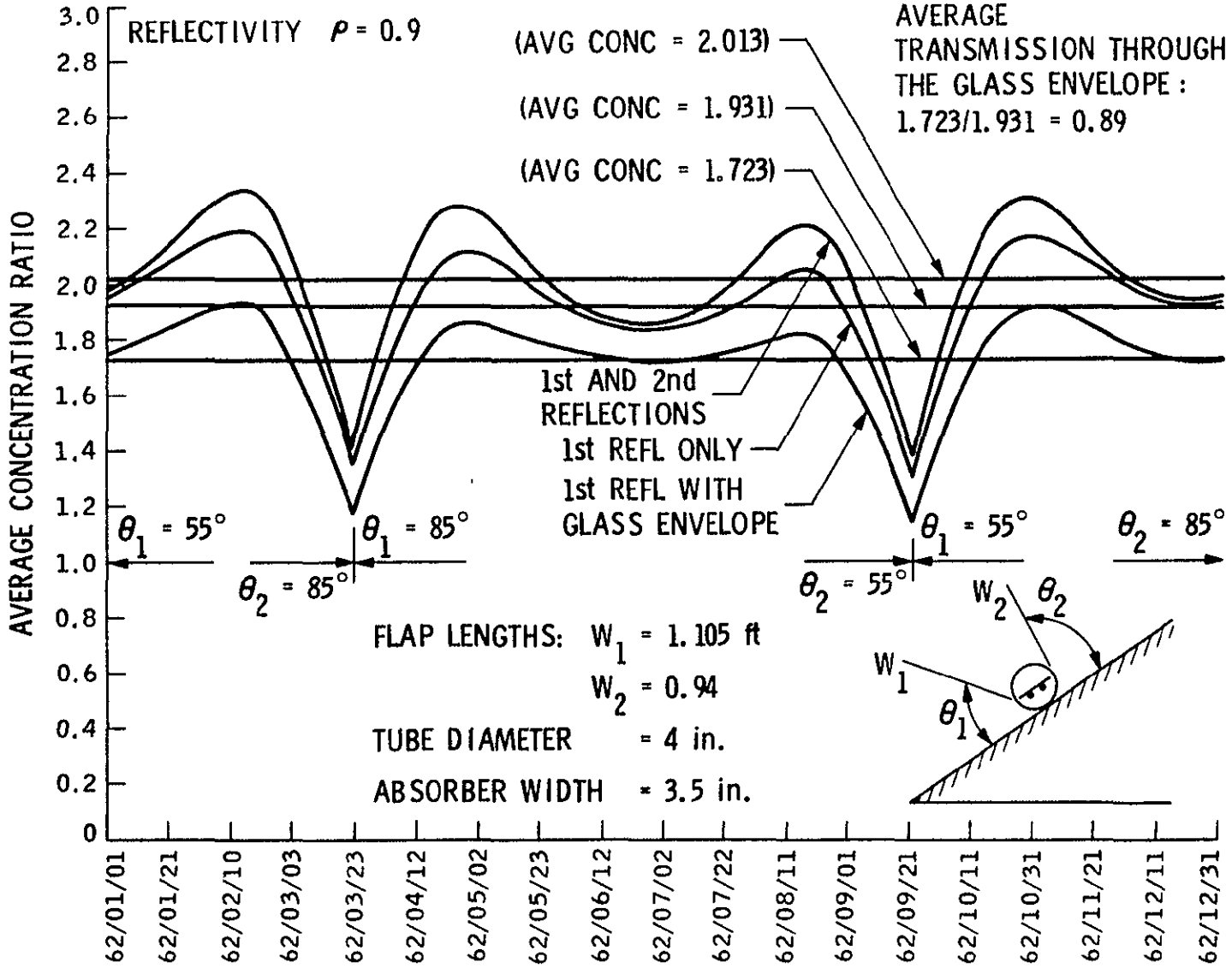

Figure 3-2. Daily Average Concentration Ratio Calculated Using Various Mathematical Models

The net effect over a year is that the first and second reflections model predicts the collection of only about 4% more energy than the first reflection-only model.

The insertion of a circular glass envelope, having an average transmissivity of 0.92, reduces the yearly average concentration ratio of 1.723. This corresponds to our equivalent transmission factor of about 1.723/1.93 = 0.89 if the first reflections are considered. If first and second reflections are considered, the transmission factor becomes 1.723/2.013 = 0.855.

Since a transmission loss of 92% had to be considered even with a clear pyrex tube, the curvature of the tube results in losses with a factor of only 0.97/0.89 = 1.033 and 0.92/0.855 = 1.076 for first and second reflection models, respectively.

Curves for mirror surface reflectivity values of 0.9, 0.85 and 0.8 are given in Figure 3-3. The effect of reflectivity is more pronounced during the solstices than the equinoxes. The reduction of the concentration ratio is not as large as the ratio of reflectivities. For example, for July 8 at solar noon, the calculated concentration ratio absorptivity product is CR $\tau\alpha$ = 1.775 for a specular reflectivity of ρ = 0.9, and CR $\tau\alpha$ = 1.667 for ρ = 0.8. The reduction of the reflectivity is 0.9/0.8 = 1.125, whereas the concentration ratio is reduced only by a factor of 1.775/1.667 = 1.064. This occurs because the net concentrated flux is a combination of directly incident beam and diffuse solar radiation as well as reflected (from both mirrors as first and second reflections) beam and diffuse radiation. The directly incident radiation on the receiver is 1/3 of the amount on the aperture plane. Even if the reflectivity of the mirror surfaces were zero, still 1/3 of the energy incident on the aperture plane could be collected. This feature, which applies to symmetrical vee grooves as well as CPC type concentrators, is the inherent advantage of the concentrator design.

3.2 THERMAL MODELS RESULTS

Solutions to the thermal model of the vacuum tube receiver with and without vee-trough concentrators were obtained. The procedures were as follows.

3.2.1 Solution Without Reflectors

Equation B.8 (see Appendix B) giving U_L contains the glass temperature T_g, which is not known. First, T_g was obtained from Equation B.9 by

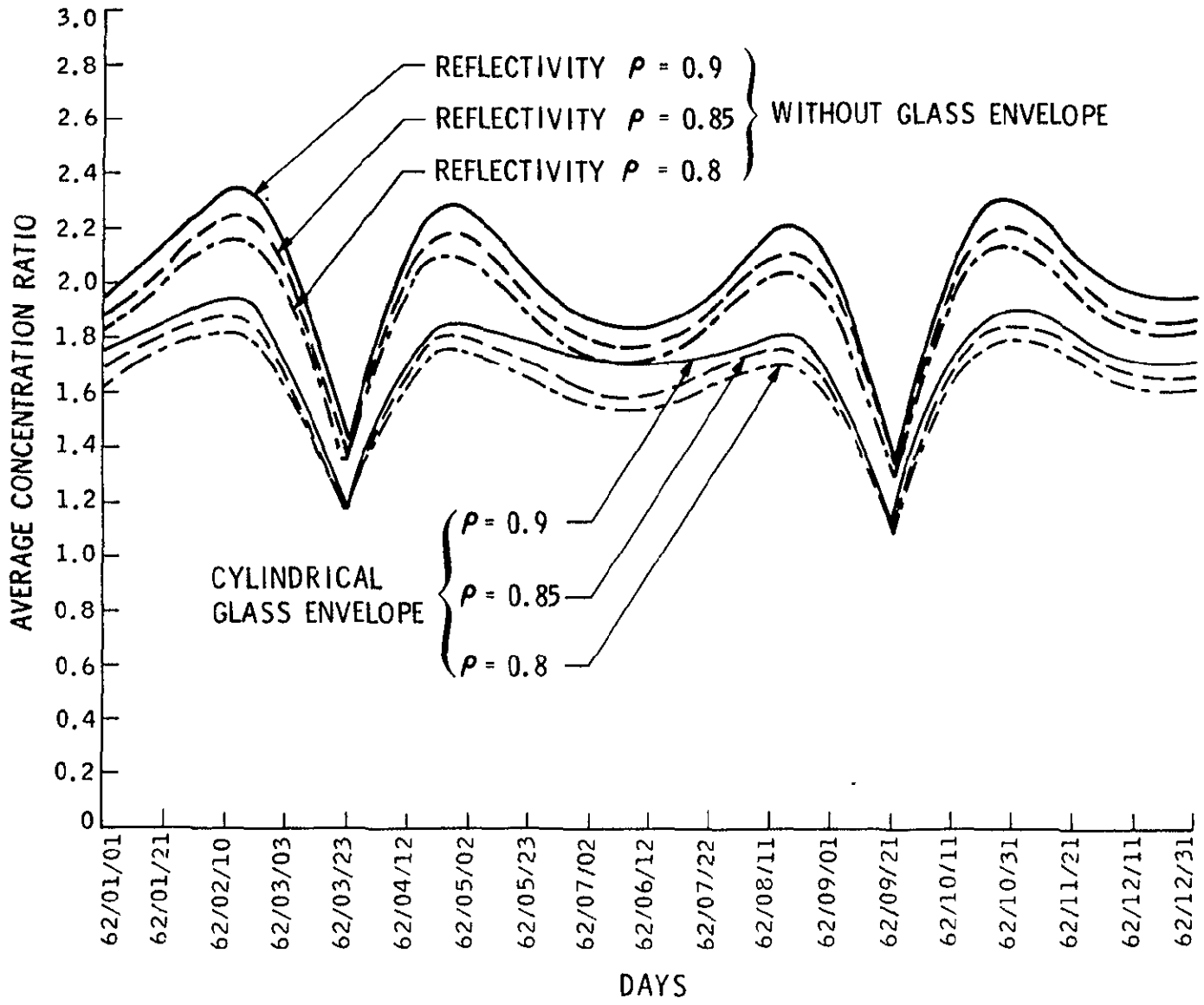

Figure 3-3. The Effect of Reflectivity on the Daily Average Concentration Ratio (Concentrated Flux Only)

using the computer for various ambient temperatures and wind velocities under the previously mentioned assumption that the sky and ambient temperatures are the same. The calculated T_g values were then put into Equation B.8 for various plate temperatures; i.e., the average working fluid temperatures. After the U_L value was determined, the heat removal factor F_R was calculated by means of Equation B.18 for various U_L, T_p and $\dot{m}$ values. Once the U_L and F_R values were obtained, the useful heat Q_u and the collector efficiency η were calculated for given solar heat fluxes by means of Equations 2.6 and 2.7, respectively.

3.2.2 Solution With Reflectors

The same procedure as in 3.2.1 has been used in order to calculate the values of T_g, U_L, F_R and consequently the values of Q_u and η by using Equations 2.9 and 2.10, taking into consideration the concentration ratio CR resulting from the optical model calculations for different type reflectors.

Figure 3-4 gives results of the thermal model of the vacuum tube receiver with and without reflectors. The tube efficiency η is plotted against $\Delta T_{f,i}$, fluid inlet temperature minus the ambient temperature. The top set of curves gives the efficiency of the receiver tube based on the flux incident on the absorber plate. Fluxes up to 350/BTU/hr ft^2 are attainable without a vee-trough concentrator.

The purpose of the vee-trough concentrator is to increase the flux on the absorber to levels around 800 BTU/hr ft^2.

The net efficiency of the vee-trough/vacuum tube collector, given as a function of the incident flux intensity on the aperture plane, is based on the aperture area. Therefore, it is lower than the receiver efficiency based on the absorber area. However, the cost of the collector based on the aperture area is also low. As a result, the cost per BTU is low and results in a cost-effective design.

Receiver tube and receiver-concentrator costs, as well as predicted energy costs, are discussed in Section V. Table 5-4 compares the results of the thermal model with test data.

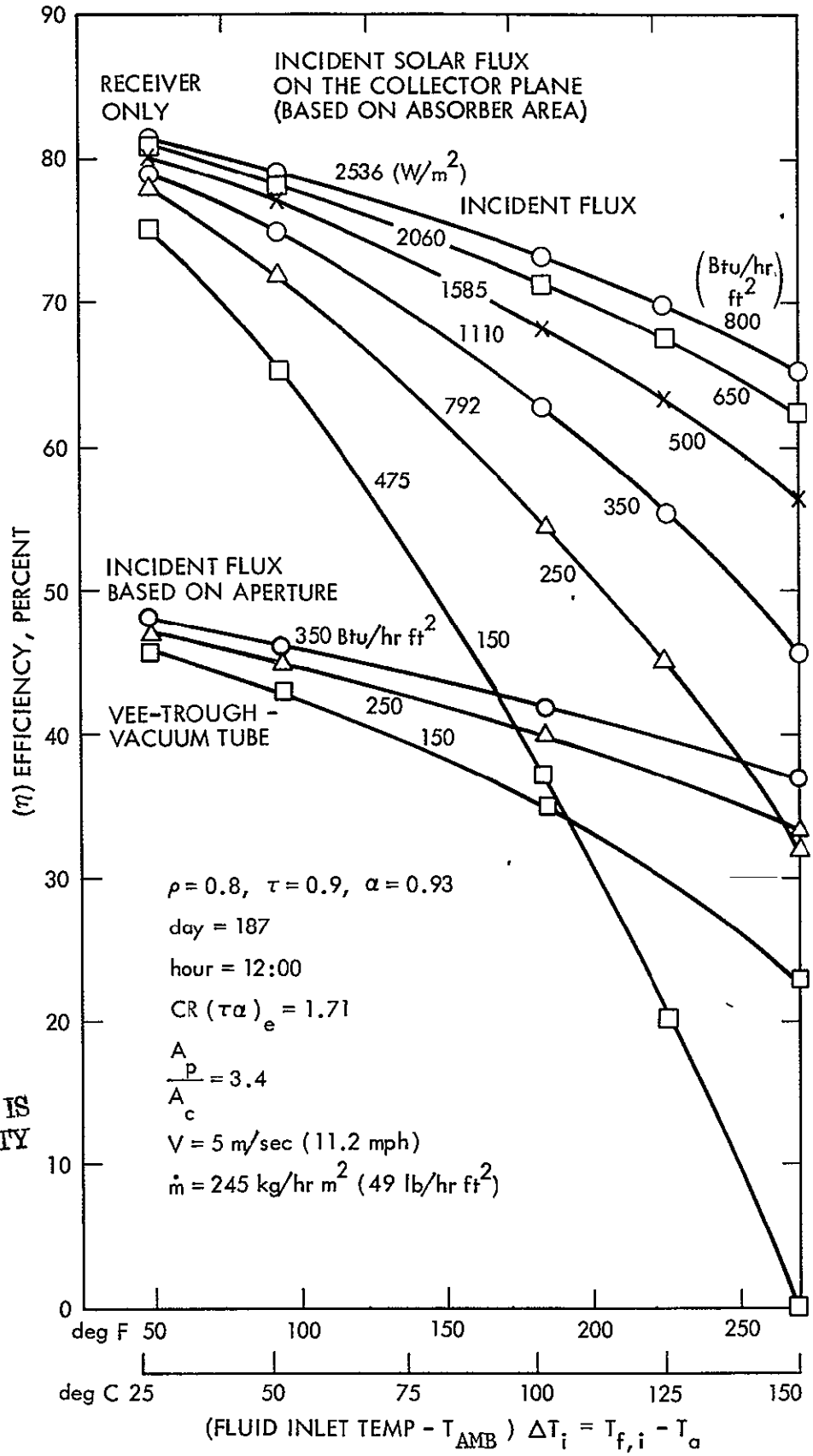

Figure 3-4. Results of the Thermal Model for the Receiver and Collector

SECTION IV

DESIGN OF THE TEST BED AND INSTRUMENTATION

4.1 TEST BED DESIGN

A test bed was designed and constructed for experimental evaluation of the vee-trough collector consisting of Corning Glass Works vacuum tube receivers and vee-trough reflectors.

The test bed consisted of the following components (as seen in Figure 4-1).

4.1.1 Pumping Station

The working fluid selected, Therminol 44, was circulated through the evacuated tubes by means of a gear type pump. The pumping station has features such as a pressure relief valve, a bypass loop used to regulate the flow, a drain line and an expansion tank. Both the tank and the flexible piping connecting the pumping station to the collector stand are insulated against heat losses.

The tank is equipped with two electrical immersion heaters and a temperature regulator for controlling the desired operation temperature. This feature is needed because of the limited number of available tubes, each tube being able to heat the fluid only about 5 - 10°C per tube. With 4 tubes connected in series, the outlet temperature from the last tube is from 20 to 40°C above the inlet temperature to the first tube. Since test data extending to 180°C were needed, the preheater was used. In the actual system, a sufficient number of tubes will have to be connected in series to elevate the collection temperature to the desired operation temperature, including an allowance for a temperature drop in the heat transport system.

4.1.2 Collector Test Stand

Vacuum tubes are installed on an adjustable tilt stand and instrumented for thermal performance evaluation. During the contract period, tests were run only at a collection plane tilt equal to the JPL latitude ($\approx 35^{\circ}$). The setup has, however, the flexibility for testing at other tilts such as (latitude + 10°) or (latitude - 10°), which were found to yield performances

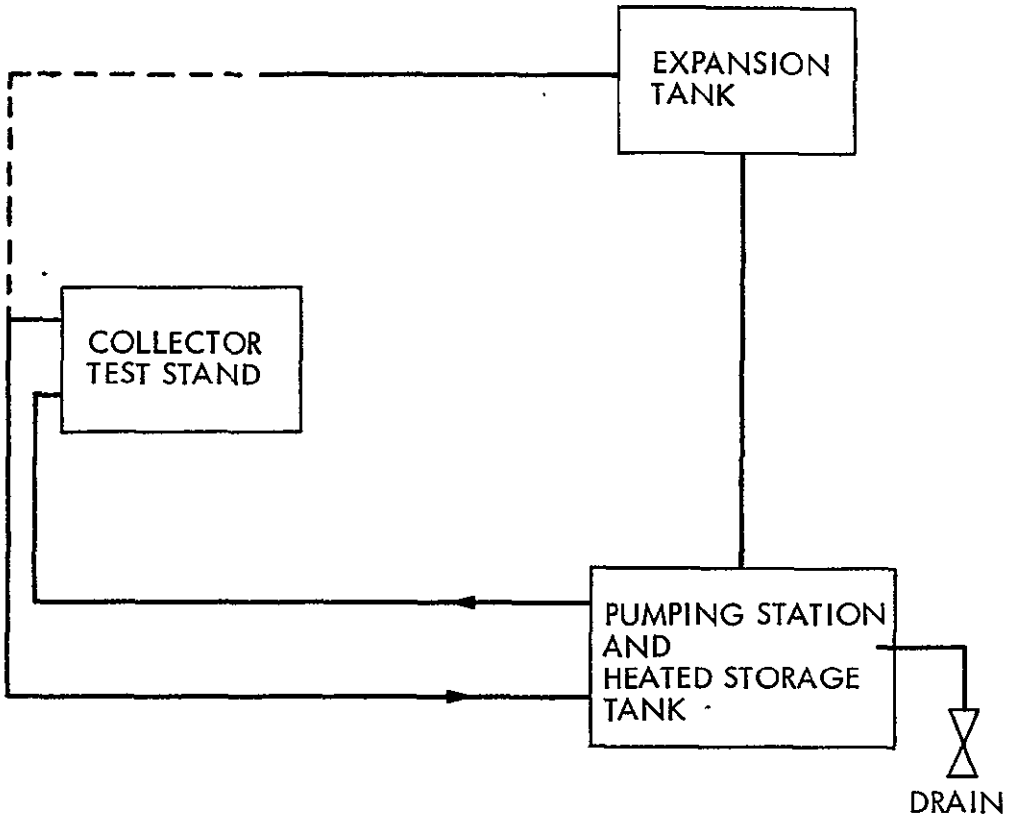

Figure 4-1. Test Bed Components

better than (tilt = latitude) for winter and summer, respectively.

The test stand is made of aluminum. The frame has aluminum channels onto which the tube supports are attached. Tube ends are connected to the manifold, which is designed for parallel or series operation of the tubes.

Figure 4-2 shows the tube and valve connections as well as the positions of probes for measuring temperatures, fluid pressure, and flow rates.

Figures 4-3 through 4-6 show progression of the construction of the test stand frame before the assembly of the tubes.

Figures 4-7 and 4-8 show the test stand at the test site before the tube assembly and the reflectors were installed. The manifold box was later insulated and closed after the leak test.

Figures 4-9 and 4-10 show the complete test bed with tubes installed, but with the manifold uninsulated. The evacuated tubes are temporarily wrapped with aluminized mylar for dry run protection.

For commercial operations, the coating must survive under stagnation temperatures. Tests by Honeywell (Ref. 24) using black chrome coating has revealed that emissivity and absorptivity values are stable up to 360^{o}, which is above the stagnation temperature of the plain tube. However, tubes with concentrators will exceed this temperature. Since high-temperature selective coating development is underway as a part of the thermal conversion program, it is expected that a coating which will survive at 500^{o}C, a level above the stagnation temperature of the evacuated tube with vee-trough concentrators, will become available. Until such a coating is developed, care has to be taken to protect the dry tubes from exposure to the sun. One accidental dry run due to an unnoticed pump failure and lasting about one-half day did not damage the coating. A heat loss experiment conducted after that dry run revealed no change. Efficiency figures of tubes before and after the exposure were almost the same. Relatively short exposure may have caused an unnoticeable change but, as mentioned before, care was exercised to cover the tubes and protect against long dry exposures.

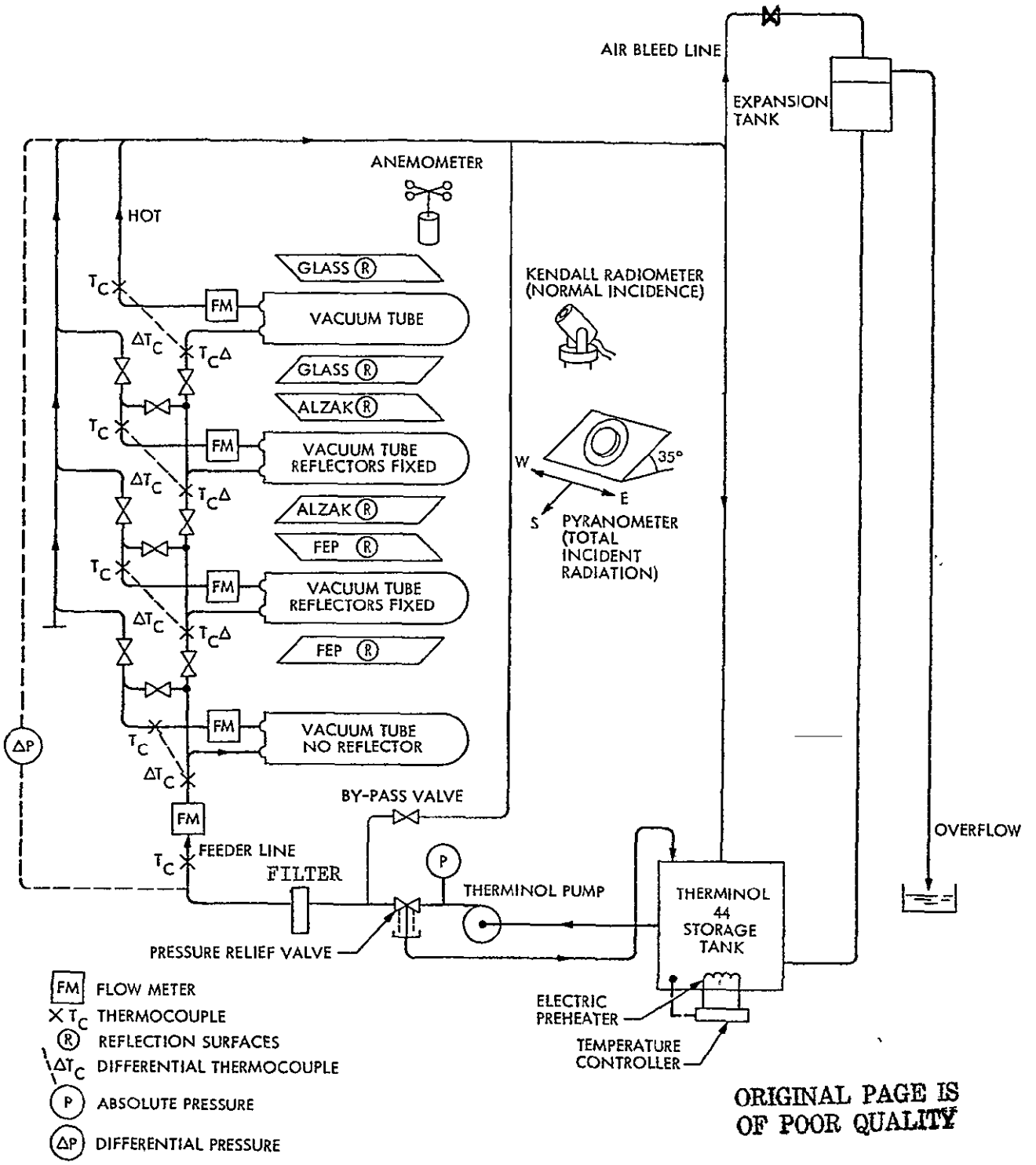

Figure 4-2. Test Arrangement for the Vacuum Tube Receivers

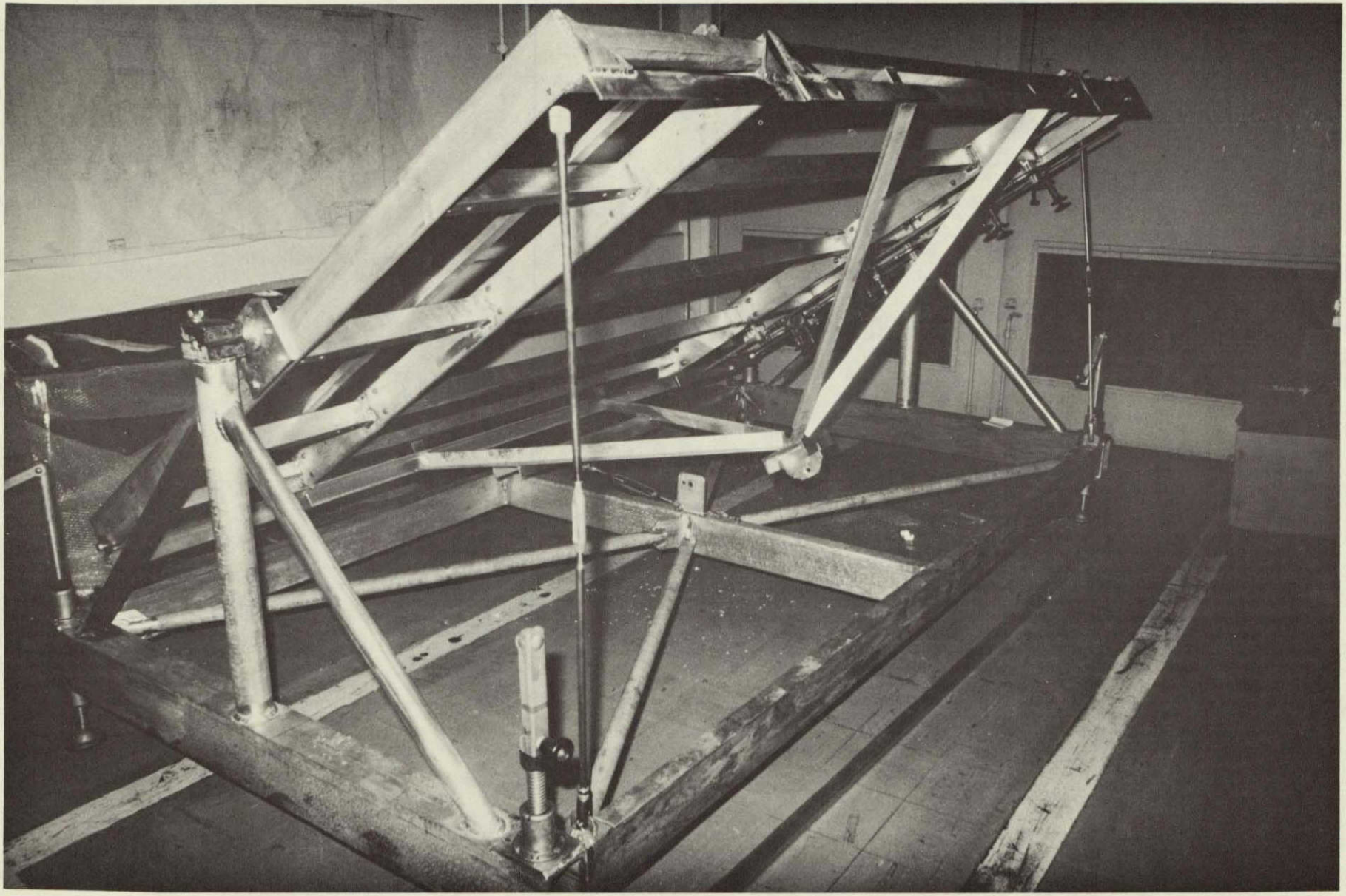

Figure 4-3. Test Stand Frame

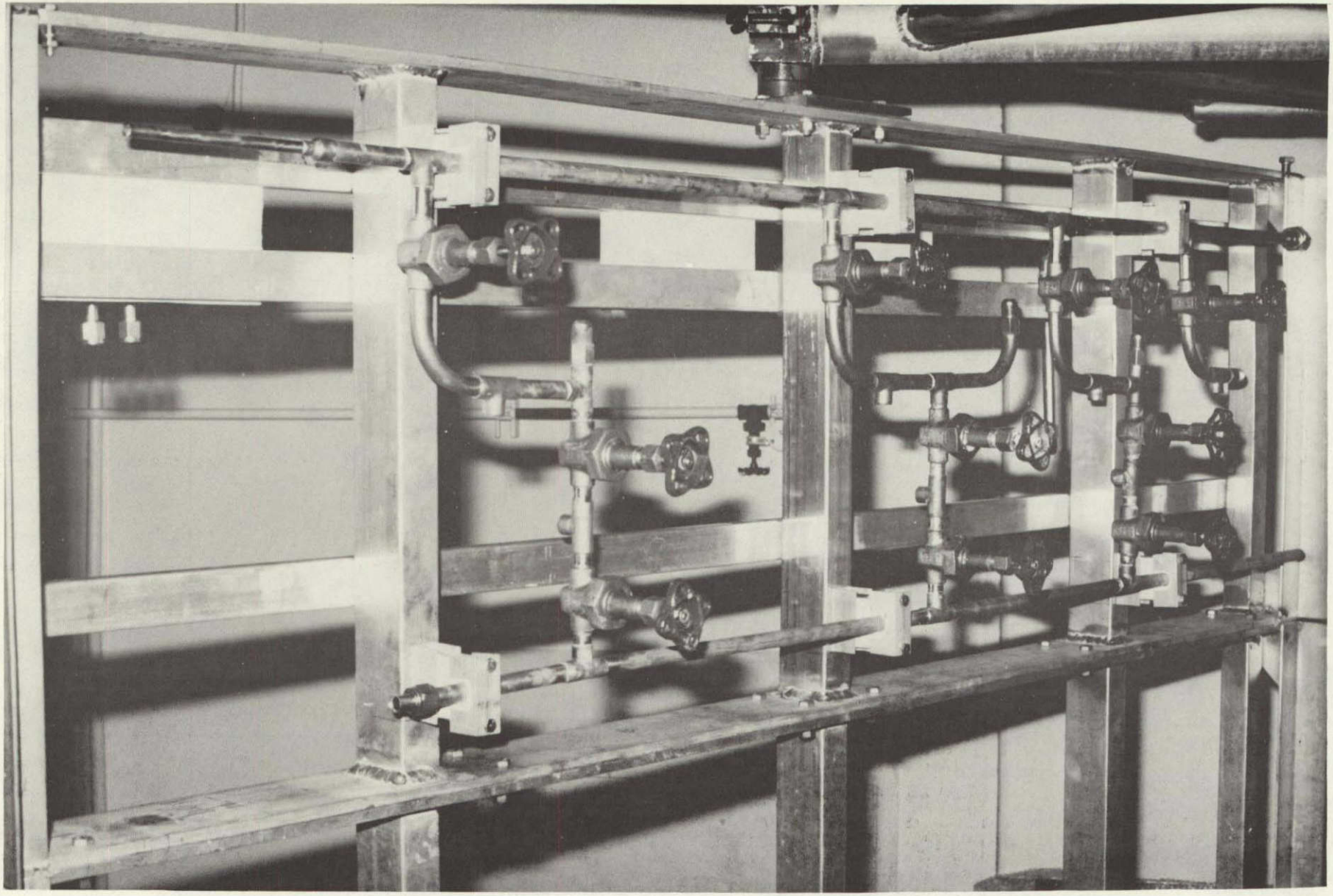

Figure 4-4. Manifolding on
Test Stand

ORIGINAL PAGE IS
OF POOR QUALITY

Figure 4-5. Tube End Y-Connection
for Inserting Thermocouple Probes

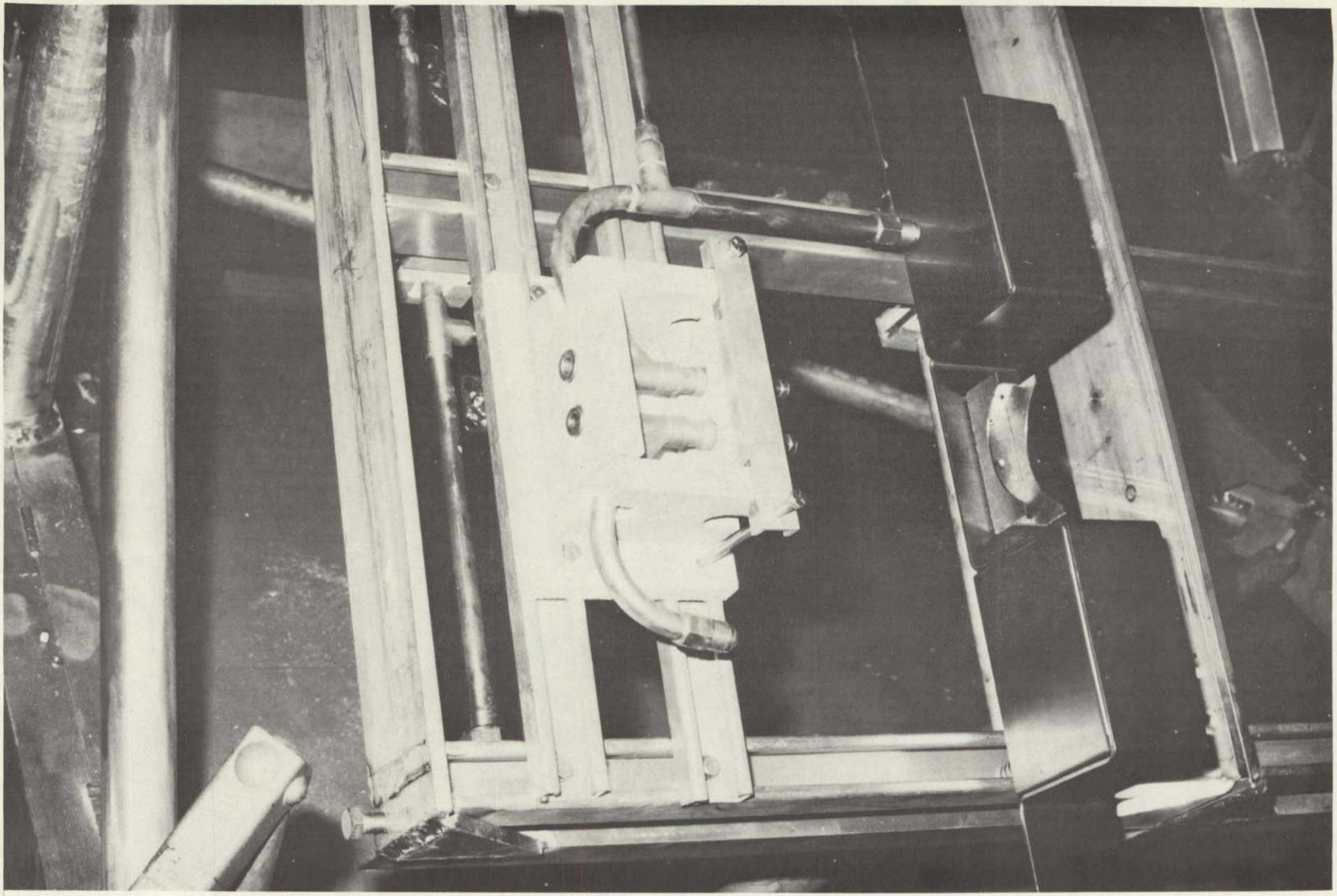

Figure 4-6. Tube End and Tube Support

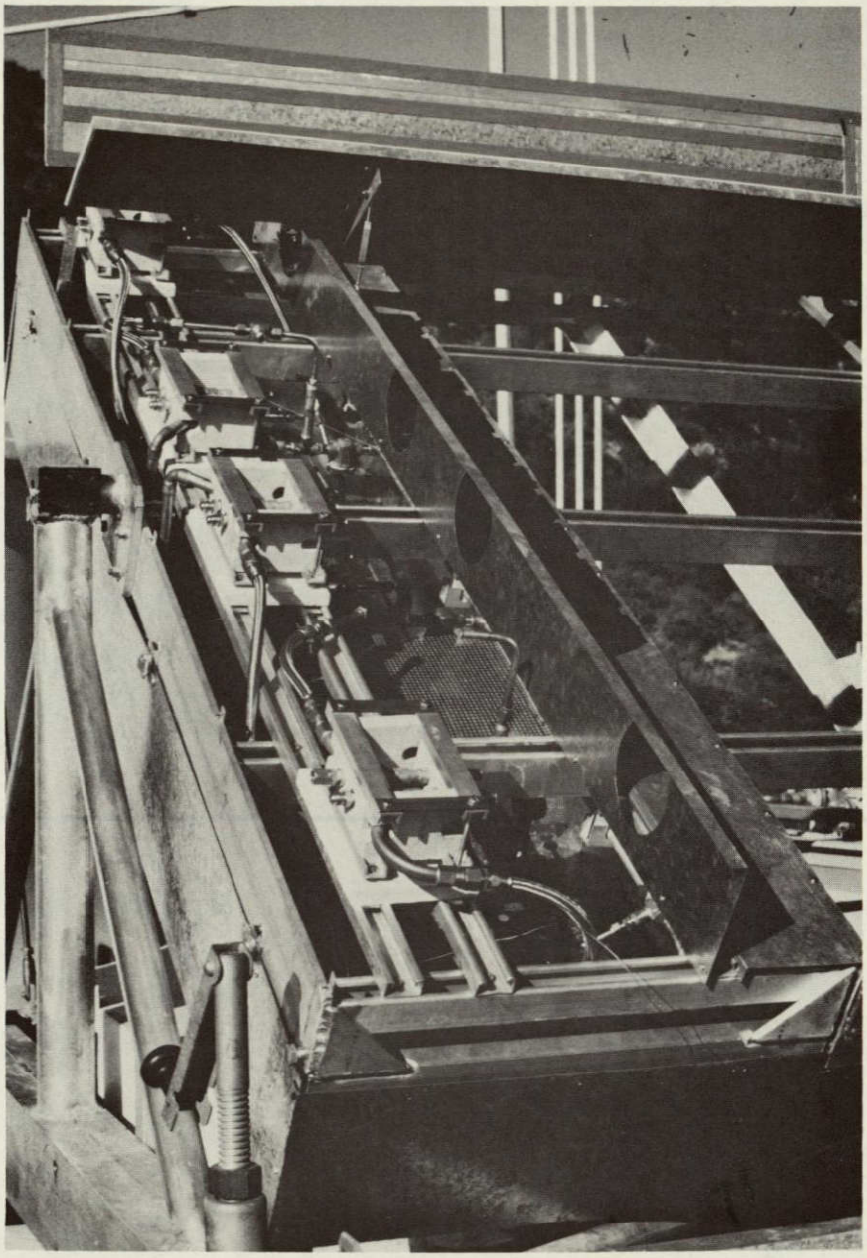

Figure 4-7. Test Stand at Test Site, Closeup View

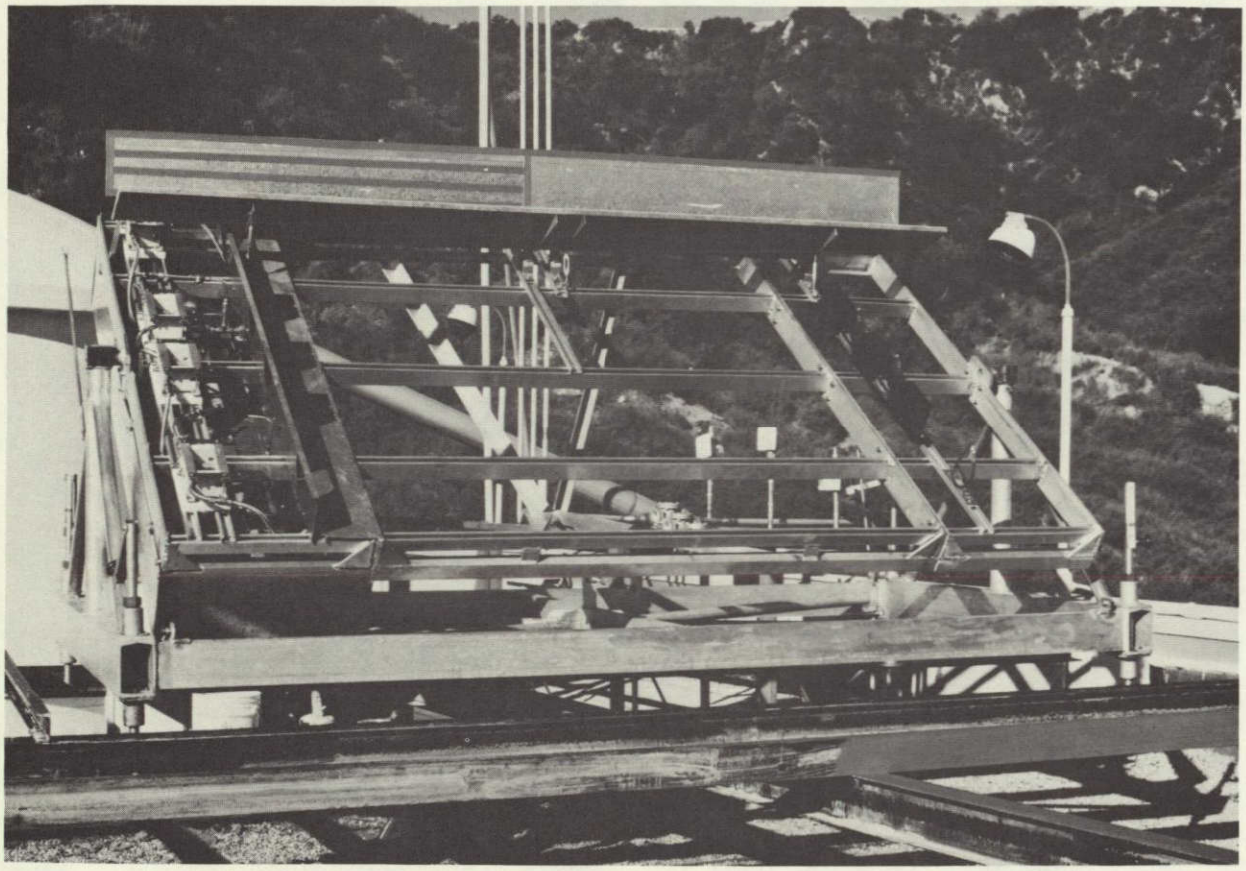

Figure 4-8. Test Stand, Overall View

Figure 4-9. Test Bed with Tubes Installed

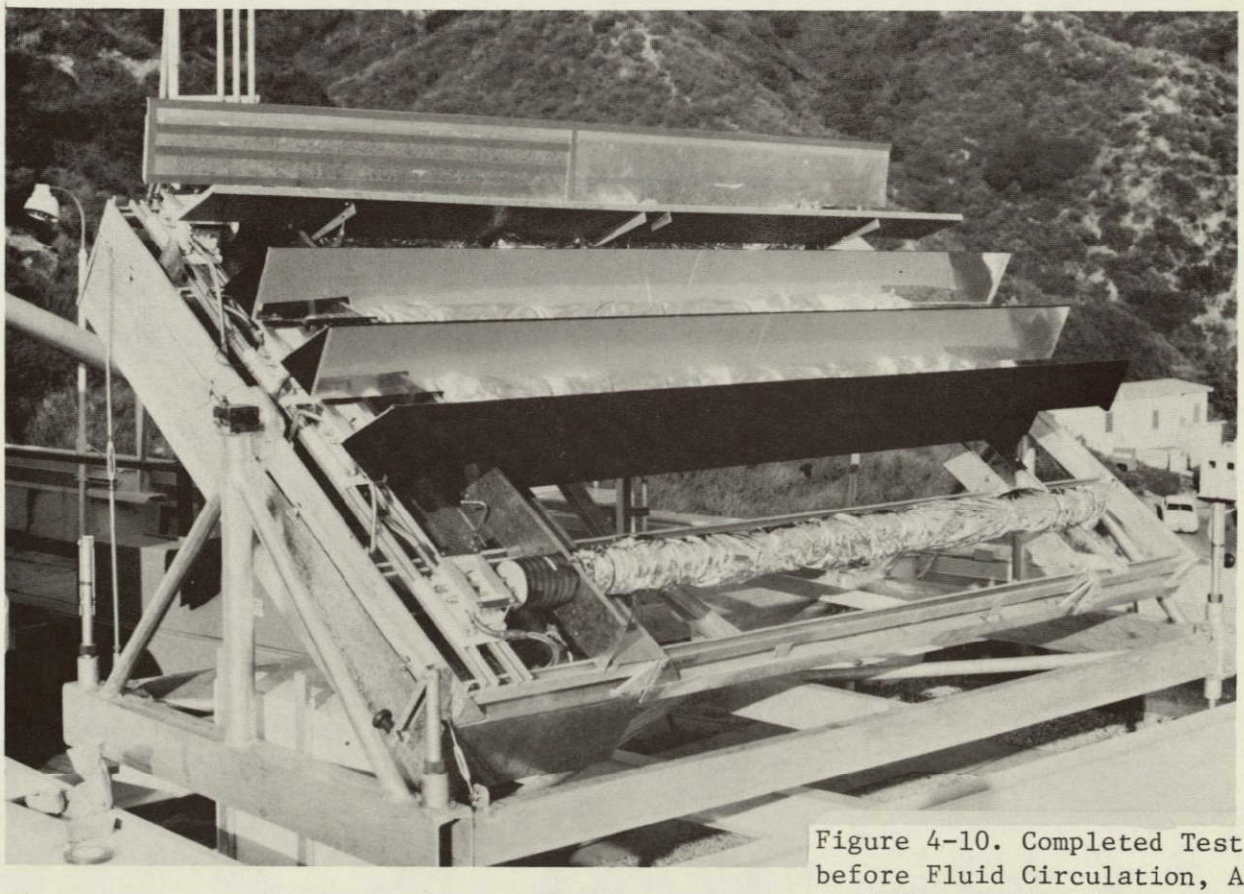

Figure 4-10. Completed Test Bed before Fluid Circulation, Aluminum Foil Wrapped for Protection

4.2 INSTRUMENTATION

The vee-trough collector test bed is fully instrumented to determine the receiver tube thermal efficiency as shown in Figures 4-2 and 4-11. The flow rate of Therminol 44 is measured by turbine-type flow meters for each tube, and flow rates are compared for series operation. Both the absolute fluid output temperature and the differential temperature between the fluid inlet and outlet are measured on four vacuum tubes. Thus, the net useful heat collected can be calculated using data from the flow meter and differential thermocouples. Additional thermocouples are attached to the surface of each vacuum tube. These thermocouples are used as an indicator of the thermal insulation status (i.e., condition of the vaccum and selective coating). Heat loss experiments (e.g., night runs with preheated fluid and measurement of ΔT of fluid) also enable the monitoring of the condition of the vacuum tubes. The tube ends, where the two copper lines come out from the vacuum tube, are further insulated to reduce conduction losses and instrumented to measure the ΔT through the insulation. The manifold at the vacuum tube ends (which consist of valves, flow meters and flexible tubing) is heavily insulated. Pressure drops through the tubes (four tubes may be connected in series or parallel by manipulating valves) and absolute pressure are determined using pressure transducers. Tests were run in the series configuration of receiver tubes.

All data acquired from the vacuum tube test bed are fed into JPL's automated data acquisition and processing system (IDAC). Figure 4-11 shows the basic measuring and recording devices for data collection. The raw data can be (1) displayed visually on a TV screen, (2) recorded on magnetic tape, or (3) printed on photosensitive paper for manual evaluation. It is also possible to load the data on a magnetic tape and then process it later. The IDAC system also has the capability of providing alarms, such as for excessive tube outlet temperature and/or for stopping the circulation of the working fluid. Data evaluation for the runs reported is done manually from the printed strip.

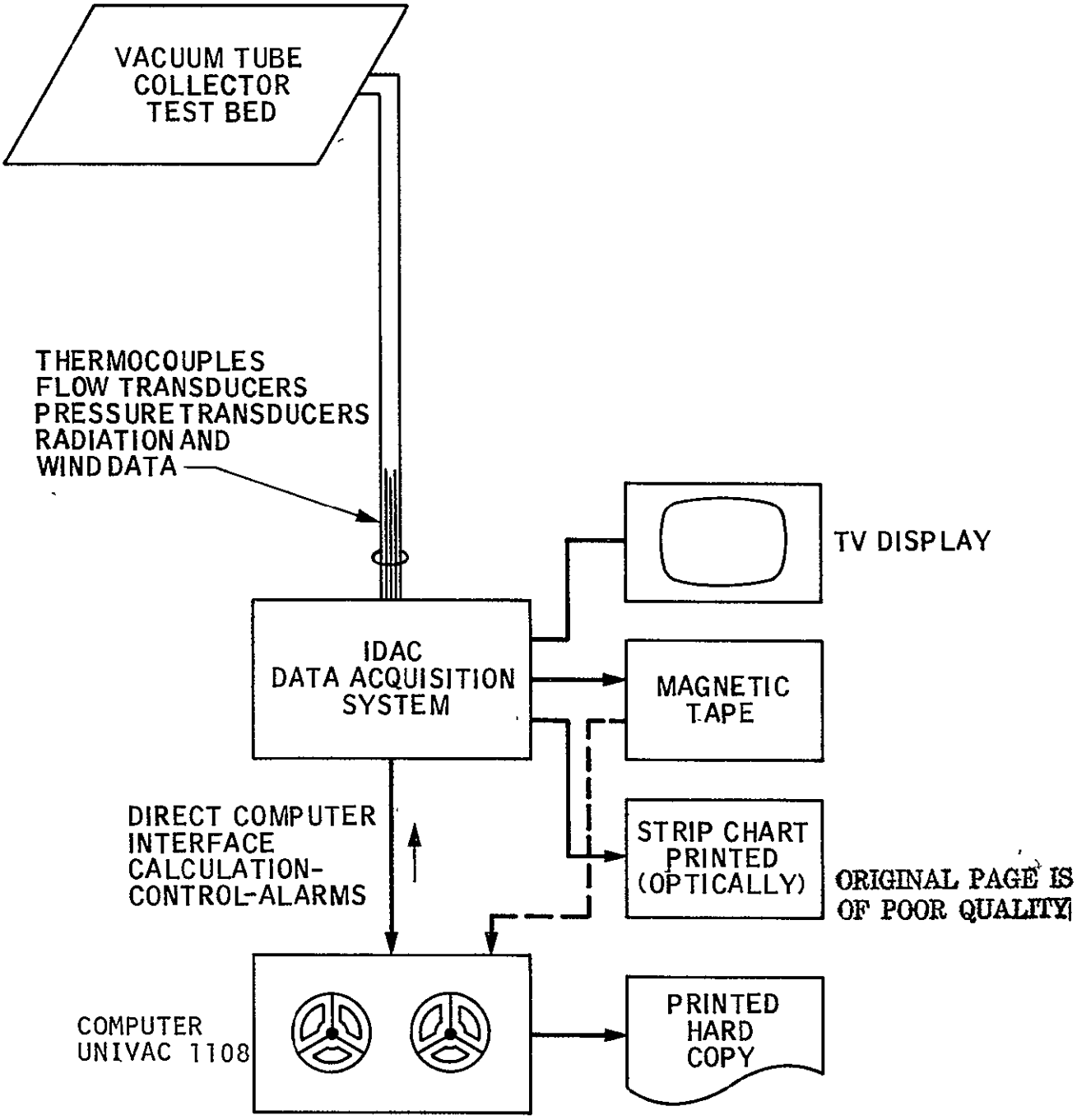

Figure 4-11. Vee-Trough Vacuum Tube Collector Data Acquisition System

SECTION V

TESTING AND EVALUATION

The test bed was first tested against any fluid leakage and other mechanical problems. The air entrapped in the manifold and lines was bled by opening the valve in the air bleed line. After the flow meter reading was stabilized, the valve was closed. The procedure was occasionally repeated to eliminate dissolved air or gas released due to decomposition of Therminol, which might have caused flow instabilities to invalidate the experiments.

5.1 CALIBRATION OF INSTRUMENTS

The useful heat calculations and efficiency determination require the following basic data, which has to be known within permissible error limits:

1) Mass flow rate of the working fluid $\dot{m}$ which consists of d (density) and V (volumetric flow) rate terms
2) Specific heat of the working fluid C_p
3) Temperature rise of the working fluid in the evacuated tube ΔT
4) Solar flux intensity at the tilted collector plane I_t

Items (1), (2), and (4) were determined using calibrated instrumentation. Specific heat of Therminol 44 was taken from the manufacturers data (Table 5-1). These figures were also verified by tests performed at JPL's Chemistry Laboratory. Table 5-2 gives these values along with JPL data at $100^{\circ}F$. Property change due to slight coloring of Therminol after several runs, was not significant. These data were used in calculations either using linear interpolation techniques or by curve fitting.

5.2 PERFORMANCE OF TESTS

Tests were run mainly under clear day conditions for daytime efficiency determinations and at night for heat loss experiments. The latter was conducted to determine actual (U_L) values for use in theoretical calculations of the collector efficiency.

Steps in data acquisition and some sample data are given below. Further measured data and processed values are given in Appendix C.

Table 5-1. Typical Properties of Therminol 44

Item	Description
Composition	Modified Ester Based Fluid
Appearance	Clear yellow liquid
Odor	Faint
Pour point	-62° to -68°C (-80 to -90°F)
Density @ 75°F	7.67 lb/gal
Flash point, coc.	207°C (405°F)
Fire point, coc.	225°C (438°F)
AIT	374°C (705°F)
Coefficient of expansion	0.0008 cc/cc/°C
Boiling range 10% 90%	 337°C (638°F) 390°C (734°F)
Average molecular weight	367

Table 5-2. Variations of Properties of Therminol 44 with Temperature

Temperature		Density			Specific Heat		Viscosity
^{o}C	^{o}F	lb/gal	lb/ft^3	kg/m^3	Btu/lb ^{o}F	kcal kg ^{o}C	lb/hr ft
-53.8	-65	8.18	61.2	980	0.421	0.421	6321
-45.6	-50	8.13	60.8	974	0.426	0.426	1948
-17.8	0	7.95	59.5	953	0.443	0.443	119
10.0	50	7.78	58.2	932	0.459	0.459	22.8
37.8	100	7.63	57.1	915	0.476	0.476	8.05
JPL DATA							
	(100)	(7.60)			(0.480)		(8.81)
66	150	7.43	55.6	890	0.492	0.492	3.92
93	200	7.23	54.1	867	0.508	0.508	2.34
121	250	7.05	52.8	845	0.524	0.524	1.54
149	300	6.88	51.5	825	0.542	0.542	1.07
177	350	6.69	50.1	802	0.558	0.558	0.84
204	400	6.51	48.7	780	0.574	0.574	0.66
232	450	6.32	47.8	757	0.590	0.590	0.52
260	500	6.14	46.0	736	0.607	0.607	0.42

DATA FROM MONSANTO, LEAFLET IC/FF-32

5.2.1 Daytime Tests

Prior to test initiation, auxiliary electric heaters were switched on and the fluid in the storage tank was heated to the temperature selected for the day. Usually, tests were started at lower temperature levels, say about 200°F for the first day, then raised to 250°F, 300°F, etc on subsequent days.

The pyroheliometer (Kendall Mark II) was aimed at the sun and the circulation pump was started. After the flow was set to a nominal value, the readings could be started within a few minutes since the thermal capacity of the vacuum tubes is quite small. All temperatures (absolute and differential), flow meters readings, pressures, solar flux intensity, wind speed, and wind direction were recorded on photosensitive paper at selected intervals, normally 10 minutes. Data was simultaneously recorded on magnetic tape at 2-minute intervals. However, since the tape recorder occasionally had parity errors, magnetic tape data evaluation was abandoned and only data recorded on the photosensitive paper was reduced.

The temperature of the working fluid gradually rose during the day since heat gain from the sun was more than the loss through lines and tank insulation. This has enabled the obtaining of test data around the set point. It is quite satisfactory for a quasi-steady-state evaluation to have input temperature varying at a rate of 14°C (27°F)/hr since the thermal capacity (response time of a tube; i.e., time required for a temperature rise of 14°C) is only 1/3 of a minute.

The present study does not examine a system incorporating a storage and a load. Instead, its purpose is to determine quasi-steady-state performance of the evacuated tube with and without the vee-trough concentrators.

Test data acquired was later processed by transposing optically printed figures into punch cards via a computer using a special computer program which calculated efficiencies and plotted the curves presented in Appendix C.

5.2.2 Night Tests

In order to evaluate the overall heat transfer coefficient U_L between the working fluid and the sky, heat losses have been measured without any heat gain during the night. U_L has been obtained from

$$U_L = \frac{\dot{m}\ c_p\ \Delta T}{A_p\ (T_{f,i} - T_a)}$$

where ΔT is the temperature decrease of the working fluid. Since the glass tube surface temperatures were measured, the U_L value could be calculated by the equation

$$U_L = F_c \epsilon \sigma (T_p^4 - T_g^4) (T_{f,i} - T_a)$$

and compared to the above value. The plate temperature has been taken as the average fluid temperature $T_m = \frac{1}{2} (T_{f,i} + T_{f,o})$.

The average plate temperature differs from the average fluid temperature due to the thermal resistance between the fluid and plate. The difference, however, is less than 1% since tubes are spaced only 2 inches apart and are bonded to the copper absorber plate by electron beam welding.

5.3 EVALUATION OF TEST DATA

Test data have been obtained for evaluation of the hourly useful heat and the efficiency of the collectors with or without the vee-trough reflectors. For this purpose the temperature increase and the outlet temperatures of the fluid for each tube, the mass flow rate, the beam and total solar flux on the tilted surface, the tube glass wall temperature, the ambient temperature, and the wind velocity and direction have been measured and recorded every 10 minutes from 7:30 am to 4:30 pm PST.

The first four data groups have been used for evaluating the useful heat and the efficiency; the rest have been used for monitoring purposes. A typical evaluation of the test data is given in Table 5-3. Additional results are in the Appendix.

Table 5-4 gives the theoretical efficiency calculation for four tubes tested under the conditions presented in Table 5-3 on July 6, 1977. Test data and theoretical predictions compare well.

In calculating useful heat and collector efficiency either curve of the Therminol 44 properties presented in Table 5-2 can be used, or simplified relations may be utilized. As an example, the temperature dependence of the specific heat and the density of Therminol 44 can be calculated by the following equations:

$$c_p = 0.443 + 0.003275\ T$$

$$d = 7.95 - 0.0036\ T$$

Table 5-3. Test Data Evaluation

Parameter			Tube No.			
			1	2	3	4
T_i	Fluid outlet temperature	F	262.1	242.2	224.4	207.3
ΔT	Fluid temperature increase	F	19.63	20.1	19.82	13.8
T_o	Fluid inlet temperature	F	242.5	222	204.5	193.5
T_m	Fluid average temperature	F	252	232	214	200
f	Flowmeter frequency	Hz	436			
V	Flow rate V = 0.02 f	gal/hr	8.72			
ρ	Density (for T_{04} = 193.5F)	lb/gal	7.2			
$\dot{m}$	Mass flow rate $\dot{m}$ = dV	lb/hr	62.7			
C_p	Specific heat (for T_m)	Btu/lb °F	0.529	0.522	0.516	0.51
Q_u	Useful heat $Q_u = \dot{m}C_p\Delta T$	Btu/hr	641.2	658.7	642	442.6
I_t	Total solar flux	Btu/hr ft^2	289.1			
A_c	Collection (aperture) area	ft^2	5.87	7	6.94	2.045
Q_{in}	Total solar input $Q_{in} = I_tA$	Btu/hr	1697	2023.7	2009.3	589.8
η	Overall collection efficiency based on total solar flux and aperture area	$\eta = \frac{Q_u}{Q_{in}}$	0.378	0.325	0.320	0.75
T_a	Ambient temperature	F	88.1			
ΔT_i	Excess temperature $\Delta T_i = T_i - T_a$	F	154.7	134	116.5	105.4
–	Reflector type	–	Glass	Alzak	TEP Teflon	None
*Test conducted at 11:50 am (PST) on July 6, 1977						

Table 5-4. Theoretical Calculation of the Useful Heat and the Overall Collection Efficiency and Comparison with Tests

PARAMETER		July 6, 1977, 11:50 Tube No.			
		1	2	3	4
v	Wind velocity, mph	3.6			
T_p	Absorber plate temperature, °F $T_p \cong T_m$	252	232	214	200
C_c	Manifold heat losses coefficient	1.03	1.03	1.025	1.025
U_L	Overall heat transfer coefficient (calculated), Btu/hr ft^2	0.37	0.36	0.33	0.29
$(\tau\alpha)_e$	Total effective transmittance	0.855			
CR	Concentration ratio*	1.6	1.6	1.6	1
A_p	Absorber plate surface, ft^2	2.045	2.045	2.045	2.045
F_R	Heat removal factor	0.95	0.95	0.95	0.96
Q_u	Useful heat, Btu/hr	657	657	678	425
η	Efficiency	0.39	0.33	0.34	0.72
η	(Test data from Table 5-3)	0.378	0.325	0.320	0.75

*The concentration ratio given is a derived figure which accounts for the surface distortions, micro and macro irregularities of the reflector surface, and dust and dirt effects on the mirrors and glass tube.

where T, C_p, and d are given in F, BTU/lbF, and lb/gal, respectively.

Table 5-5 gives test results for July 8, 1977, during which time the operating temperature was up to 166°C (332°F). Results of various tests run during July 1977 are summarized in Figure 5-1. Measured efficiencies of the bare tube receiver and receivers with various reflectors are plotted against $\Delta T_i = (T_{in} - T_{amb})$.

Daily total incident fluxes and useful heats collected by each tube are tabulated in Table 5-6 for selected days during the summer of 1977. Operating temperatures varied throughout the day, as will be seen in Table 5-6. Although the heater was set to a fixed temperature, additional solar heating resulted in temperatures above the set point.

Due to variation of temperature, daily average efficiencies presented in Table 5-6 do not exactly match with the predictions given in Appendix D. The results are, however, within reasonable limits. Unless a precise fluid inlet temperature control loop is installed, such deviations are expected.

Table 5-5. Vee-Trough/Vacuum Tube Collector Typical Test Data

PARAMETER	UNIT	July 8, 1977, 11:50 PDST			
		Tube*No.			
		1	2	3	4
Fluid inlet temperature T_i	°C	166.5	161.5	155.5	154
Total pressure drop (4 tubes in series) (P)	kp/cm^2	0.21			
Average mass flow rate $\dot{m}$	kg/hr	22.53			
Specific heat C_p	KJ/kg C	2.319	2.307	2.294	2.282
Fluid temperature rise ΔT	°C	11.53	11.62	11.72	5.22
Useful heat $Q_u = \dot{m}C_p\Delta T$	KJ/hr Btu/hr	602 (571)	604 (572)	606 (574)	268 (254)
Solar flux					
Pyranometer: Total flux I_t	W/m^2	908			
Pyroheliometer: Beam flux I_b	W/m^2	808			
Collection Aperture Area A	m^2	0.545	0.65	0.645	0.19
Concentration ratio (aperature/bottom area)		2.87	3.0	3.0	1.0
Total solar input: $Q_{in} = I_t A$	KJ/hr Btu/hr	1781 (1690)	2125 (2014)	2108 (1998)	621 (598)
Overall collection efficiency based on total solar flux and aperture area	-	0.34	0.285	0.29	0.43
Ambient temperature T_a	°C	29.7			
$\Delta T_i = T_{in} - T_a$	°C	136.8	131.8	125.8	124
Reflector type	-	Glass	Al-zak	FEP Teflon	None

* Tube 1: glass mirrors; Tube 2: Alzak mirrors;
Tube 3: FEP Teflon - aluminized; Tube 4: no mirrors;
Working fluid: Therminol 44

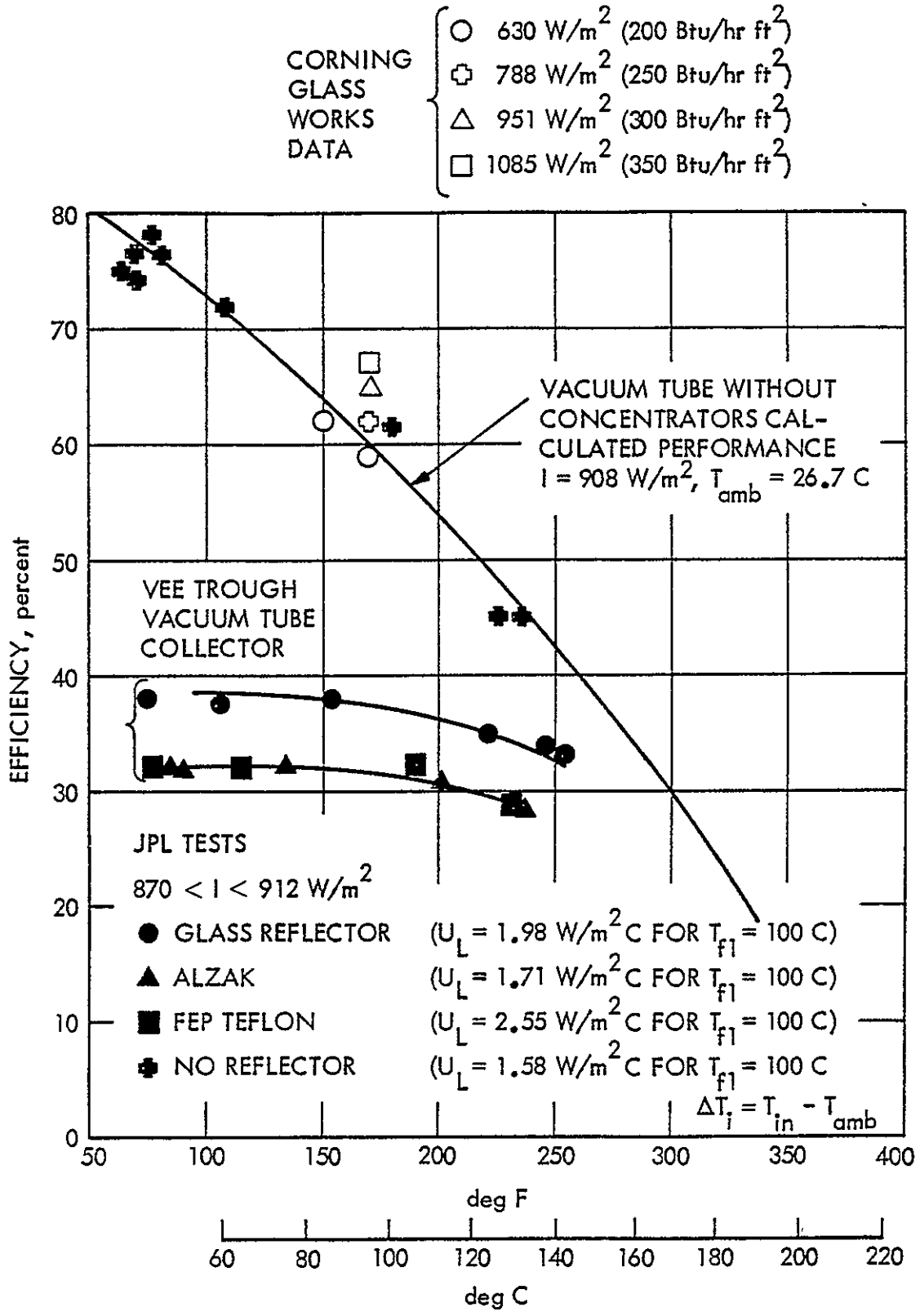

Figure 5-1. Test Data for Collector Efficiency Versus Temperature

Table 5-6. Daily Total Incident Fluxes and Useful Heats Collected

Date, 1977	Temperature range, °F	Q_u, Btu/day	Q_{in}, Btu/day	η_{daily}, %	Tube No.
June 1 Day 152	280 - 350	2579	7518	34	1
		2522	8967	28	2
		2276	8913	26	3
		803	2611	31	4
June 16 Day 167	275 - 335	2973	10485	28	1
		3197	12503	26	2
		2979	12438	24	3
		1843	3644	51	4
July 5 Day 186	80 - 240	3224	9620	34	1
		3206	11320	28	2
		3106	11250	28	3
		2429	3300	74	4
July 6 Day 187	165 - 265	3353	9777	34	1
		3445	11658	30	2
		3355	11575	29	3
		2384	3397	70	4
July 8 Day 189	250 - 365	3129	10599	30	1
		3187	12642	25	2
		3006	12553	24	3
		1310	3683	36	4
Aug. 10 Day 222	210 - 260	3572	10641	34	1
		1797	3698	49	4

SECTION VI

OPTIMIZATION STUDIES

Optimization of design and operation parameters is essential for obtaining the most economical performance of the vee-trough/vacuum tube collector. The ultimate purpose of the optimization study is to identify the combination of parameters yielding the lowest energy cost. This section discusses the optimization approach and results.

The optimization studies were performed in two steps:

1) Optimization of the vee-trough design for maximum thermal energy collection.

2) Search for the lowest cost collector.

6.1 OPTIMIZATION OF THE VEE-TROUGH DESIGN FOR MAXIMUM THERMAL ENERGY COLLECTION

The concentrated solar flux intensity must be maximized for the best vee-trough performance for year-round operation. The evacuated tube receiver efficiency also has to be as high as possible at the operation temperature for the best performance of the combination of vee-trough reflector and receiver.

Factors influencing the vee-trough and evacuated receiver performance are:

1) Flap angles: Aperture angle.

2) Flap length: Aperture size.

3) Physical properties of the vee-trough reflectors:
   Reflectivity of the surface mirror surface.

4) Design and material properties of the evacuated receiver:
   Transmissivity of the glass envelope.
   Absorptivity of the selective absorber surface.
   Emissivity of the absorber surface.

5) Collector plane tilt (in case it may be other than the latitude).

Although other factors such as the flow rate and properties of the working fluid (density, viscosity, coefficient of heat transfer, flow velocity) are important, they are not as important as the design factors listed above.

One purpose of this project is to optimize the design of the vee-trough/vacuum tube receiver combination. Optimization of the complete system incorporating the vee-trough/vacuum tube collector, a thermal storage unit, and a load is beyond the scope of this project.

6.1.1 Optimization of the Flap Angle

First the flap angles θ_1 and θ_2 must be optimized. If the aperture angle η and/or flap angle θ_1 and θ_2 are varied, the daily average concentration ratio is affected as shown in Figure 6-1. If the vee-trough were symmetrical, the concentration ratio would be at its maximum during the equinoxes. Figure 6-1 indicates that either good summer and good winter performance or good year-round performance can be obtained by choosing θ_1, θ_2 and η properly.

Flap angles θ_1 and θ_2 may be varied to obtain the combination which yields the maximum year-round averaged concentration ratio for the case in which there is a demand for both heating and cooling. In the case of only heating or only cooling, the optimum combination of θ_1 and θ_2 would be different.

In the search of the maximum yearly averaged concentration ratio, the computer programs labeled VTFR and VTCGE, which were previously described, were run or θ_1 ranging from 49° to 69°, for θ_2 ranging from 75° to 89° and for the aperature angle η ranging from 30° to 42°.

Figure 6-2 gives the results of these runs in which the concentration ratio is plotted against θ_1, η being a parameter. The flap widths are $W_1 = 10.93$ in. and $W_2 = 9.5$ in. and the mirror reflectivity is $\rho = 0.9$. Results given in Figure 6-2 suggest a set of $\theta_1 = 55^\circ$, $\theta_2 = 85^\circ$ and $\eta = 40^\circ$ for the best year-round concentration ratio. For that case, the optical concentration ratio (i.e., $A_{aperture}/A_{bottom}$) is 3. Although the concentration ratio improves slightly for $\eta < 40^\circ$, there are sharp peaks and valleys on the curves of concentration ratio as seen in Figure 6-1. Therefore, $\eta = 40^\circ$ was selected as the optimum aperture angle.

6.1.2 Optimization of the Flap Widths

The effect of the variation of the flap widths W_1 and W_2 on the concentration ratio is illustrated in Figure 6-3. Increasing the flap length for a fixed aperture angle η would increase the geometric concentration ratio almost linearly. The actual year-round concentration ratio increases at a much slower rate, as seen in Figure 6-3. A compromise has to be sought between the increased

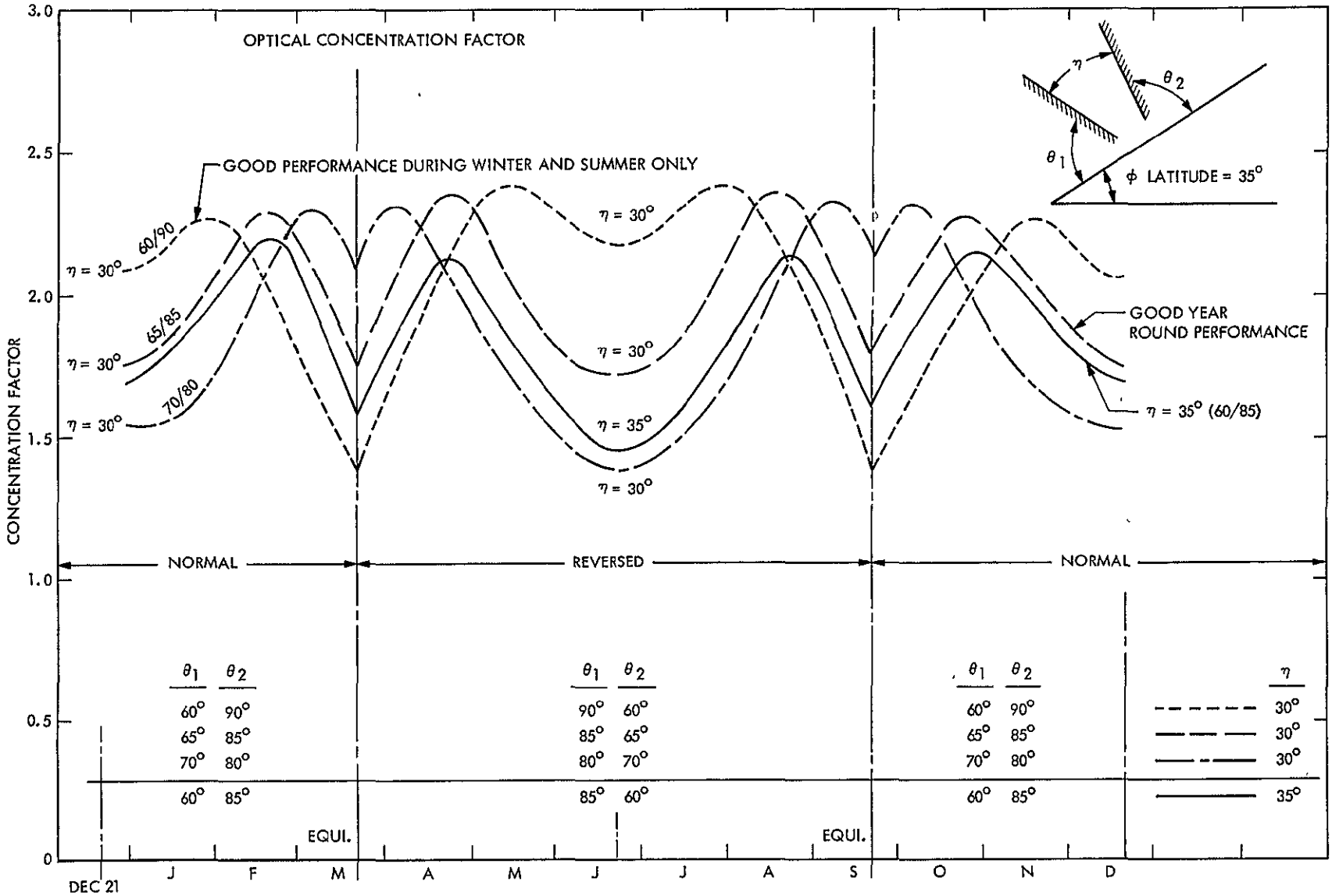

Figure 6-1. Variation of the Daily Averaged Concentration Ratio with Flap Side Tilt and Aperture Angles

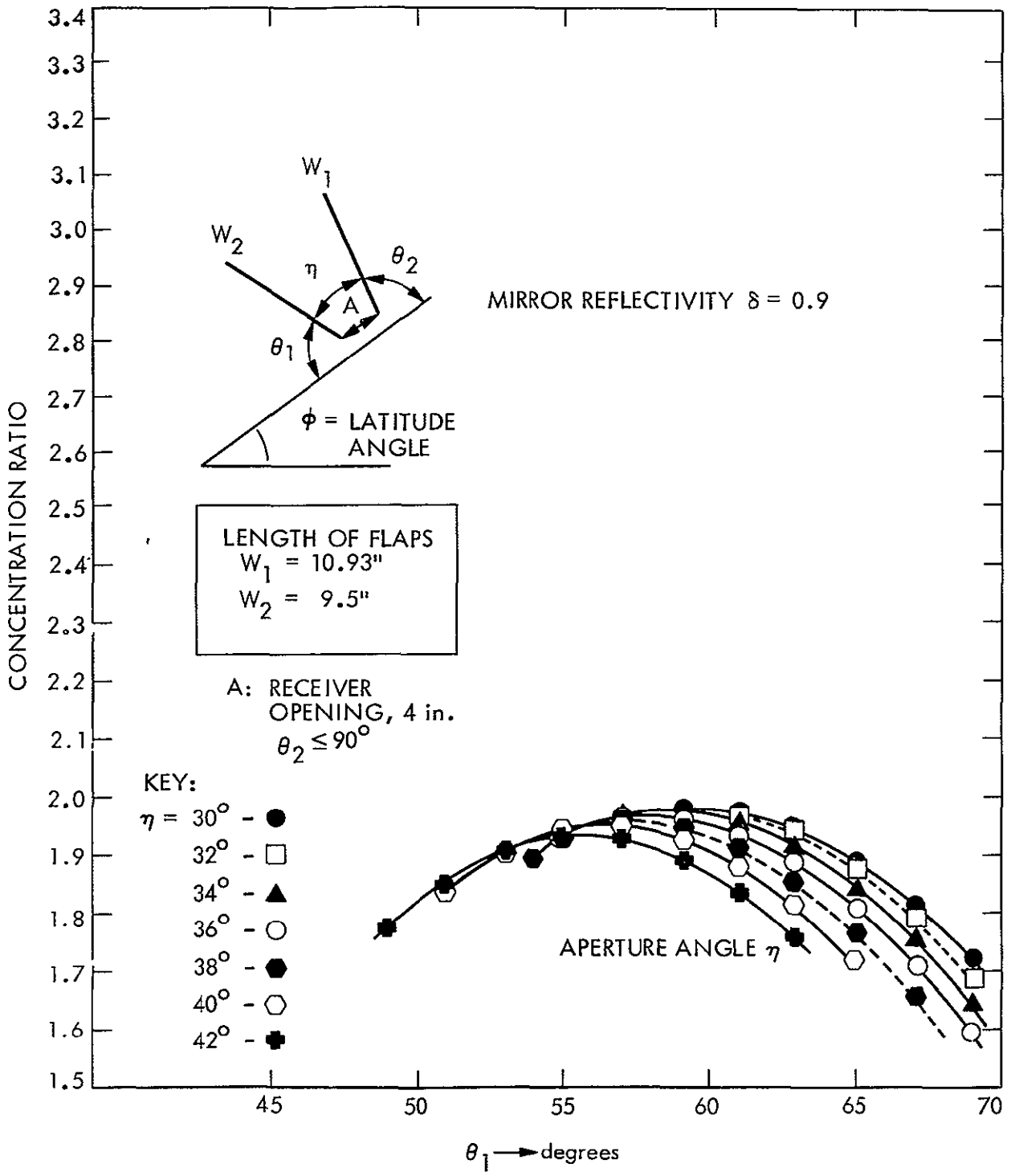

Figure 6-2. The Effect of Vee-Trough Aperture Angle Tilt on the Average Year-Round Concentration Ratio

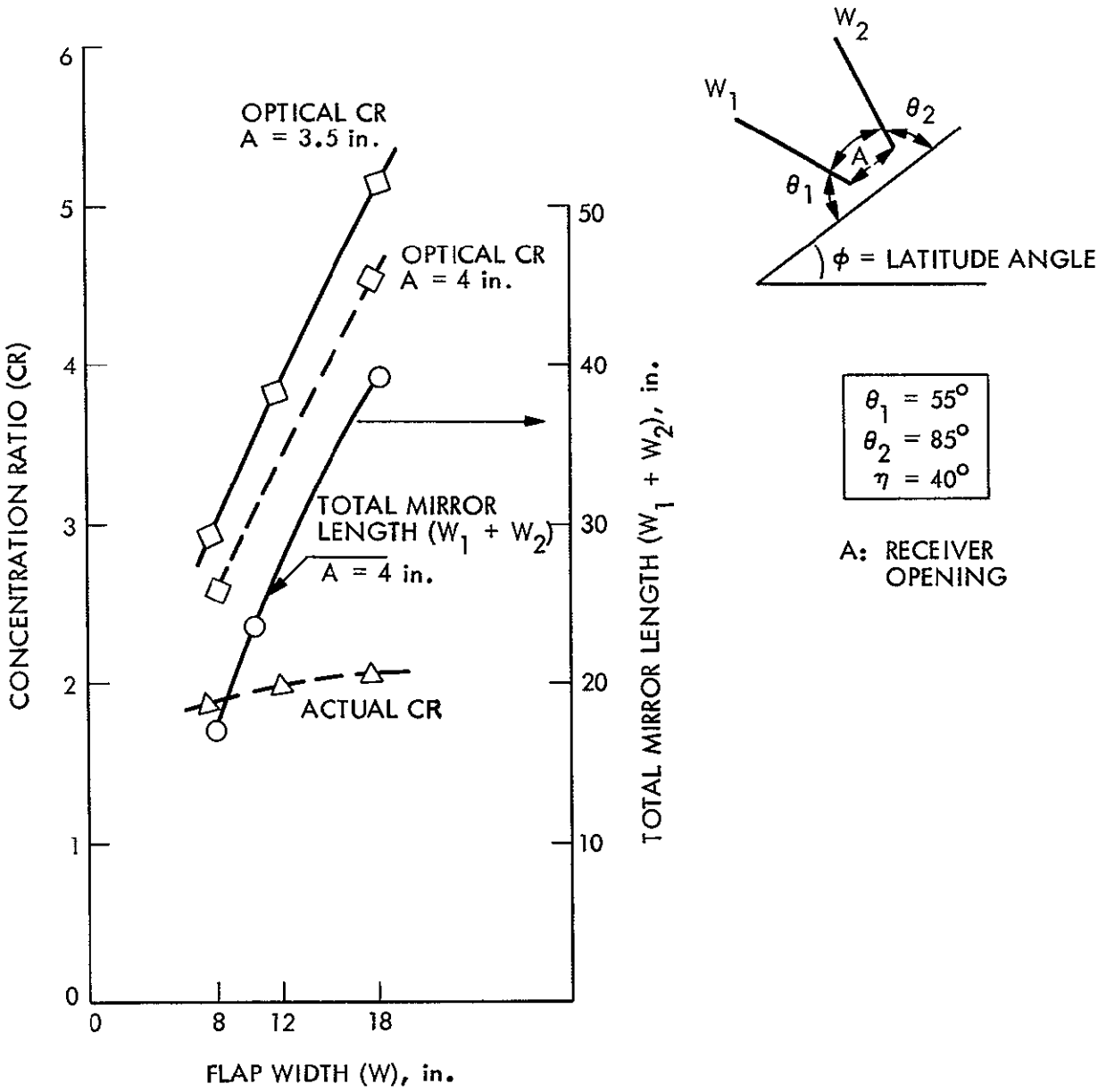

Figure 6-3. The Effect of Vee-Trough Width on the Concentration Ratio

mirror length and improvement of the actual concentration ratio. An optical concentration ratio increase beyond 3 is not usually justified, since the total mirror length almost doubles for an actual concentration ratio change of 5%.

6.1.3 Reflectivity Optimization

The reflectivity of the mirror surfaces has a significant effect on the concentration ratio as seen in Figure 6-4. The concentration ratio on the absorber plate, after transmission losses through the glass envelope have been taken into account, is less sensitive to the variation of the surface reflectivity. Ideally, the higher the reflectivity, the better the concentration ratio. A low value of $\rho = 0.8$ is attainable with an Alzak reflector, where a $\rho = 0.9$ requires glass mirrors. The choice of the reflecting surface must be made on a cost-effective basis rather than on the basis of the highest concentration ratio.

6.1.4 Design and Material Properties of the Evacuated Tube Receiver

Performance of the evacuated tube receiver can be improved by:

1) Improving the transmissivity of the glass envelope. Since major losses are due to surface reflection, new techniques of anti-reflection coatings are recommended. Transmissivity can thus be increased up to 98 percent.

2) Improving the absorptivity of the selective coating. Presently available black chrome coatings are known to be the best among the inexpensive processes. An absorptivity value improvement to 94.4% is expected.

3) Improving the emissivity of the absorber surface. The present value for the emissivity ϵ is around 0.09. Refinements to lower the emissivity ϵ to about 0.066 are expected.

All of these improvements will increase the receiver performance and make it closer to its theoretical limits. Economic constraints, however, limit the use of expensive materials and processes.

6.1.5 Optimization of the Collector Plane Tilt

Results of tests run on the test bed and earlier curves of the concentration ratio apply to a collector tilted to the latitude. If ϕ, the collector plane tilt, is changed, then the daily average concentration ratio throughout a year is affected, as seen in Figure 6-5. As expected, if the tilt is more than the

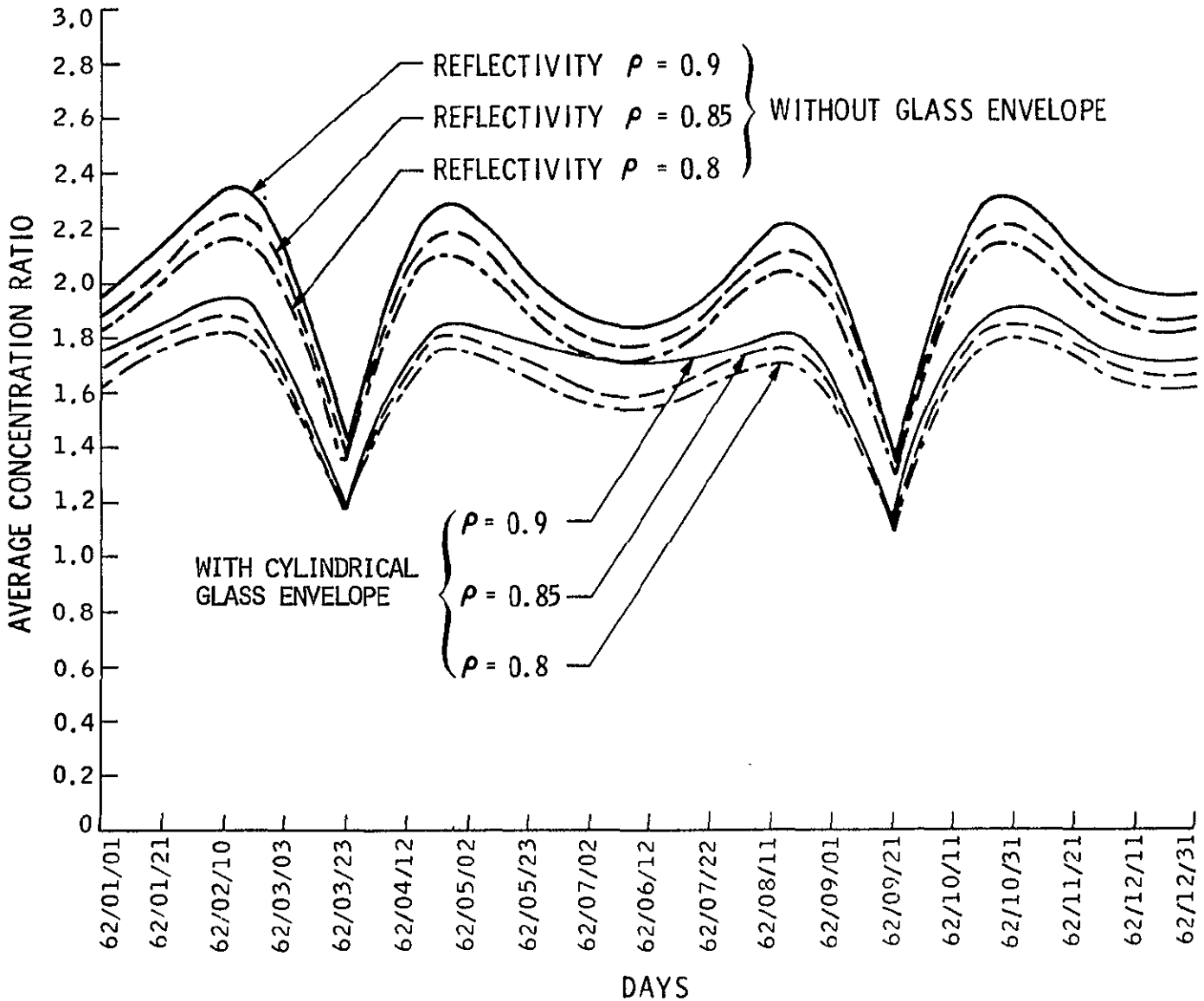

Figure 6-4. The Effect of Reflectivity on the Daily Average Concentration Ratio

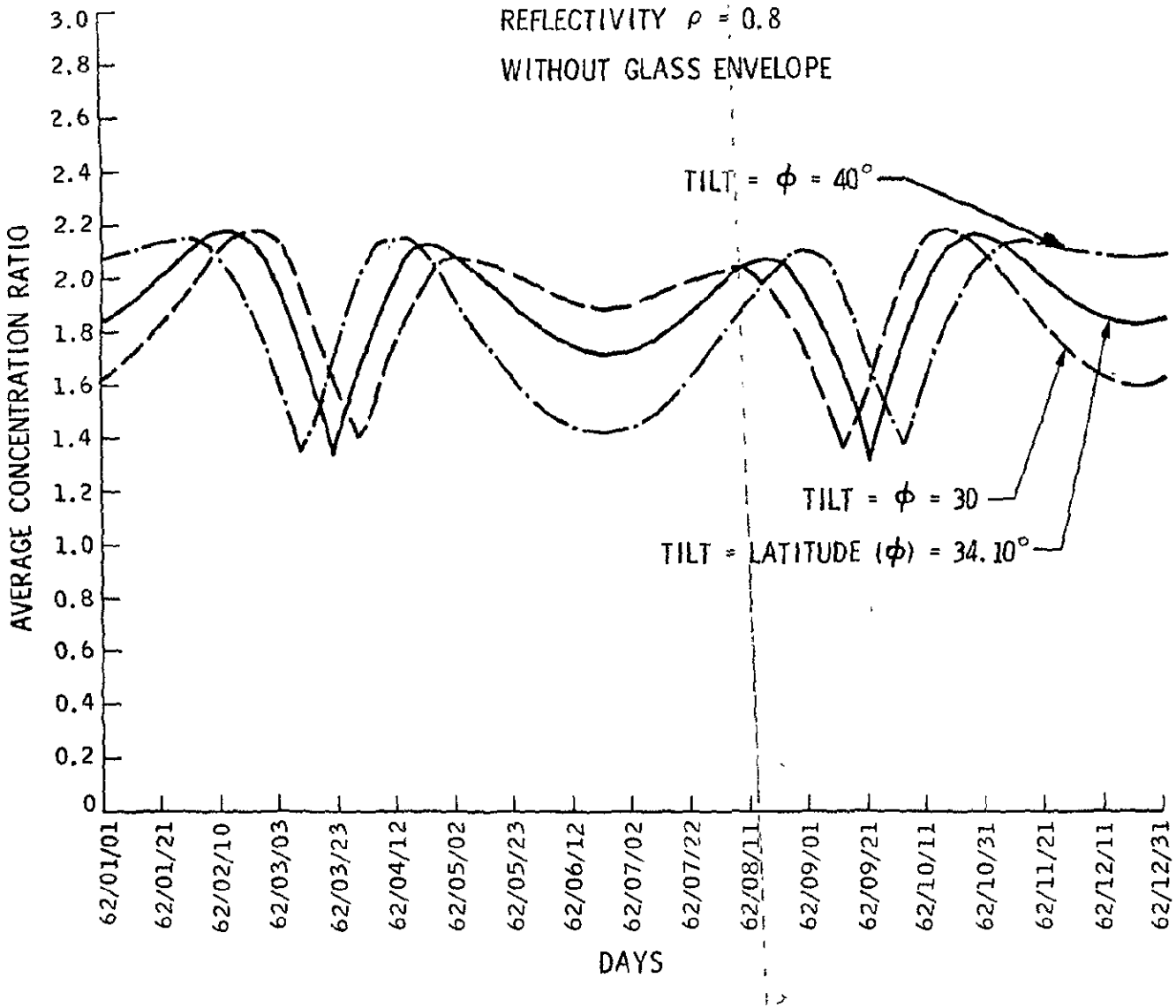

Figure 6-5. The Effect of the Collector Plane Tilt ϕ on the Daily Average Concentration Ratio

latitude, for example 40^{o}, then the winter performance is better than the performance of a vee-trough tilted to the latitude (34.10^{o} in this example). Similarly if the tilt is less than the latitude, for example 30^{o}, then the summer performance is better than the performance of the collector tilted to the latitude, 34.10^{o}. This feature of the vee-trough would be very useful for those applications requiring winter heating or summer cooling only. In such instances the collector tilt may be about ϕ -(10 to 15^{o}) for summer operation and ϕ +(10 to 15^{o}) for winter operation, respectively. Its exact value must be determined by a simulation model which would consider the climatic variables, load and storage relations for the system studies.

6.2 OPTIMIZATION OF THE USEFUL HEAT COLLECTION

The thermal output (net heat collection) of the vee-trough/vacuum tube collector, based on year-round operation, can be maximized employing the thermal performance model described in Section II. The vee-trough configuration yielding the highest daily and year-round concentration ratio also yields the maximum useful heat. Since the thermal output (net useful heat) is dependent upon the operation temperature, various sets of operating conditions and vee-trough configurations were tested using the thermal model of the vee-trough/evacuated tube collector. Hour-by-hour radiation and ambient temperature data for Burbank, California, during 1962 was utilized. Computer-plotted curves of useful heat and efficiencies are presented in Appendix D. Two sample curves plotted by the computer are presented in Figure 6-6. These curves give day-long average efficiencies at operation temperatures of 150 and 350^{o}F for one year. Yearly averages are also summarized for two design conditions. One of the sets (ρ = 0.8, etc.) describes the performance of the vee-trough collector as designed and tested at JPL. The latter (ρ = 0.94 employing silvered Teflon reflectors, etc.) gives the output of an advanced idealized collector which we believe can be designed soon. Additional curves of incident flux, concentration ratio and useful heat are presented in Appendix D. Table 6-1 gives the summary of the year-round predicted performance data for a vee-trough/vacuum tube collector operating at temperatures of 150, 250, 350 and 450^{o}F. The first set is for the presently available collector. The latter is for the advanced collector.

6.3 OPTIMIZATION OF THE VEE-TROUGH COLLECTOR FOR THE LOWEST ENERGY COST

As previously mentioned, the lowest energy cost requires maximization of the thermal output and minimization of the collector cost to obtain the lowest energy cost. It usually turns out that neither maximum heat collection nor the

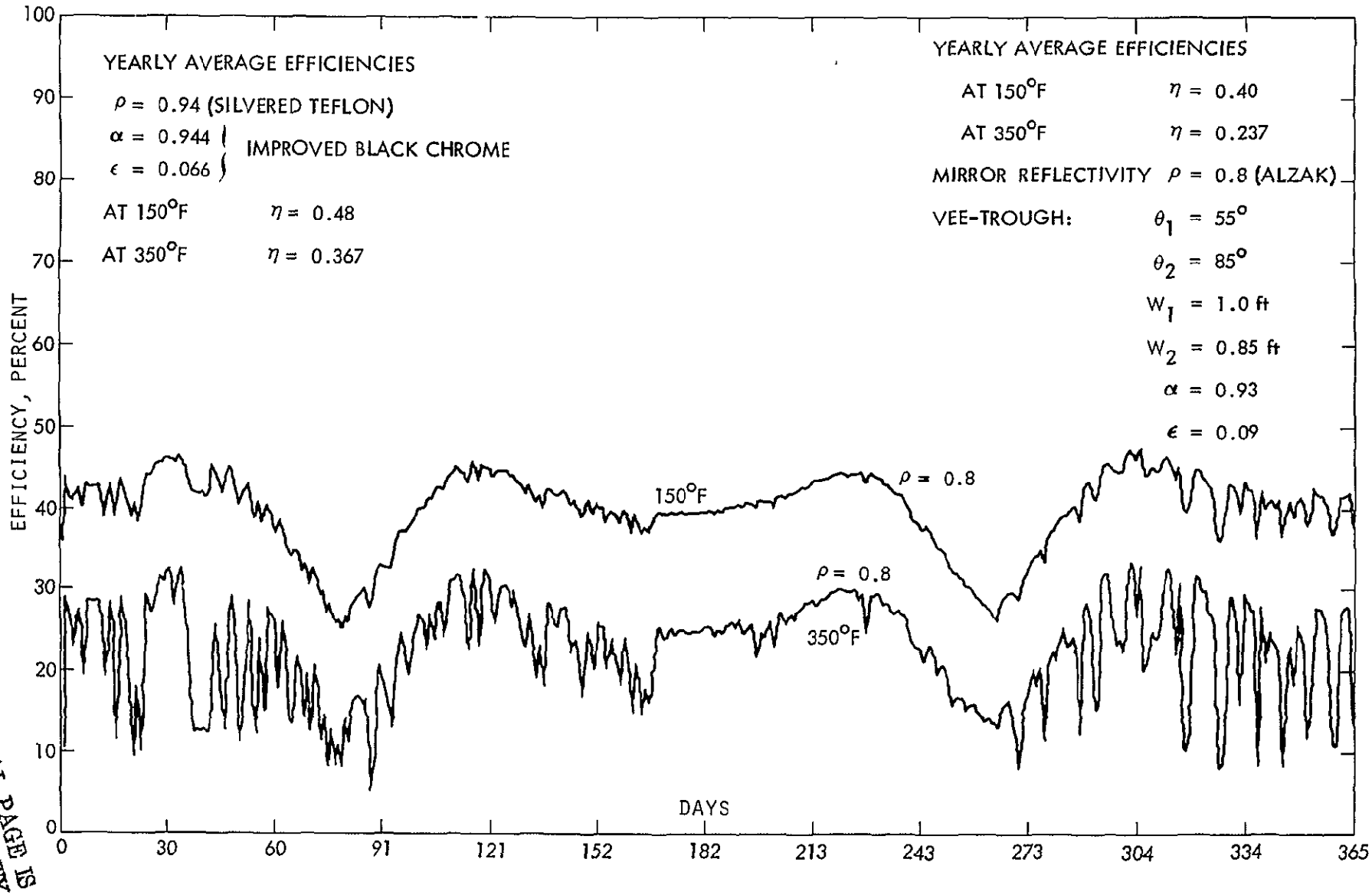

Figure 6-6. Variation of Daily Average Efficiencies at Operation Temperatures of 150°F and 350°F

Table 6-1. Summary of the Computed Year-Round Performance Predictions

Operation Temperature, °C	Total Useful Heat, Btu/tube-year	Overall Efficiency, η
Collector as Tested $\delta = 0.8, \epsilon_p = 0.9, \epsilon_b = 0.12, \tau = 0.9, \alpha = 0.93$		
150	1,677,000	0.398
250	1,387,000	0.329
350	1,000,000	0.237
450	547,000	0.13
Advanced Collector $\delta = 0.94, \epsilon_p = 0\ 0665, \epsilon_b = 0.0665, \tau = 0.98, \alpha = 0.944$		
150	2,027,000	0.481
350	1,832,088	0.434
250	1,549,300	0.367
450	1,183,800	0.281

NOTE $Q_{incident} = 4,217,000$ Btu/tube-year; $\theta_1 = 55^\circ$, $\theta_2 = 85^\circ$

lowest collector cost figures are the answers to the cost-effective design. Therefore a compromise is usually sought.

The yearly total heat collected and overall collector efficiencies tabulated in Table 6-1 are predictions. There is little uncertainty in these performance predictions, whereas cost estimates are much more uncertain.

Since evacuated tube manufacturers were reluctant to supply a reliable cost estimate, an attempt was made to predict the cost of the evacuated tube and vee-trough reflectors. These costs are only approximate since they are our own estimates based on the cost of available base materials. Details of the evacuated tube receiver and collector module cost are given in Appendix E. Cost estimates are summarized in Table 6-2 for glass tube diameters ranging from 2 to 7 in. and two sets of reflector costs ($0.5/ft^2 and $1.0/ft^2 of the reflector surface area). The module suggested measures approximately 6 x 17 ft for small tubes, or 7 x 17 ft for 7-in. diameter tubes. From the data in Table 6-2, the optimum (minimum cost) appears to correspond to 5 - 6 in. Present tubes are 4 in. in diameter. Unless a smaller diameter is preferred due to factors such as ease of fabrication, handling, etc., it would appear that a 6-in. diameter tube would be better than a 4-in. tube based on the tube cost data available to us.

Instead of reaching conclusions by using cost data we have estimated, a parametric study of the energy cost has been made. The energy cost has been predicted for a set of receiver tube and reflector costs and is presented in Table 6-3. Results are also presented in graphical form in Figure 6-7 for easy visualization. Present cost estimates yield energy costs of about $5.2/GJ ($5.5/MBtu) and $5.97/GJ ($6.3/MBtu) at 65 and 121^{o}C, respectively.

Figure 6-2. Summary of the Evacuated Tube Receiver and Collector Module Cost Estimates

CATEGORY	Tube Diameter, in.					
	2	3	4	5	6	7
	Aperture Area, ft^2					
	84	84	84	87.5	84	98
	Module Size, ft					
Width x Length of Module	6 x 17	6 x 17	6 x 17	6.25 x 17	6 x 17	7 x 17
Tube and frame cost, $	1279	950	855	770	693	846
Vee-trough @ 1.0 $ ft^2, $	231	201	190	195	189	234
Total module cost, $	1510	1151	1046	965	882	1080
Absorber area, ft^2	21.0	23.3	24.5	26.2	25.6	30.3
Collector cost per unit area (absorb), $/$ft^2$	71.9	49.4	42.7	36.8	34.4	35.6
Collector cost per unit area (aperture), $/$ft^2$	18.0	13.7	12.45	11.02	10.5	11.02
Vee-trough @ 0.5 $/$ft^2$						
Tube & frame, $	1279	950	855	770	693	846
Vee-trough, $	189.5	157.4	142	140	131.5	156
Total module cost, $	1468.5	1107.5	997	910	824.5	1002
Collector cost per unit area (absorb), $/$ft^2$	69.2	47.5	40.7	34.7	32.2	33.1
$/$m^2$					346	
Collector cost per unit area (aperture), $/$ft^2$	17.5	13.2	11.7	10.4	9.81	10.2
Collector cost per unit area (aperture), $/$m^2$	188.3	142	125.9	111.9	105.6	109.8

Table 6-3. Energy Cost Estimates

Cost Characteristic	Units	Operation Temperature, °C/(°F)		
		65 (150)	121 (250)	177 (350)
$Q_{incident}$	KJ/m^2 yr Btu/ft^2 yr	8.17×10^6 (720,000)		
Overall collector Efficiency $\rho = 0.8$		0.40	0.34	0.26
$\rho = 0.94$		0.48	0.43	0.37
(Suggested) $\rho = 0.9$		0.46	0.40	0.345
Net yearly energy collection (Q_t)	KJ/m^2 yr Btu/ft^2 yr	3.75×10^6 331200	3.26×10^6 288000	2.81×10^6 248400
Energy cost From Ref. 14: $C = 0.196\, C_c/Q_t$ (C_c*) Collector cost $\$/m^2$				
Tube cost at 100 $\$/m^2$ Reflector cost at 10 $\$/m^2$ C_c =	$\$/m^2$	70.0		
C = Energy cost	\$/GJ	3.65	4.20	4.88
	(\$/MBtu)	3.84	4.42	5.14
Tube cost at 100 $\$/m^2$ Reflector cost at 5 $\$/m^2$ C_c =	$\$/m^2$	60.0		
C = Energy cost	\$/GJ	3.13	3.60	4.18
	(\$/MBtu)	3.30	3.79	4.41
Tube cost at 150 $\$/m^2$ Reflector cost at 10 $\$/m^2$ C_c =	$\$/m^2$	85		
C = Energy cost	\$/GJ	4.44	5.11	5.92
	(\$/MBtu)	4.68	5.39	6.24
Tube cost at 150 $\$/m^2$ Reflector cost at 5 $\$/m^2$ C_c =	$\$/m^2$	75		
C = Energy cost	\$/GJ	3.92	4.50	5.23
	(\$/MBtu)	4.13	4.74	5.52
Tube cost at 250 $\$/m^2$ Reflector cost at 10 $\$/m^2$ C_c =	$\$/m^2$	115.0		
C = Energy cost	\$/GJ	6.01	6.91	8.02
	(\$/MBtu)	6.32	7.29	8.46
Tube cost at 250 $\$/m^2$ Reflector cost at 15 $\$/m^2$ C_c =	$\$/m^2$	105.0		
C = Energy cost	\$/GJ	5.49	6.31	7.32
	(\$/MBtu)	5.79	6.65	7 72

*Collector cost (C_c) is calculated from:

$C_c = C_{tube} \times A_{tube} + C_{reflec} \times A_{ref}$ + frame and assembly

$A_{tube} = 0.3\ m^2/m^2$ aperture

$A_{ref} = 2.0\ m^2/m^2$ aperture, frame + assembly = 20 $\$/m^2$

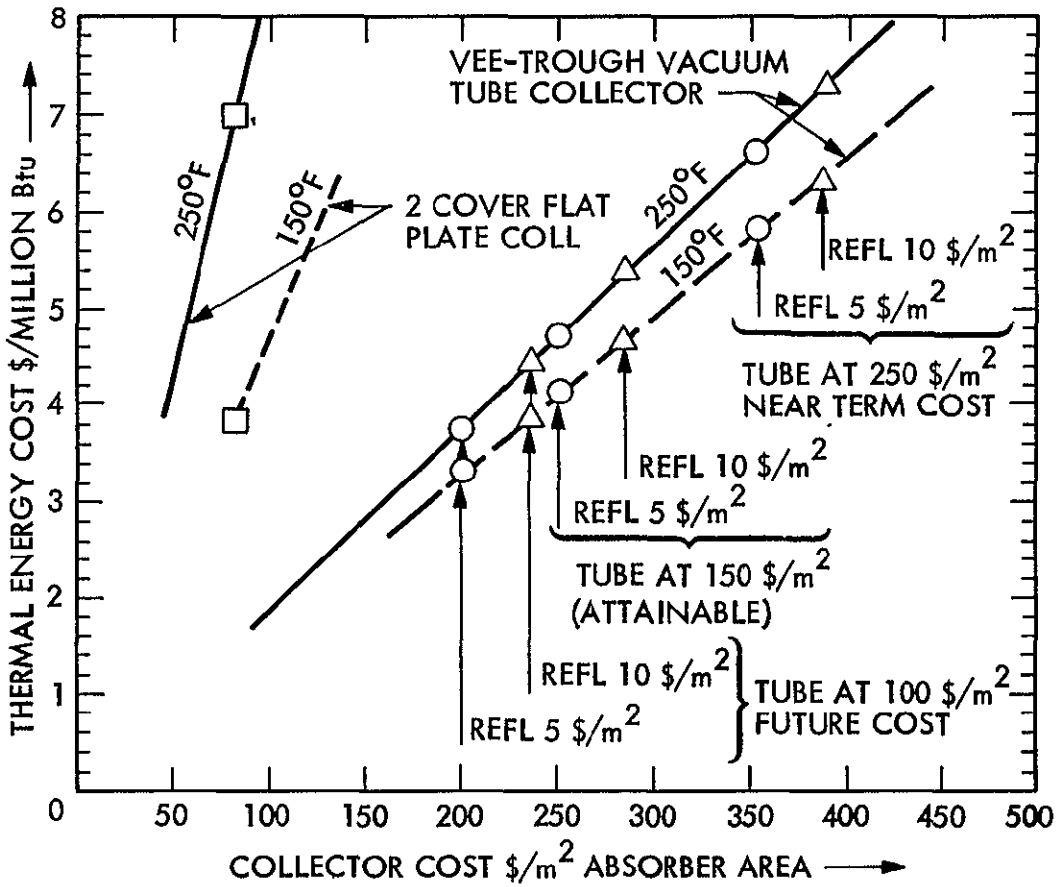

Figure 6-7. Thermal Energy Cost Versus Collector Cost Based on the Absorber Area

SECTION VII

CONCLUSIONS AND RECOMMENDATIONS

7.1 CONCLUSIONS

This report outlines the mathematical analysis and early test data of the vee-trough/vacuum tube collector proposed for use in solar heating and cooling applications. Owing to its high-temperature capabilities (300-400^{o}F), the proposed scheme could also be used for power generation purposes in combination with an organic Rankine conversion system. It is especially recommended for those unattended pumping stations since the reflectors only require reversal once every six months.

Mathematical models of both the vee-trough concentrator and vacuum tube receiver have enabled the prediction of both the concentrated flux intensity and net useful heat at any time and for any configuration. Production runs based on Burbank, California, weather data have yielded an optimum design as described previously. Optimal design of the vee-trough/vacuum tube collector for localities at different latitudes and having different weather patterns might be different from those given in this report. The methodology developed during this project, however, enables the determination of the optimum collector dimensions and enables the prediction of the yearly useful heat collection.

Test results reported represent the performance of the vee-trough/vacuum tube collector combination based on the aperture area. The data are defined for the total incident flux on the collector plane tilted 35^{o} to the south. All instruments used for the measurement of temperature, flow rate and solar radiation were calibrated. Differential thermocouples were accurate to $\pm$0.08^{o}C ($\pm$0.14^{o}F) whereas absolute temperatures were measured within 0.1^{o}C. Errors due to the measurement of millivolt output on the IDAC terminal were less than 0.02^{o}C for the differential and 0.1^{o}C for the absolute temperature measurements. The combination of these two errors still yielded $\pm$0.1^{o}C for the differential temperatures and $\pm$0.4^{o}C for the absolute temperature measurements. Volumetric flow of the working fluid, Therminol 44, was measured within $\pm$3%. The effect of the viscosity on the calibration factor for the flow meters was found to be negligible for the range of operation 65 to 205^{o}C. Total solar radiation measurements were made using a spectran precision pyranometer ($\pm$1%). Combination accuracy of measurements is within $\pm$6%.

Efficiencies shown in Figure 5-1 and those tabulated in Tables 5-4 and 5-5 are the values obtained from the test bed without any corrections due to differences in U_L values of tubes. As will be noted, U_L varies from 1.58 W/m^{2o}C

to 2.55 $W/m^{2o}C$ at $100^{o}C$ for the tubes tested. A fair comparison of reflector surfaces requires using vacuum tubes having the same U_L values. Since such tubes were not available, actual tests could not be run. However, it is obvious from the test data that the aluminized FEP Teflon reflector output would have been improved if U_L were 1.71 instead of 2.55 $W/m^{2o}C$ at $100^{o}C$ over Alzak reflectors. Similarly, the tube with a glass reflector would yield a higher efficiency if U_L were 1.71 instead of 1.98 $W/m^{2o}C$ at $100^{o}C$.

Results of the thermal performance analysis given in Figure 3-4 were based on a mathematical model without reflector end effects and without losses due to copper tube axial conduction and supporting clip conduction. Year-round performance prediction averages the effect of overcast and low solar intensity periods for an 8-hour duration and applied to Burbank, California, for one particular year. The trend of the efficiency curves would, however, be unchanged for different localities and years.

Therefore, efficiencies given in Figures 3-4 and 5-1 and Table 5-5 are higher than the year-round predictions. The difference, however, is not large. Table 5-5 gives $\eta = 0.285$ for Alzak at $166^{o}C$ ($322^{o}F$) whereas the averaged collector efficiency at $177^{o}C$ ($350^{o}F$) is 0.237 as given in Figure 6-6. Interpolation to $\pm 161^{o}C$ gives $\eta = 0.26$. The difference is only 2.5 percentage points. Tests revealed that the pressure drop and power requirements were not serious matters. The test bed was designed to compare various reflector surfaces, and the piping was arranged for both parallel and series operation. Flow meters, valves, bends or Y's in the loop, which would not be needed in a normal operation, add more resistance to flow; therefore pressure drop is increased. The pressure drop was on the order of 0.2 kg_f/cm^2 (3 psi) for 4 tubes in series. The suggested module design may use at most 6 tubes in series for 4 inch tubes or 4 tubes in series for 6 inch tubes. In both cases, the pressure drop is within reasonable limits and the pumping power is small.

Energy cost predictions are given in terms of the collector cost based on the unit absorber area. Such a presentation enables one to visualize the effect of component costs. Since there are no firm cost figures available for the evacuated tube receiver, a definite energy cost cannot be quoted. A cost estimate was, however, presented using suggested net prices for off-the-shelf pyrex tube to give an idea about the near future costs. When these tubes are mass produced, the evacuated receiver will most probably be fabricated at the site where the tubes are drawn. Thus, the glass tube cost, which includes packaging, transportation and profit, will be reduced.

Long-range mass production costs could be as low as $\$150/m^2$ for the evacuated tube receiver and $\$5/m^2$ for the reflector. These figures were obtained

from conversations with industry personnel. Although not firm, it is believed that these costs are attainable.

The vee-trough/vacuum tube collector competes with conventional flat plate collectors costing $\$80/m^2$ and operating at 121°C. The predicted vee-trough collector cost with $\$150/m^2$ tubes and $\$5/m^2$ reflectors yields thermal energy costs 2/3 that of a flat plate collector costing $\$80/m^2$. At 65°C, the vee-trough collector has to be assembled with tubes which cost less than $\$150/m^2$ and reflectors costing less than $\$5/m^2$ in order to be competitive. Noting that flat plate collectors even today, after considerable marketing and developmental effort, cost more than $\$100/m^2$, it can be said that the vee-trough has some potential even at temperatures lower than 121°C. At 121°C and higher, the advantages of the vee-trough collector are obvious.

The merit of the collector concept is in combining the relatively expensive vacuum tube with an inexpensive concentrator, which enhances the tube performance by increasing the incident flux and reducing its cost due to the low cost feature of the vee-trough concentrator. The present report is considered a confirmation of the magnitude of the efficiency of the proposed collector based on test data obtained during the short test season. Further tests and analysis, especially simulations of systems with storage and variable load features, are needed.

In conclusion, it can be said that the first phase of the vee-trough program has fulfilled its objective, which was to demonstrate the performance improvement possible by combining vee-trough reflectors with vacuum tube receivers. Such nontracking solar collectors can produce useful heat within a temperature range of 100 to 200°C. The cost reduction potential of this concept was also demonstrated. Clearly the cost figures presented, like any other preliminary cost estimate of an item not yet mass-produced, are not as firm as the thermal performance data, which are based both on complete mathematical models of the collector and extensive test bed data.

7.2 RECOMMENDATIONS FOR FUTURE WORK

Since the first phase of the project was to analyze, design, construct and test the vee-trough collector within a limited time, test data could be acquired only during the late spring and summer of 1977. Additional testing is essential to verify the theoretical year-round performance predictions given in this report. Therefore, it is recommended that tests be run during fall and winter of 1977 and spring of 1978 to complete a one year cycle.

Other suggested studies and experiments include:

1) Development of a full-sized module based on the experience gained and results of the optimization studies.
2) Investigations using other options of evacuated tube receivers such as the one employing heat pipe receivers and thermos-bottle-type double-wall evacuated tubes which do not employ glass to metal seals.
3) Experiments with systems which use the vee-trough/vacuum tube collector in an absorption or Rankine air conditioning system.
4) System simulation studies to investigate the performance characteristics of the vee-trough collector using an actual system with thermal capacity, variable load and variable operation temperatures.

SECTION VIII

REFERENCES

1. M. K. Selçuk, "A Fixed Collector Employing Reversible Vee-Trough Concentrator and a Vacuum Tube for High Temperature Solar Energy Systems," Proceedings from the 11th Intersociety Energy Conversion Engineering Conference, 1976, State Line, Nev., Paper No. 769222.
2. H. Tabor, "Mirror Boosters for Solar Collectors," Journal of Solar Energy, Vol. 10, No. 3, pp. 111-118, 1966.
3. "Corning Tubular Collector," Corning Glass Works, Corning, N. Y., Jan. 23, 1975.
4. D. C. Beekley and G. R. Mather, Jr., "Analysis and Experimental Tests of High Performance Tubular Solar Collectors," ISES International Conference, Paper No. 32/10, Los Angeles, Calif., 1975.
5. K. G. T. Hollands, "A Concentrator for Thin Film Solar Cells," Solar Energy, Vol. 13, page 149, 1971.
6. H. Durand, et al., "Periodically Adjustable Concentrators Adapted to Solar Cell Panels," COMPLES International Meeting, 1975, University of Petroleum and Minerals, Dhahran, Saudi Arabia.
7. R. B. Bannerot and J. R. Howell, "Moderately Concentrating Flat Plate Solar Collectors," ASME Paper No. 75 HT-54.
8. R. Winston and H. Hinterberger, "Principles of Cylindrical Concentrators for Solar Energy," Journal of Solar Energy, Vol. 17, No. 4, pp. 255-258, Sept. 1975.
9. K. G. T. Hollands, "Honeycomb Devices in Flat Plate Solar Collectors," Journal of Solar Energy, Vol. 9, No. 3, pp. 159-164, 1965.
10. H. A. Blum, et al., "Design and Feasibility of Flat Plate Solar Collectors to Operate at 100°-150°C," Proceedings UNESCO Conference, Sun in the Service of Mankind, Paris, July 1973, Paper No. E 118.
11. P. A. Kittle and S. L. Cope, "Outside Performance of Moderate Vacuum Solar Collectors," ISES Conference, Paper No. 32/8, Los Angeles, 1975.
12. E. Speyer, "Solar Energy Collection with Evacuted Tubes," Transactions ASME (Power), pp. 270-276, 1965.
13. F. F. Simon, "Solar Collector Performance Evaluation with the NASA Lewis Simulator - Results for an Overall Glass Evacuated Tubular Selectively Coated Collector with a Diffuse Reflector," NASA TM-X-71695, Lewis Research Center, Cleveland, Ohio, Apr. 1975.

14. U. Ortabaşı and W. Buehl, "Analysis and Performance of an Evacuated Tubular Collector," paper presented at ISES 1976 Conference at Los Angeles, Calif.
15. U. Ortabaşı, "Indoor Test Methods to Determine the Effect of Vacuum on the Performance of a Tubular Flat Plate Collector," ASME Paper No. 76-WA/SOL-24.
16. S. Karaki and D. M. Frick, "Performance of an Evacuated Tube Solar Collector," paper presented at ISES 1976 Conference, Winnipeg, Manitoba, Canada.
17. W. Schertz, Argonne National Laboratories, private communication.
18. A. Rabl, "Collectors with Cusplike Compound Parabolic Concentrator and Selective Absorber," Proceedings ISES 1976, Vol. 2, pp. 327-350.
19. G. Thodos, "Predicted Heat Transfer Performance of an Evacuated Glass-Jacketed CPC Receiver, Countercurrent Flow Design," Argonne National Laboratories, Report No. ANL-76-67, Argonne, Ill., 1976.
20. W. F. Moore, General Electric Company, Valley Forge Space Center, private communication, Jan. 5, 1977.
21. W. I. Jacobs, "Use of Flexible Reflective Surfaces for Solar Energy Concentration," Journal of Vac. Sci. Technol., Vol. 12, No. 1, Jan/Feb 1975.
22. J. A. Duffie and W. A. Beckman, Solar Energy Thermal Processes, Wiley Interscience, New York, N.Y., 1974.
23. S. I. Abdel Khalik, "Heat Removal Factor for a Flat Plate Solar Collector with a Serpentine Tube," Journal of Solar Energy, Vol. 18, No. 1, pp. 59-67, 1976.
24. B. Gupta, Honeywell, Inc., private communication, July 1977.

APPENDIX A

LIST OF PUBLICATIONS & PRESENTATIONS
RELATED TO THE VEE-TROUGH VACUUM TUBE
COLLECTOR

1. Selçuk, M. K., "A Fixed Collector Employing Reversible Vee-Trough Concentrator and a Vacuum Tube for High Temperature Solar Energy Systems," Proceedings 11th Intersociety Energy Conversion Engineering Conference, 1976, State Line, Nevada, Paper No. 769222.

2. Selçuk, M. K., "Fixed Flat Plate Collector with a Reversible Vee-Trough Concentrator," ASME Paper No. 76-WA/HT-12, New York, N. Y., December 1976.

3. Selçuk, M. K., "A Vacuum Tube Vee-Trough Collector For Solar Heating and Air Conditioning Applications," ERDA, U. of Miami Forum on Solar Heating & Cooling Miami Beach, Fl., December 1976.

4. Selçuk, M. K., "Experimental Evaluation of a Fixed Collector Employing Vee-Trough Concentrator and Vacuum Tube Receivers," For Presentation at the American Society of Mechanical Engineers 1977 Winter Annual Meeting, Atlanta, Georgia.

5. Selçuk, M. K., "A Fixed Tilt Solar Collector Employing Reversible Vee-Trough Reflectors and Vacuum Tube Receivers," Presentation Only ERDA Contractors Meeting Solar Heating and Cooling Branch, Reston, Virginia, Aug. 8-10, 1977.

6. Selçuk, M. K., "A Fixed Moderately Concentrating Collector With Reversible Asymmetric Vee-Trough and Vacuum Tube Receiver," ERDA Concentrating Collectors Conference, Atlanta, Georgia, Sept. 1977.

APPENDIX B

DERIVATION OF U_L, $(\tau\alpha)_e$ AND F_R IN COLLECTOR EFFICIENCY EQUATION

The collector efficiency equation given in Section II is

$$\eta = F_R \left[(\tau\alpha)_e - \frac{U_L}{I_t} (T_{f,i} - T_a) \right]$$

Overall heat transfer coefficient U_L, ignoring the heat resistance of the working fluid, may be calculated as follows. By definition of U_L,

$$U_L = \frac{Q_\ell}{A_p (T_p - T_a)} \tag{B.1}$$

$$Q_\ell = Q_{\ell r} + Q_{\ell conv} + Q_{\ell c} = C_c Q_{\ell r} \tag{B.2}$$

$$Q_{\ell r} = \varepsilon \delta_o A_p (T_p^4 - T_g^4) = h_{r,pg} A_p (T_p^4 - T_g^4) \tag{B.3}$$

$$\varepsilon = \left[\frac{1}{\varepsilon_p} + \frac{A_p}{A_g/2} \left(\frac{1}{\varepsilon_g} - 1 \right) \right]^{-1} + \left[\frac{1}{\varepsilon_{pb}} + \frac{A_p}{A_g/2} \left(\frac{1}{\varepsilon_g} - 1 \right) \right]^{-1} \tag{B.4}$$

$$h_{r,pg} = \varepsilon \delta_o (T_p + T_g) (T_p^2 + T_g^2) \tag{B.5}$$

where $Q_{\ell r}$, $Q_{\ell conv}$, $Q_{\ell c}$ express the heat losses by reradiation, convection and conduction through supports respectively, ε is the reciprocal emissivity between the absorber plate and the glass tube, δ_o is the Stefan Boltzmann coefficient for black body, T_g is the glass temperature, and A_g is the glass tube surface area. The convection heat losses ($Q_{\ell conv}$) are negligible because of the vacuum in the glass tube. The conduction losses ($Q_{\ell c}$) are also small because of the insulation applied over the tubes in the manifold. As mentioned before, Q_l is taken into consideration by increasing the radiation losses by a factor, $C_c > 1$.

On the other hand, the heat loss Q_ℓ will be

$$Q_\ell = (h + \frac{1}{2} h_{r,gs})\ A_g(T_g - T_a) \tag{B.6}$$

where h = heat transfer film coefficient between the glass tube wall and the ambient, and $h_{r,gs}$ = radiation coefficient from the glass tube wall to the sky.

In equation (3.6), backward radiation from the glass wall to the surroundings is neglected since the ground to glass wall temperature difference is quite small; $h_{r,gs}$ can be written as

$$h_{r,gs} = \varepsilon_g\ \delta_o(T_g^4 - T_{sky}^4)/(T_g - T_a) \tag{B.7}$$

where T_{sky} is the sky temperature.

The overall heat transfer coefficient U_L can be calculated as

$$U_L = \left(\frac{1}{C_c\ h_{r,pg}} + \frac{1}{h + \frac{1}{2} h_{r,gs}}\ \frac{A_p}{A_g}\right)^{-1} \tag{B.8}$$

This equation contains the unknown glass temperature because of the $h_{r,pg}$ and $h_{r,gs}$ values. However, the glass temperature T_g can be obtained by iterative process from the equation

$$Q_\ell = C_c\ h_{r,pg}\ A_p(T_p - T_g) = (h + \frac{1}{2} h_{r,gs})\ A_g(T_g - T_a) \tag{B.9}$$

assuming that the film coefficient h and the sky temperature T_{sky} are known. The coefficient h depends on the wind velocity and direction, and T_{sky} depends on the temperature, humidity and pollutants of the air. There are several correlation equations for both h and T_{sky}, but these equations give only approximate values; h and T_{sky} have only negligible effect on U_L even if they change considerably.

Therefore, the following approximate equations can be used without introducing large errors:

$$h = 5.7 + 3.8V \ (w/m^2c) \tag{B.10}$$

$$T_{sky} = T_a \tag{B.11}$$

where v(m/s) is wind velocity. For $A_p = B.L = 0.19m^2$,

$$A_g = \pi DL = 0.68m^2$$

$$\delta_o = 5.77 \times 10^{-8} \ W/m^2 \ K^4$$

Equations B.4, 5, 7, 8, and 9 can be simplified as

$$\varepsilon = 0.208 \tag{B.4a}$$

$$h_{r,pg} = 1.2 \times 10^{-8} \ (T_p + T_g) \ (T_p^{\ 2} + T_g^{\ 2}) \tag{B.5a}$$

$$h_{r,gs} = 5.077 \times 10^{-8} \ (T_a + T_g) \ (T_a^{\ 2} + T_g^{\ 2}) \tag{B.7a}$$

$$\frac{1}{U_L} = \frac{1}{h_{r,pg}} + \frac{0.279}{h + \frac{1}{2} h_{r,gs}} \tag{B.8a}$$

$$\frac{1}{U_L} = \frac{83.333}{C_c \left(\frac{T_p}{100} + \frac{T_g}{100}\right)\left[\left(\frac{T_p}{100}\right)^2 + \left(\frac{T_g}{100}\right)^2\right]} + \frac{0.279}{5.7 + 3.8V + 0.0259 \left(\frac{T_a}{100} + \frac{T_g}{100}\right)\left[\left(\frac{T_a}{100}\right)^2 + \left(\frac{T_g}{100}\right)^2\right]} \tag{B.8b}$$

$$Q_{\ell} = 0.228 \times 10^{-8}\ C_c(T_p^{\ 4} - T_g^{\ 4})$$

$$= 0.68\ \left[(5.7 + 3.8V)\ (T_g - T_a) + 2.539 \times 10^{-8} \times (T_g^{\ 4} - T_a^{\ 4})\right] \tag{B.9a}$$

The plate temperature may be taken as

$$T_p = T_{f,0} - \frac{1}{2}\Delta T \tag{B.12}$$

where $T_{f,0}$ is the fluid outlet temperature and ΔT is the fluid temperature increase between the inlet and outlet.

All temperatures in the above equations are given in Kelvin. The coefficient C_c for heat losses through manifold connections can be estimated without a great error between 1.02 and 1.05 increasing with the plate temperature.

The transmissivity of the glass tube can be calculated from

$$\tau = \tau_r \tau_a \tag{B.13}$$

where τ_r, τ_a are transmittance values considering only reflection with absorption respectively, which can be calculated by the following equations:

$$\tau_r = \frac{1 - \rho}{1 + \rho} \tag{B.14}$$

where ρ is the reflectivity and can be expressed as

$$\rho = \frac{1}{2}\left\{\frac{\left[\sin^2 \sin^{-1}(n \sin\theta) - \theta\right]}{\left[\sin^2 \sin^{-1}(n \sin\theta) - \theta\right]} + \frac{\left[\tan^2 \sin^{-1}(n \sin\theta) - \theta\right]}{\left[\tan^2 \sin^{-1}(n \sin\theta) - \theta\right]}\right\} \tag{B.15}$$

where n is the index of refraction of the glass and θ is the incidence angle of the beam. For normal incidence the reflectivity will be

$$\rho = \left(\frac{n - 1}{n + 1}\right)^2 = \left(\frac{1.492 - 1}{1.492 + 1}\right)^2 = 0.04$$

The transmittances at normal incidence, τ_r and τ_a, will be found as

$$\tau_r = \frac{1 - \rho}{1 + \rho} = 0.923$$

$$\tau_a = e^{-K\delta_g} = e^{-0.078 \times 0.24} = 0.98 \qquad \text{(B.16)}$$

where δ_g is the glass tube thickness. The total transmittance becomes

$$\tau = \tau_r \tau_a = 0.9$$

The effective transmittance-absorptance product including multiple reflections between the glass tube and the absorber plate can be calculated as

$$(\tau\alpha)_e = \frac{\tau\alpha}{1 - (1 - \alpha)\rho_d} \qquad \text{(B.17)}$$

The diffuse reflectance ρ_d can be estimated equal to 0.15 without any great error.

Finally, the transmittance-absorptance product at normal incidence becomes

$$(\tau\alpha)_e = \frac{0.9 \times 0.935}{1 - (1 - 0.935)0.15} = 0.85$$

As the overall heat transfer coefficient U_L is based on constant absorber plate temperature, a correction factor F_R must be introduced to take into consideration the two-dimensional heat flow; i.e., between the branches of the tube and along the tube and also the heat resistance of the working fluid.

F_R can be calculated according to a procedure described in Ref. 23 by Abdel Khalik:

$$F_R = \frac{\dot{m}\, c_p}{A_p U_L} \left(1 + \frac{2\ell\lambda - \beta_1 - \lambda}{\beta_2}\right) \tag{B.18}$$

where

$$\beta_1 = \frac{LX}{\dot{m}\, c_p} \frac{XR(1+\gamma)^2 - 1 - \gamma - XR}{[XR(1+\gamma) - 1]^2 - (XR)^2} \tag{B.19}$$

$$\beta_2 = \frac{LX}{\dot{m}\, c_p} \frac{1}{XR(1+\gamma) - 1^2 - (XR)^2} \tag{B.20}$$

$$\lambda = (\beta_1^2 - \beta_2^2)^{0.5} \tag{B.21}$$

$$\ell = \frac{(\beta_1 - \beta_2 + \lambda)}{[(\beta_2 - \beta_1 + \lambda)e^{-2\lambda} + (\beta_1 - \beta_2 + \lambda)]} \tag{B.22}$$

$$X = \frac{k\delta n}{(w - d)\sin hn} \tag{B.23}$$

$$n = (w - d)\ (U_L/k\delta)^{0.5} \tag{B.24}$$

$$\lambda = -2 \cos hn - U_L \frac{d}{X} \tag{B.25}$$

$$R = \frac{1}{\pi d_i h_{f,i}} + R_b \qquad (B.26)$$

where d_i is the tube inner diameter, $h_{f,i}$ the film coefficient of the fluid, R_b the bond heat resistance between the absorber plate and the tube, and R the total heat resistance between fluid and the absorber plate. The bond resistance, being small, can be neglected.

APPENDIX C

DAY-LONG PERFORMANCE DATA

Collector outlet temperatures, temperature rise of the working fluid (ΔT), and collector efficiencies for the four collector configurations are presented for the following days:

June 1 and 16, 1977

July 5, 6 and 8, 1977

August 9, 10 and 11, 1977.

COMPARISON OF OUTLET TEMPERATURES.

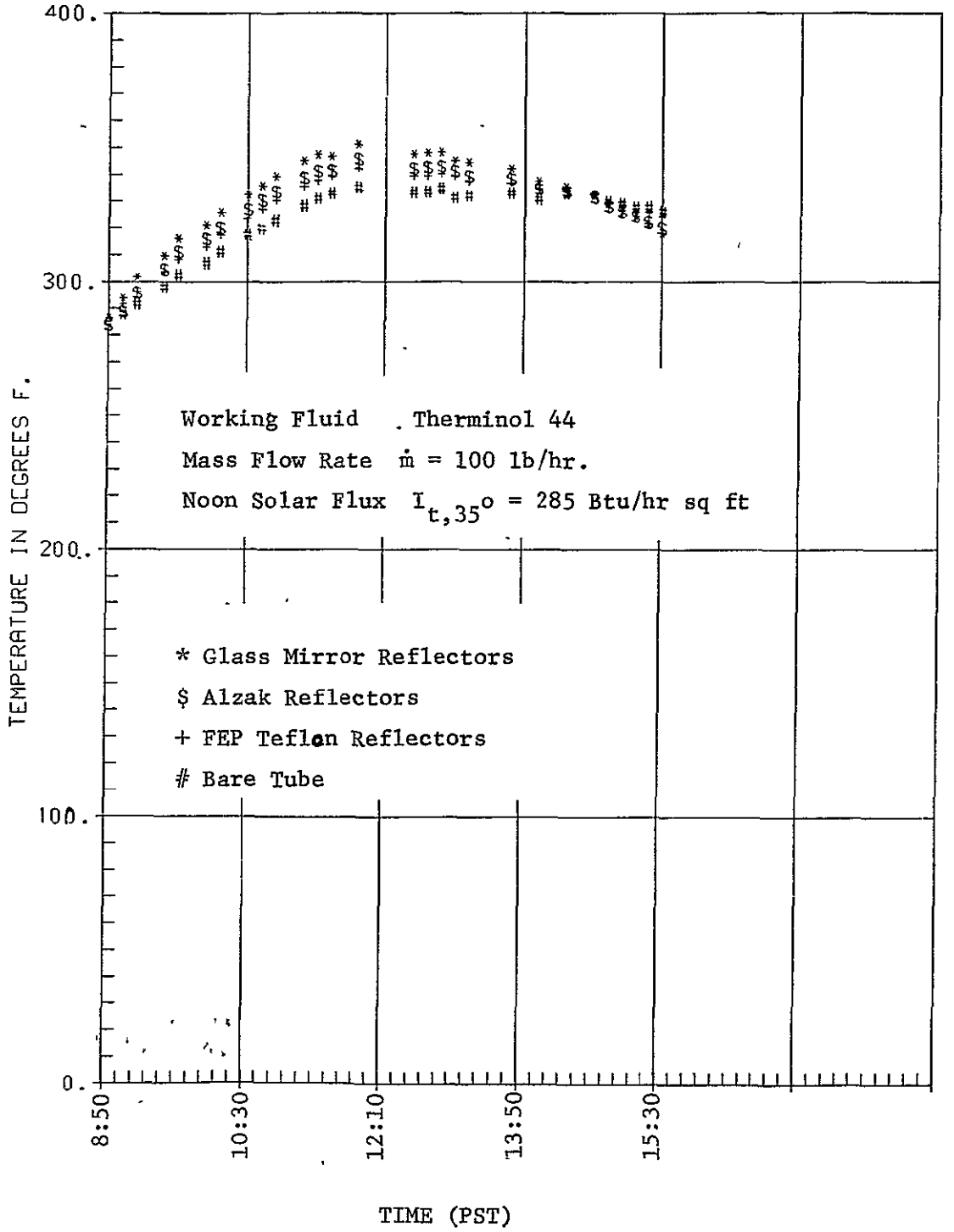

C-2

COMPARISON OF DELTA TS

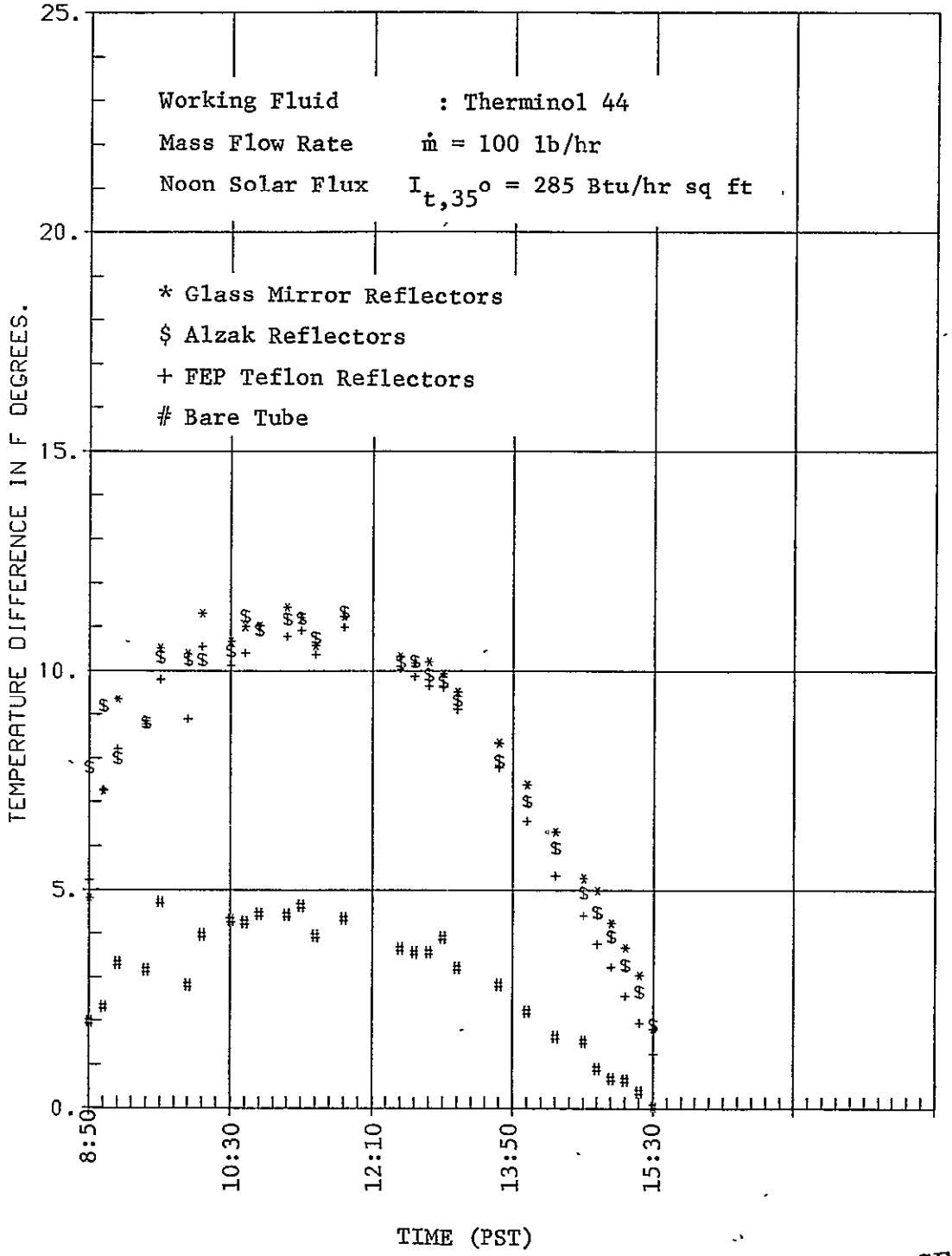

COMPARISON OF EFFICIENCIES.

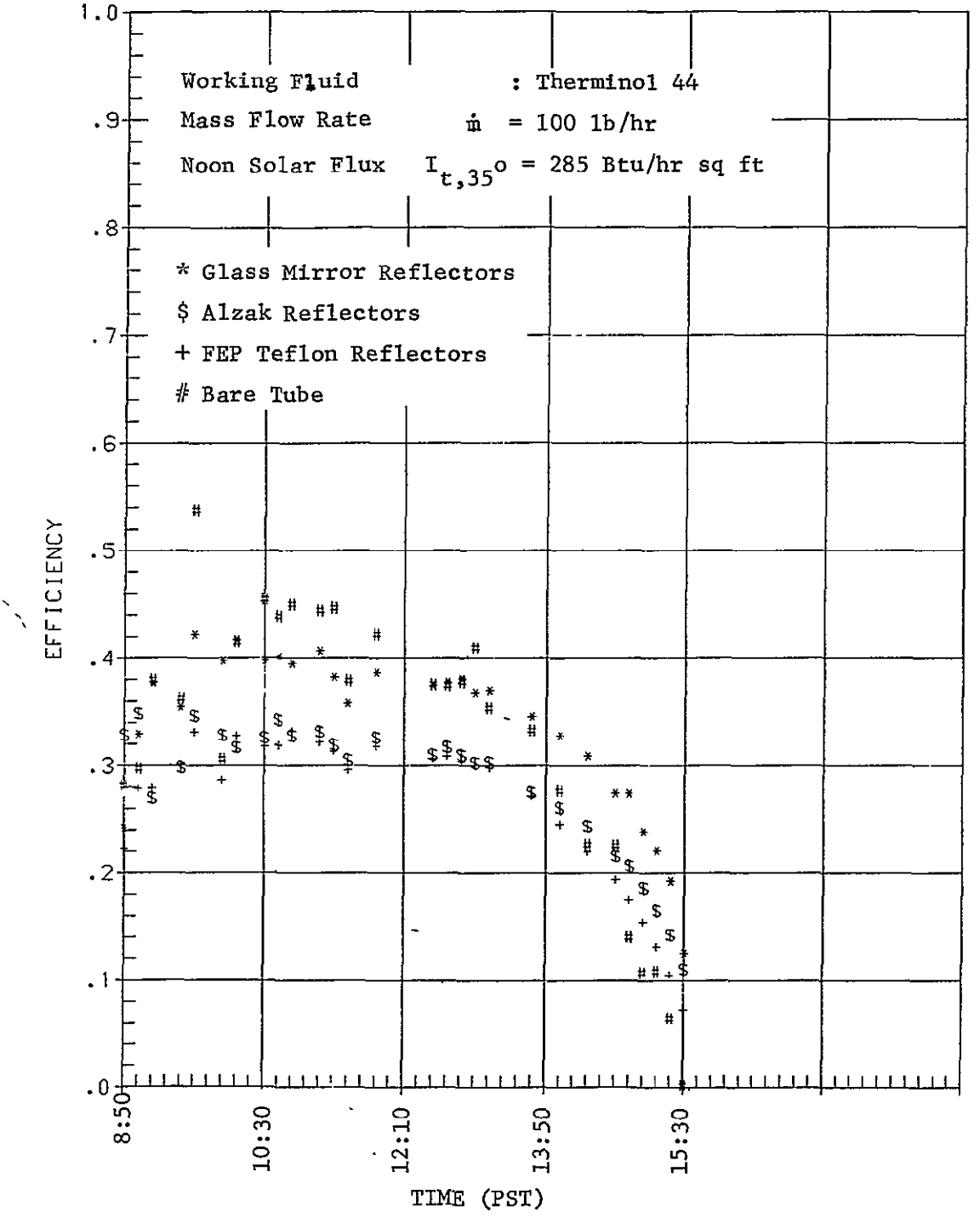

COMPARISON OF OUTLET TEMPERATURES.

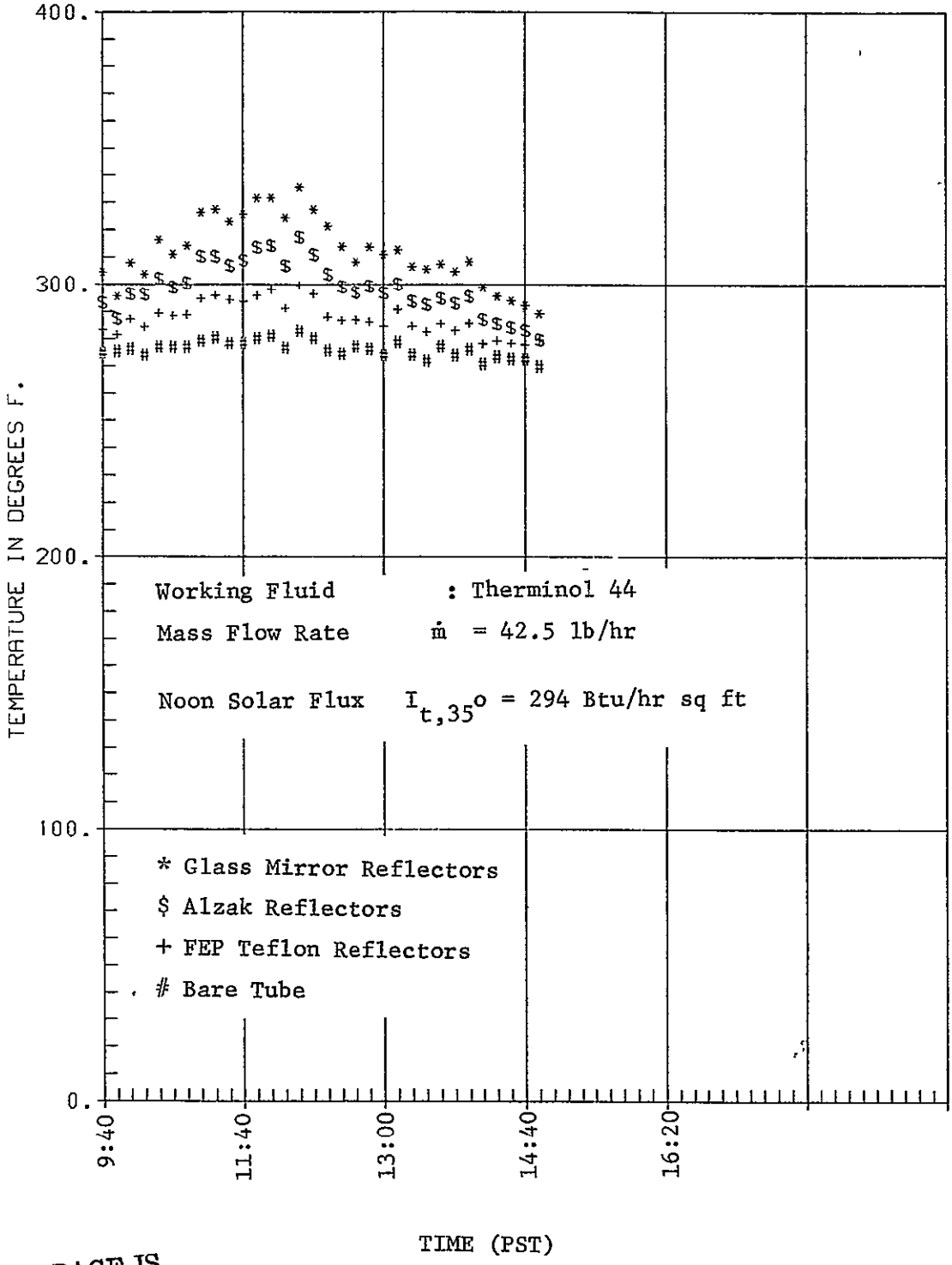

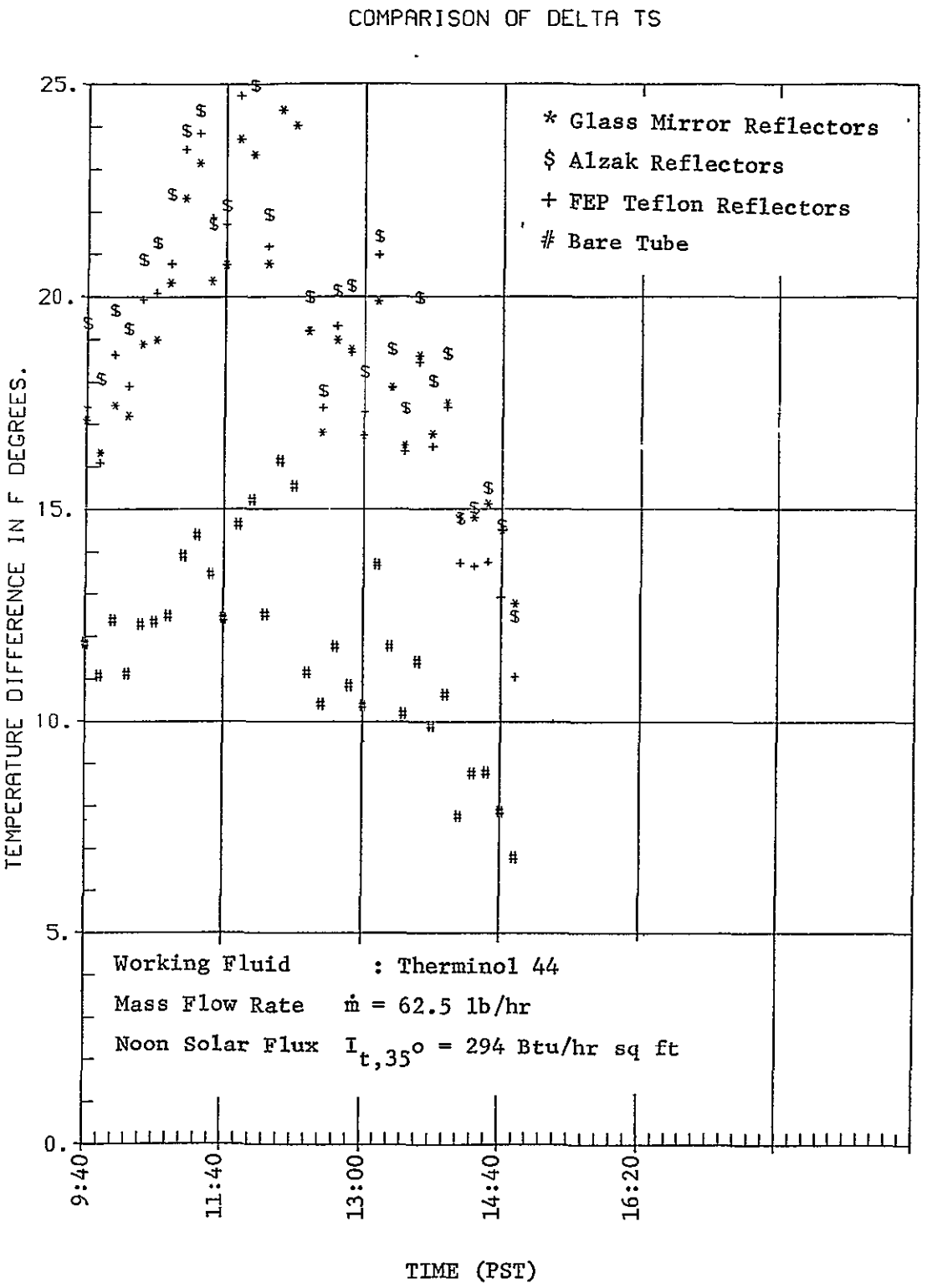
COMPARISON OF DELTA TS
* Glass Mirror Reflectors
$ Alzak Reflectors
+ FEP Teflon Reflectors
# Bare Tube
25.
20.
15.
10.
5.
0.
TEMPERATURE DIFFERENCE IN F DEGREES.
Working Fluid : Therminol 44
Mass Flow Rate ṁ = 62.5 lb/hr
Noon Solar Flux $I_{t,35^o}$ = 294 Btu/hr sq ft
9:40
11:40
13:00
14:40
16:20
TIME (PST)

COMPARISON OF EFFICIENCIES.

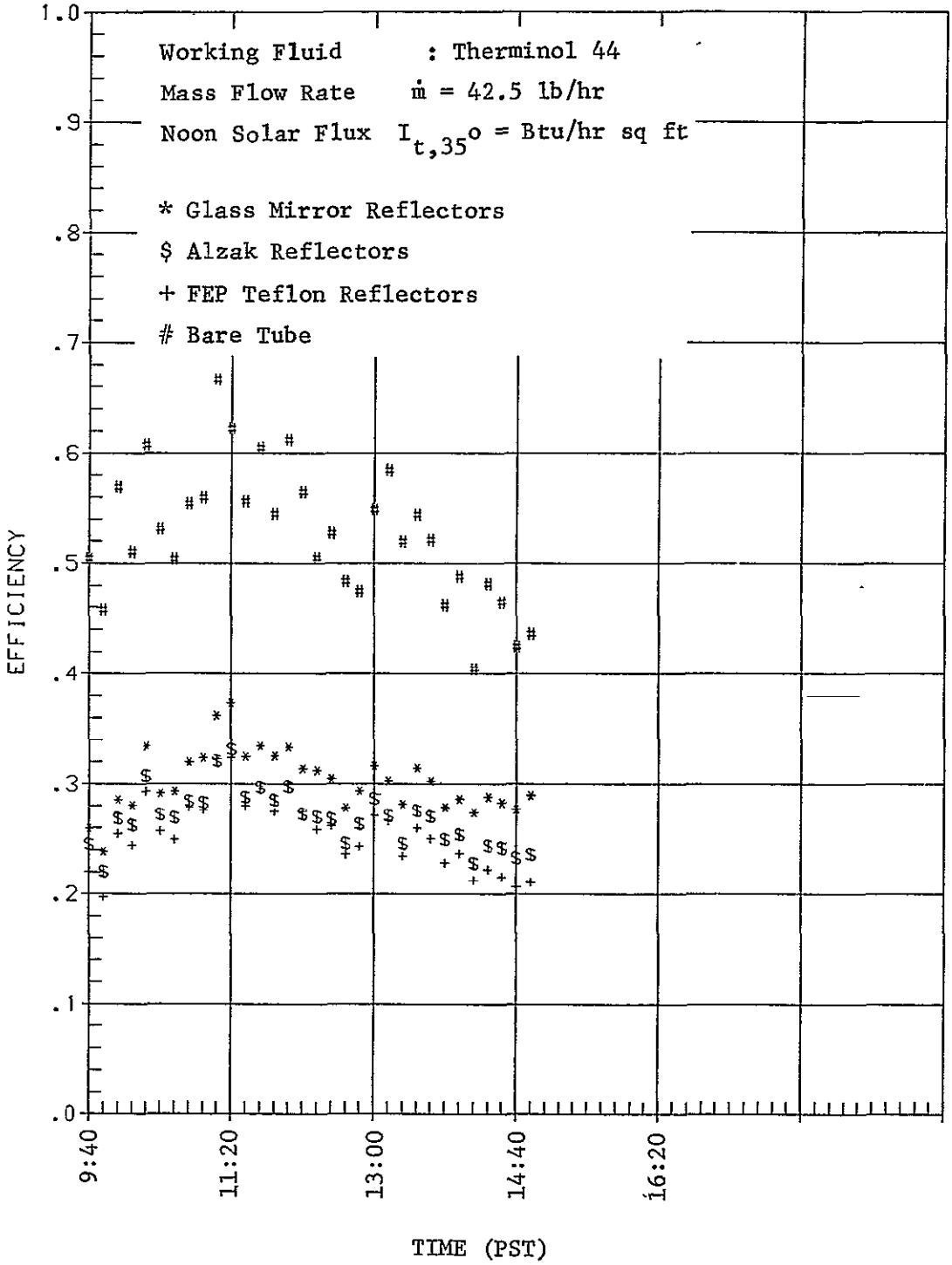

ORIGINAL PAGE IS
OF POOR QUALITY

COMPARISON OF OUTLET TEMPERATURES.

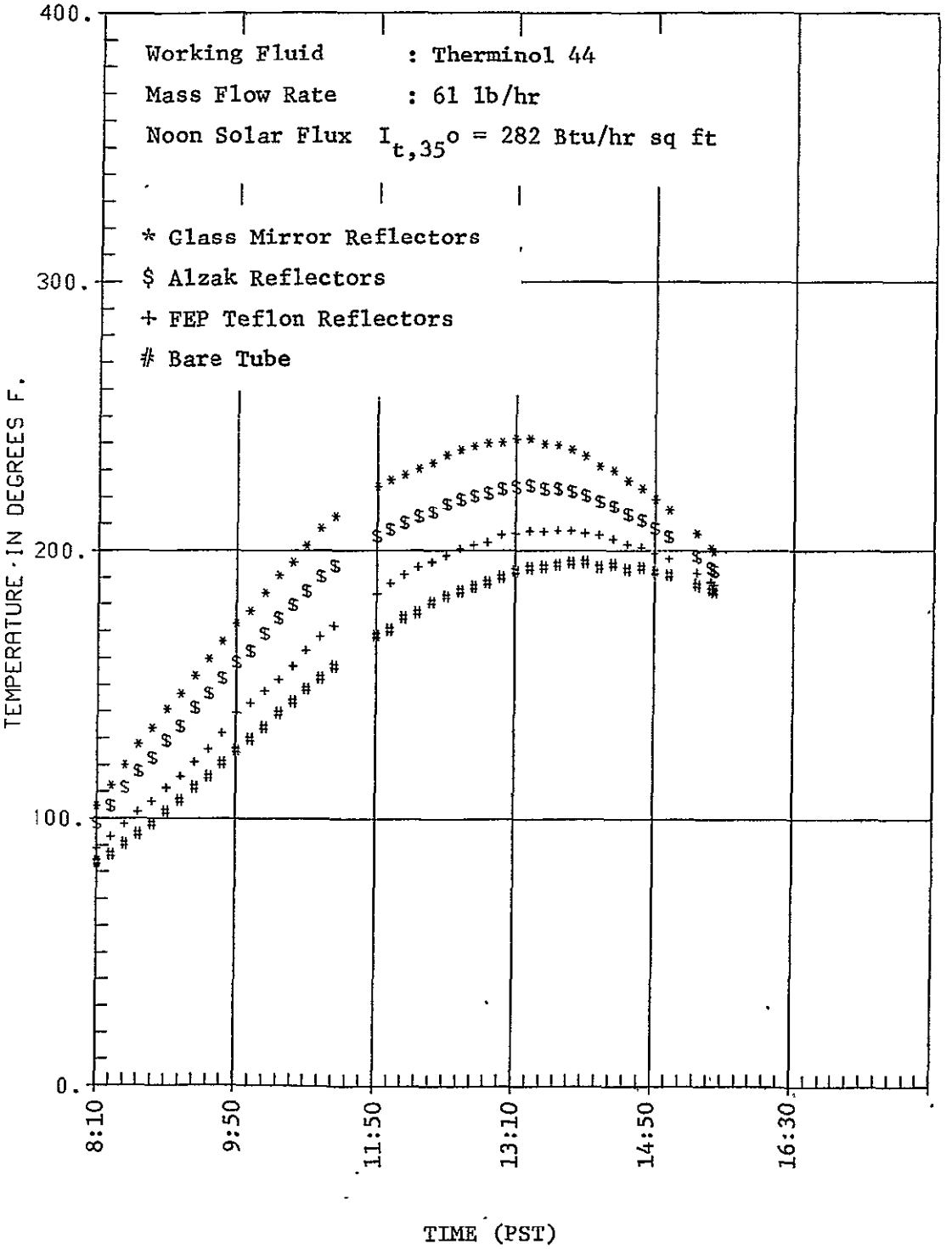

COMPARISON OF DELTA TS

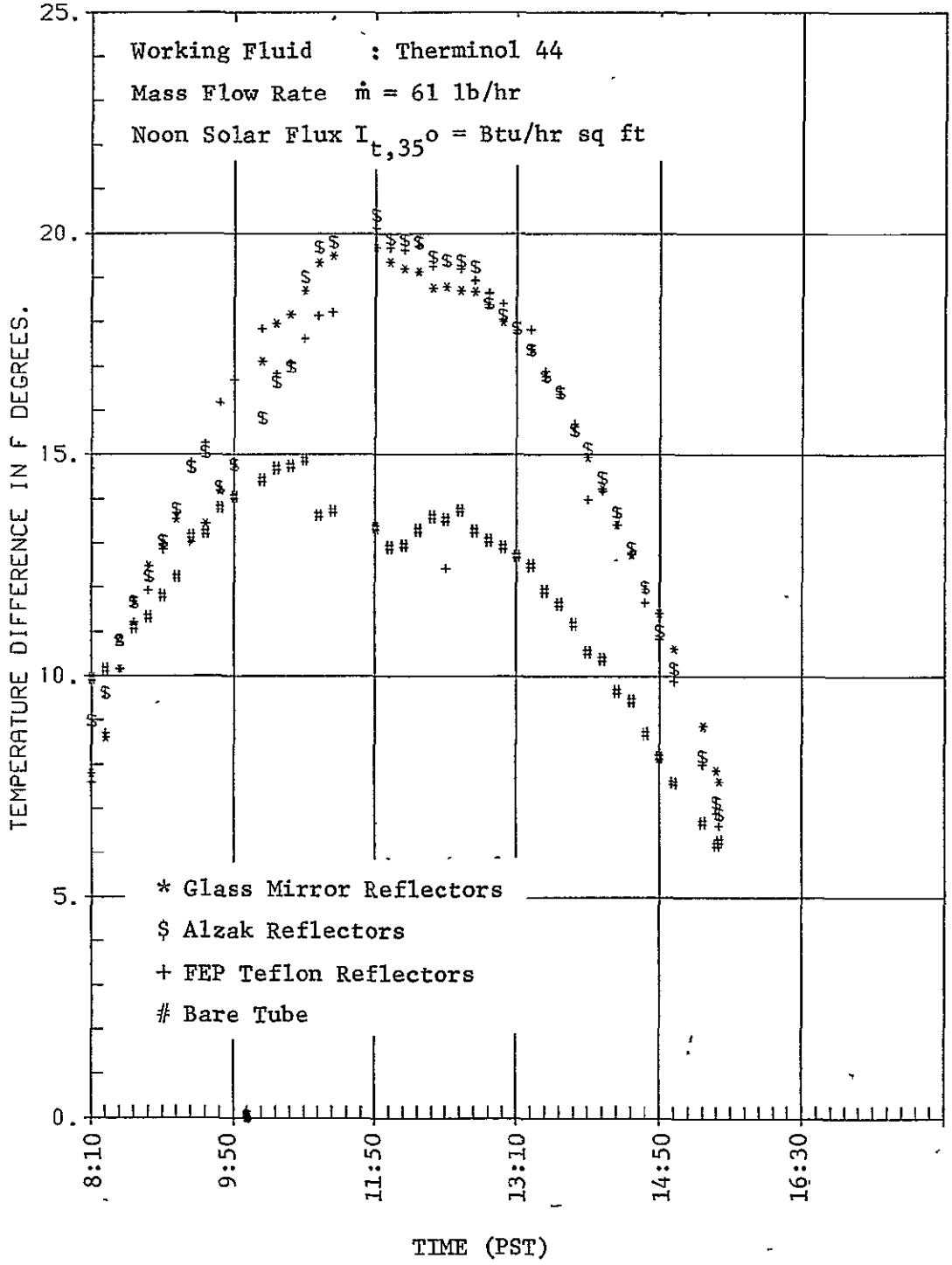

ORIGINAL PAGE IS
OF POOR QUALITY

COMPARISON OF EFFICIENCIES.

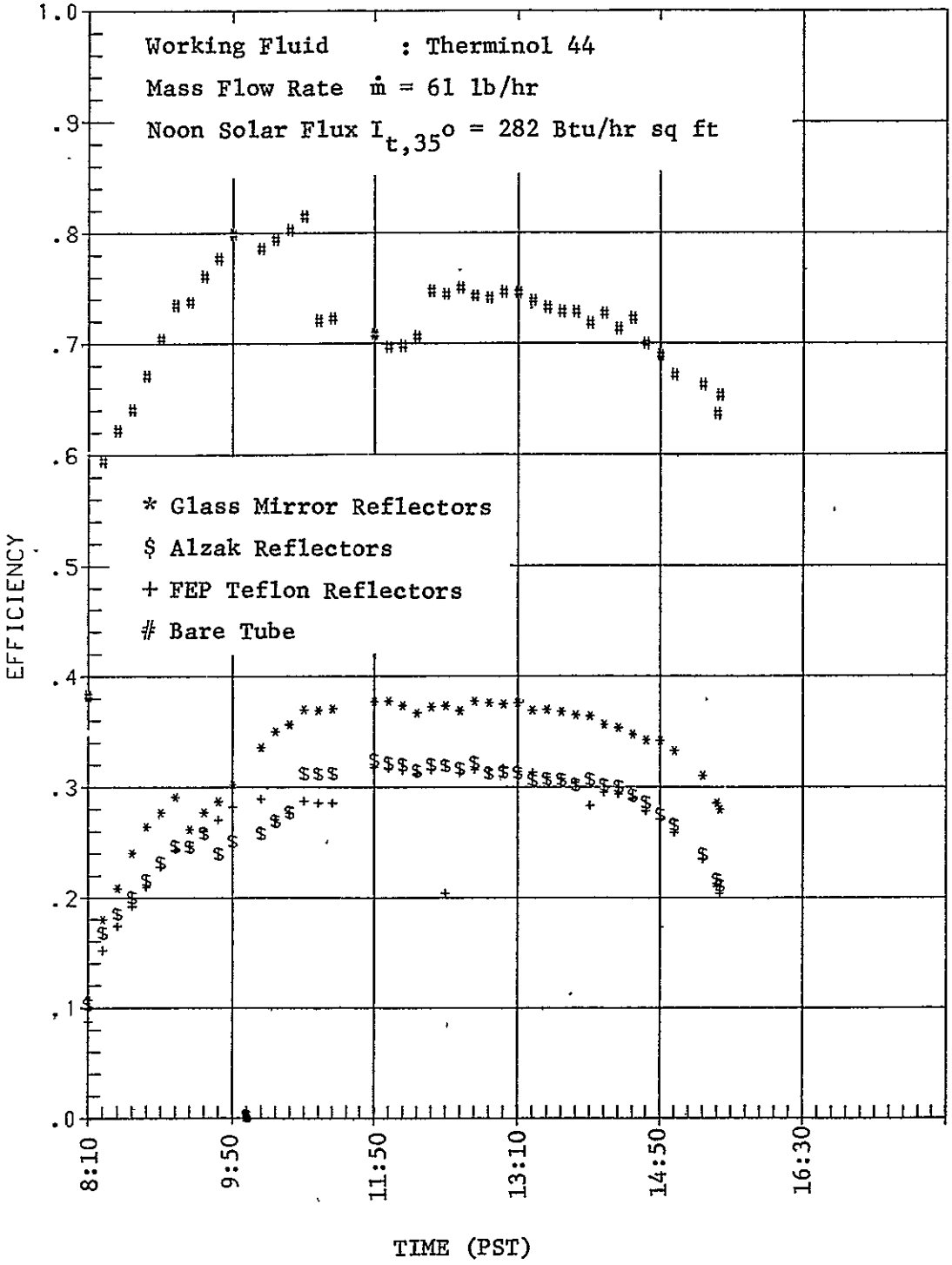

COMPARISON OF OUTLET TEMPERATURES.

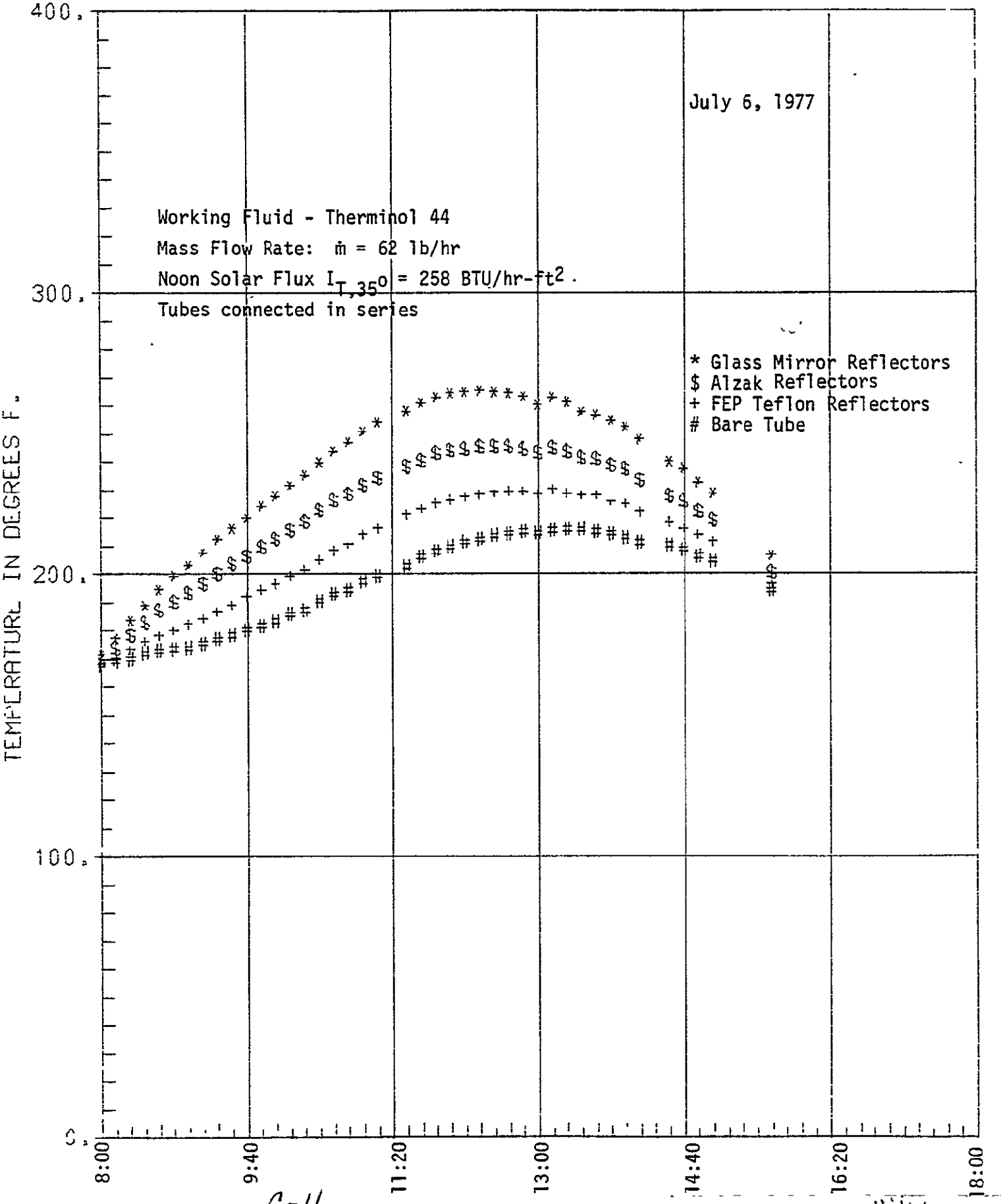

C-11

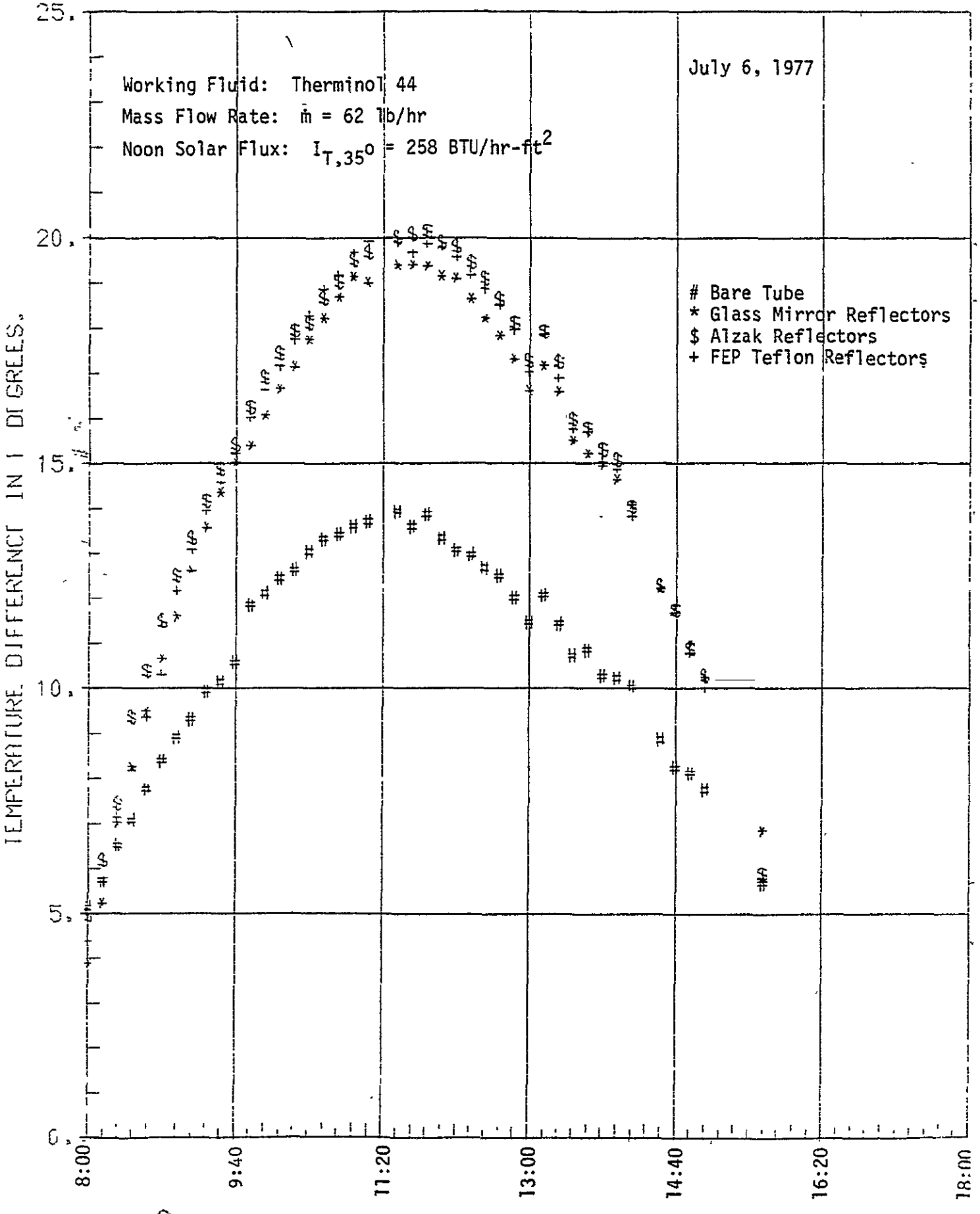
Working Fluid: Therminol 44
Mass Flow Rate: $\dot{m}$ = 62 lb/hr
Noon Solar Flux: $I_{T,35^o}$ = 258 BTU/hr-ft^2
July 6, 1977
Bare Tube
* Glass Mirror Reflectors
$ Alzak Reflectors
+ FEP Teflon Reflectors
TEMPERATURE DIFFERENCE IN I DEGREES.
25.
20.
15.
10.
5.
0.
8:00
9:40
11:20
13:00
14:40
16:20
18:00
TIME (PST)

COMPARISON OF EFFICIENCIES.

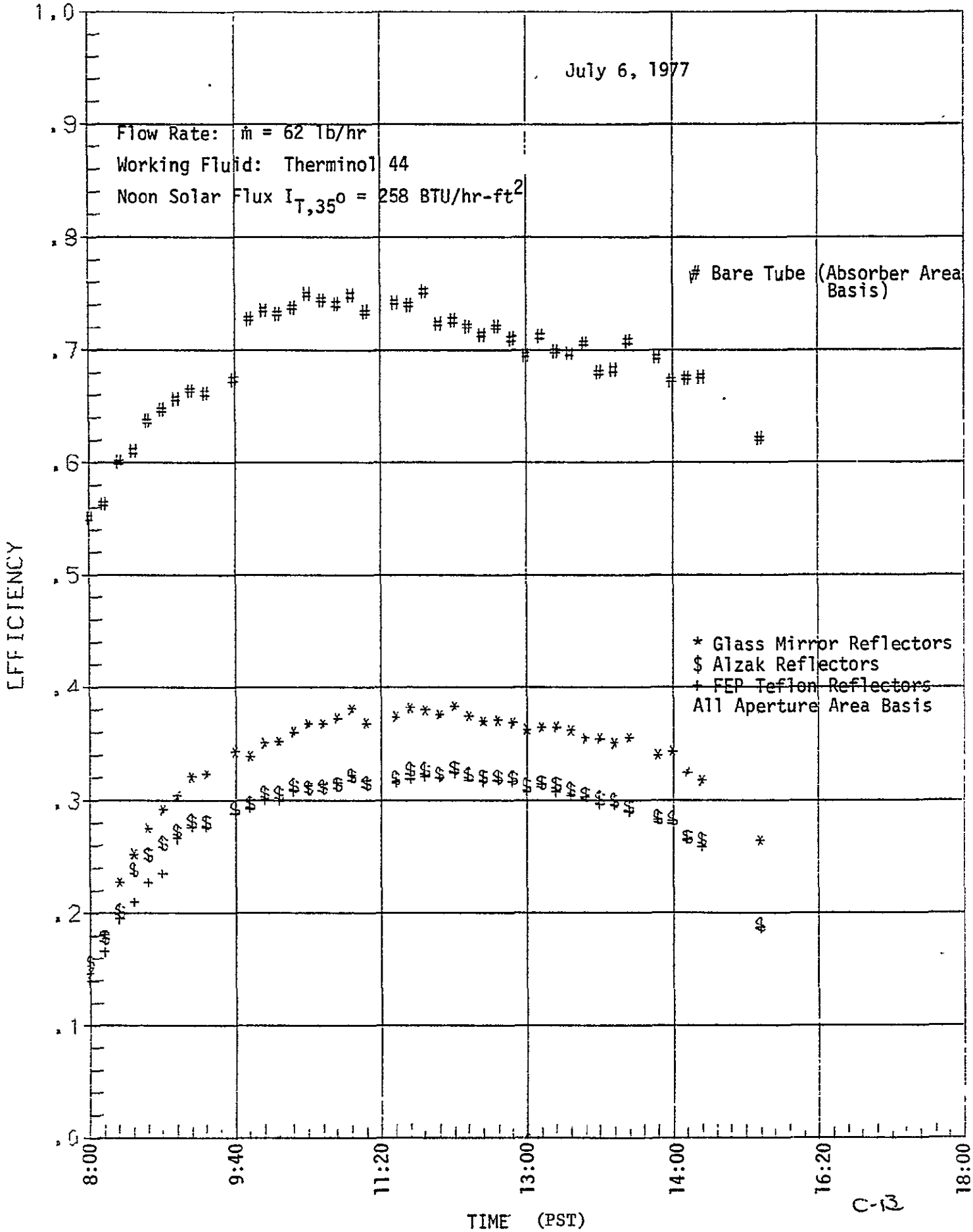

COMPARISON OF OUTLET TEMPERATURES.

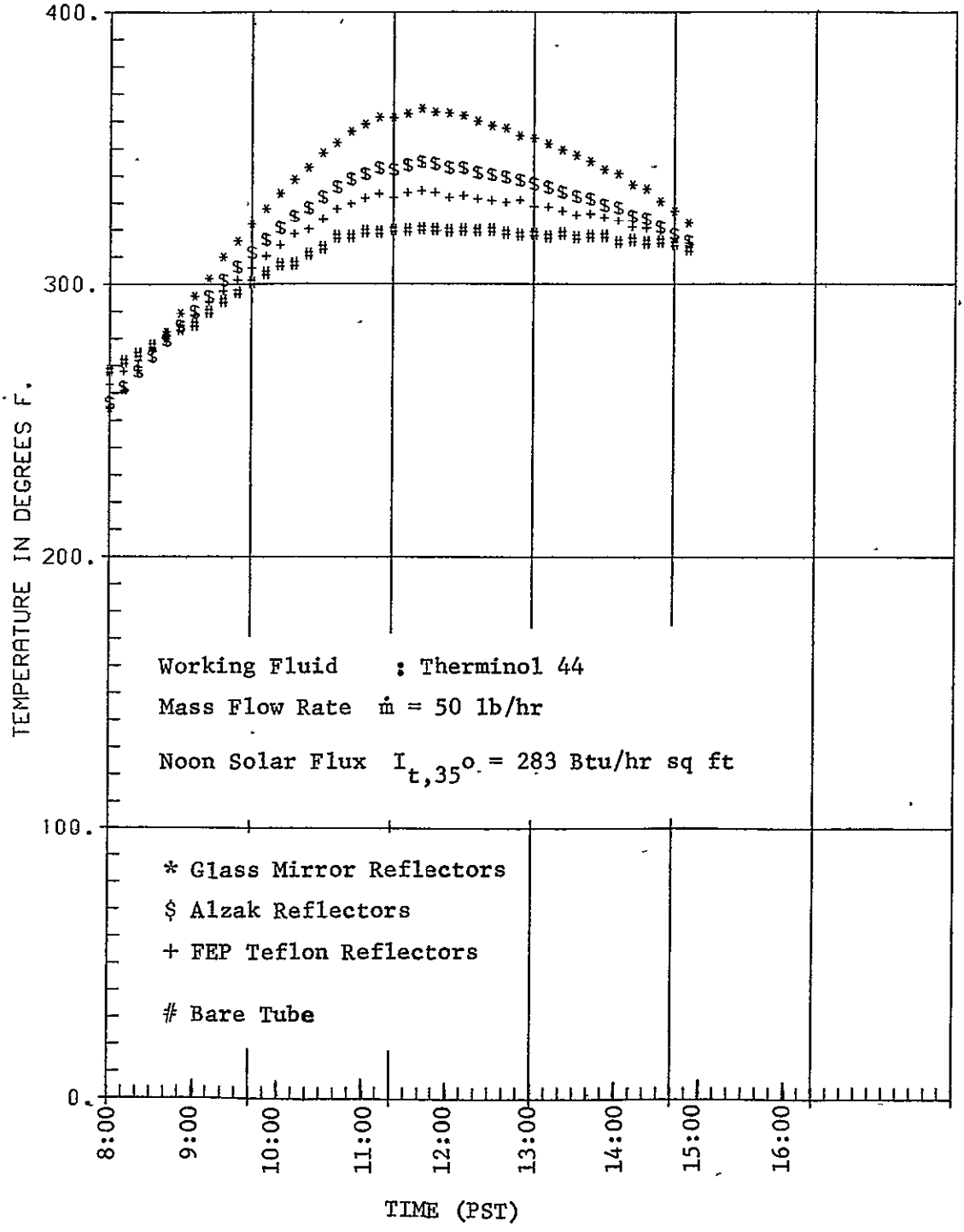

COMPARISON OF DELTA TS

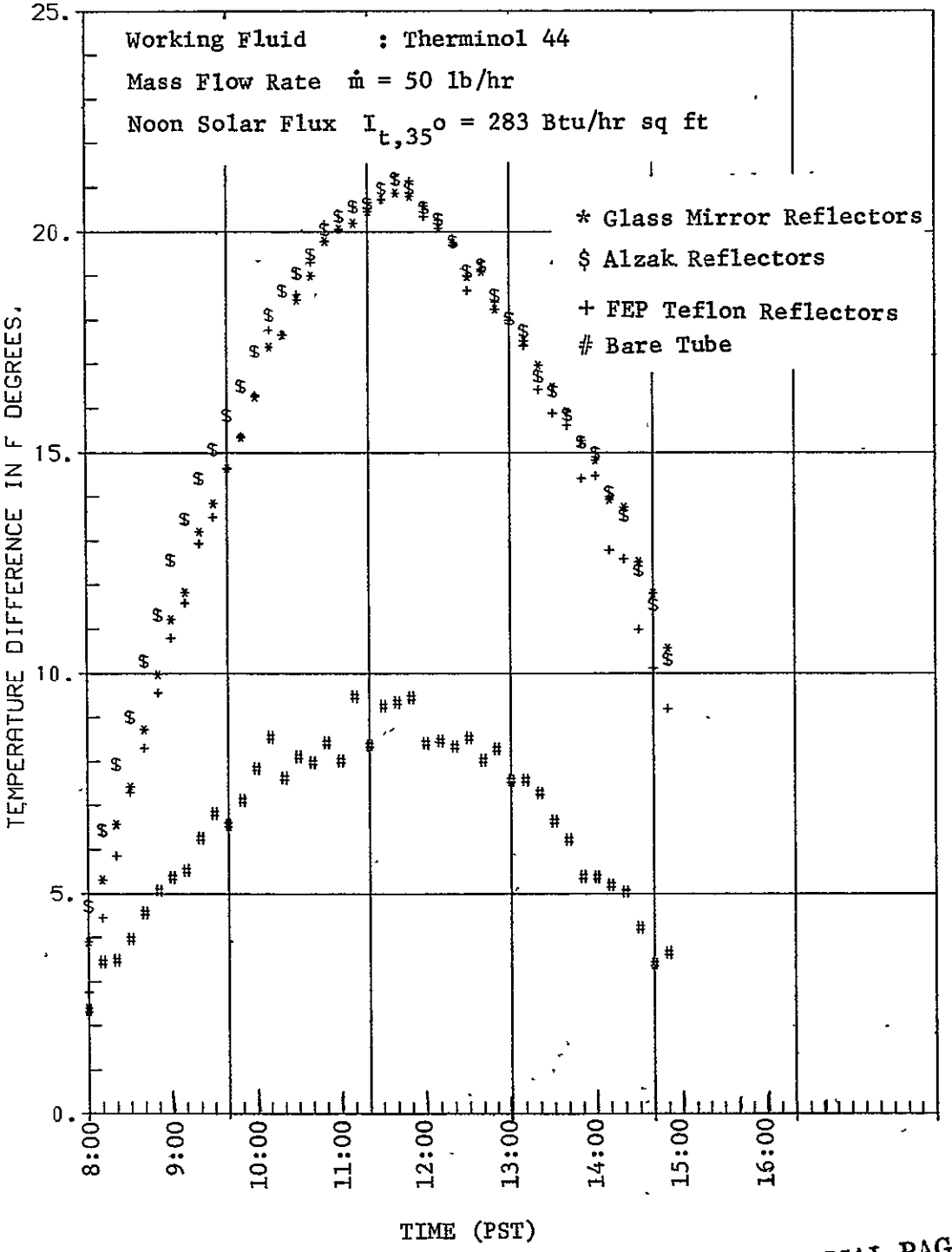

COMPARISON OF EFFICIENCIES.

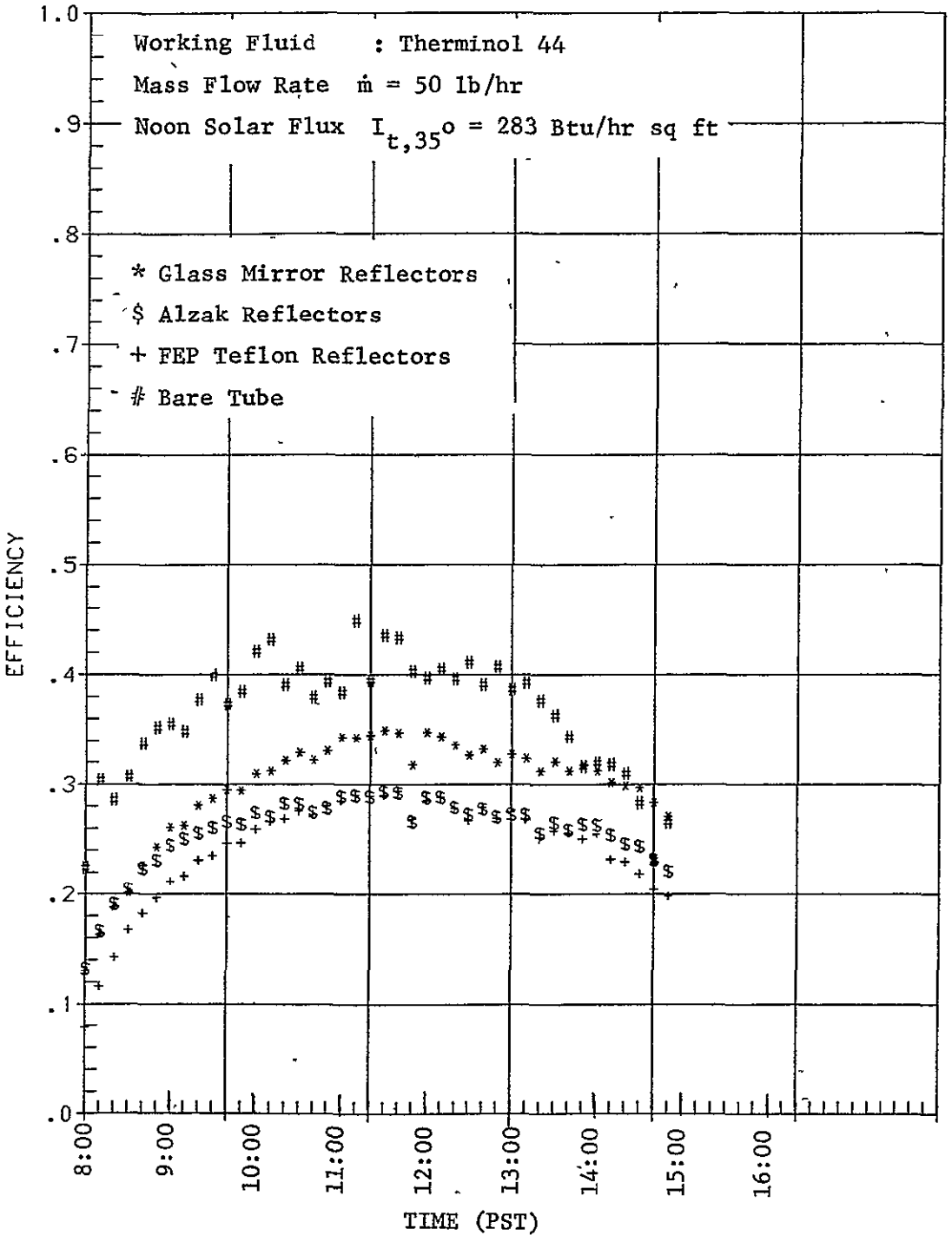

IMPORTANT NOTE:

Results of Tubes #2 and #3 for August 9, 10 and 11 MUST BE DISCARDED as it was discovered that differential thermocouple readings were erroneous.

COMPARISON OF OUTLET TEMPERATURES.

AUG. 9, 1977

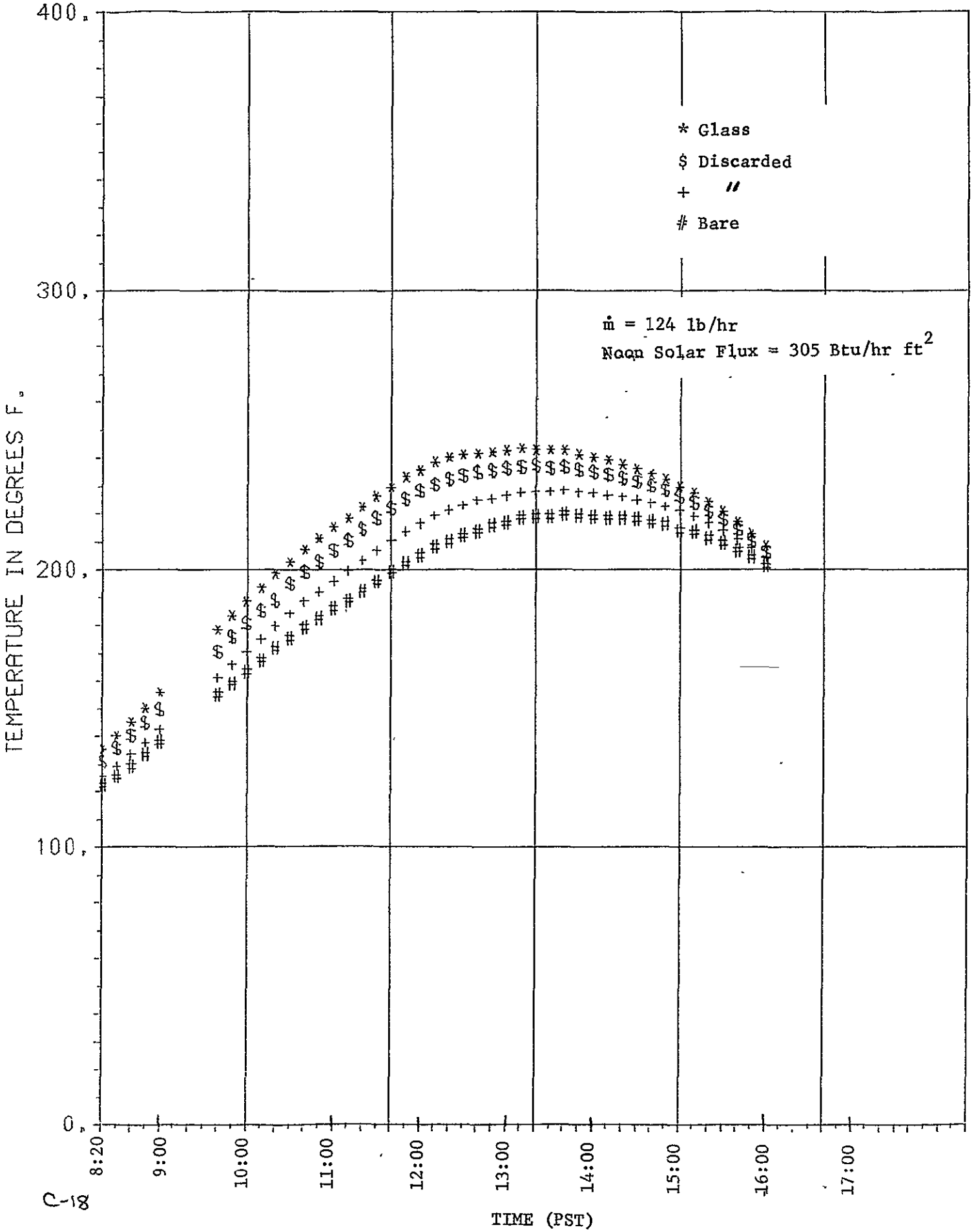

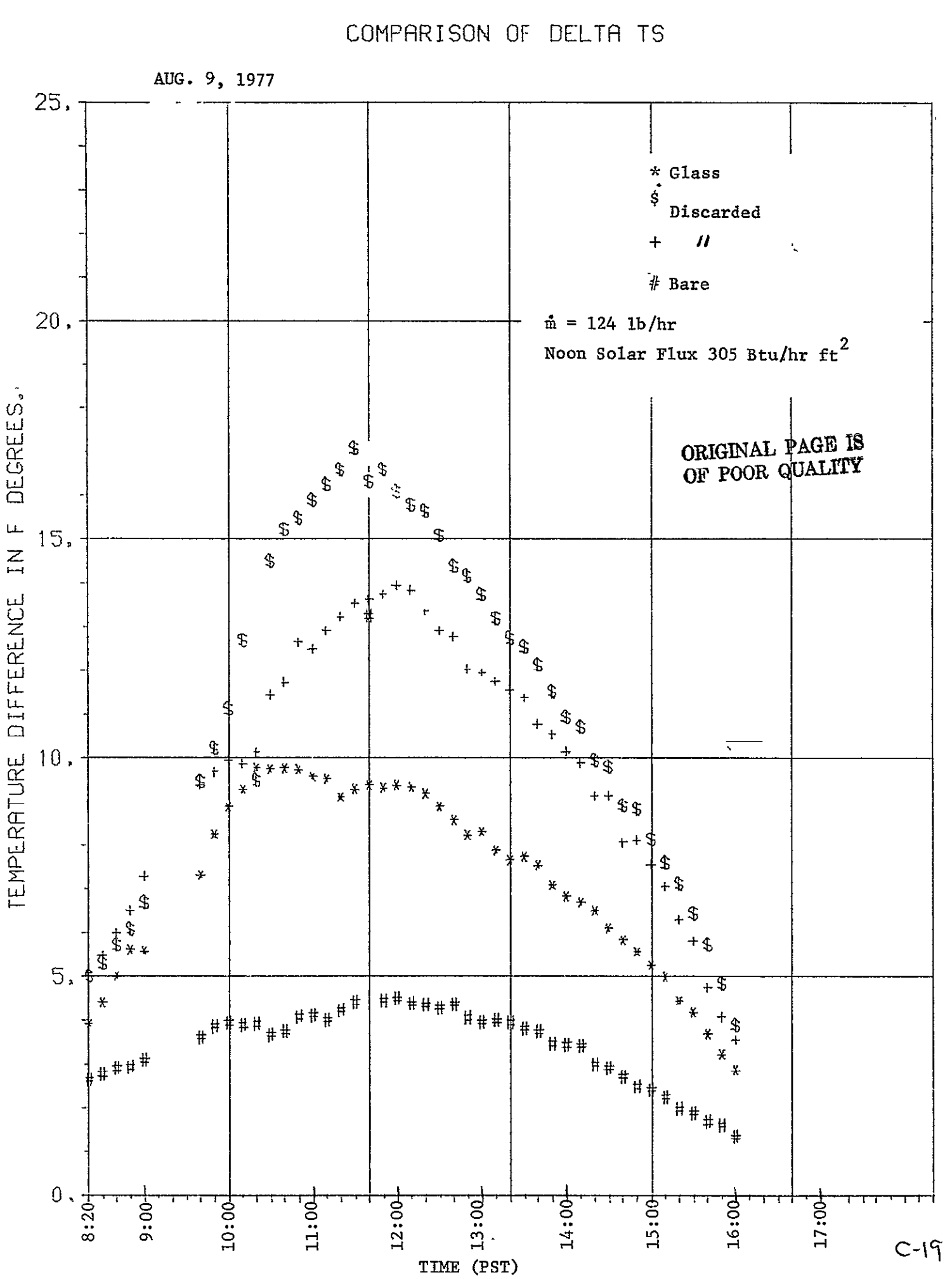
COMPARISON OF DELTA TS
AUG. 9, 1977
25.
20.
15.
10.
5.
0.
TEMPERATURE DIFFERENCE IN F DEGREES.
* Glass
$ Discarded
+ //
# Bare
ṁ = 124 lb/hr
Noon Solar Flux 305 Btu/hr ft2
ORIGINAL PAGE IS
OF POOR QUALITY
8:20
9:00
10:00
11:00
12:00
13:00
14:00
15:00
16:00
17:00
TIME (PST)

COMPARISON OF EFFICIENCIES.

AUG. 9, 1977

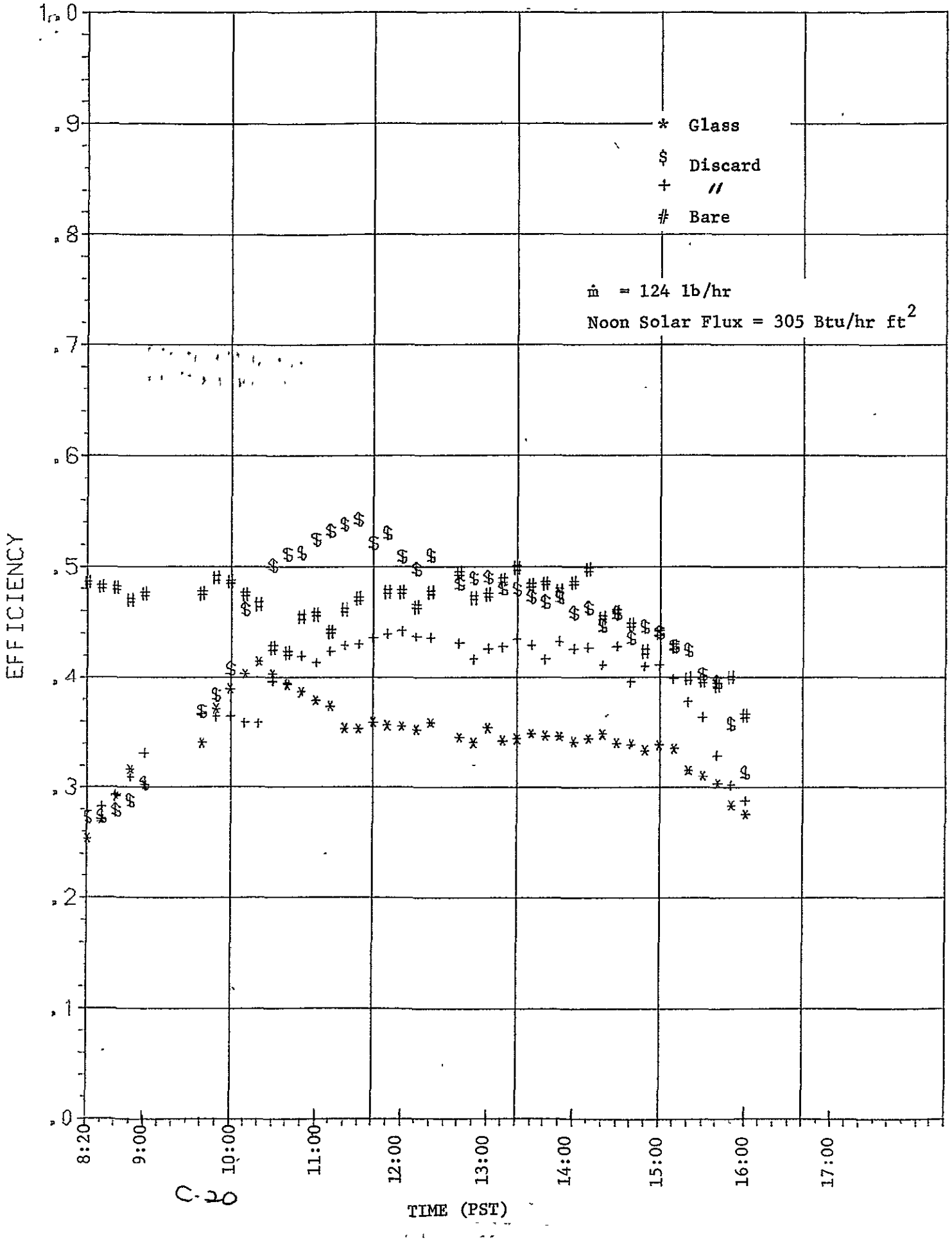

COMPARISON OF DELTA TS

AUG. 10, 1977

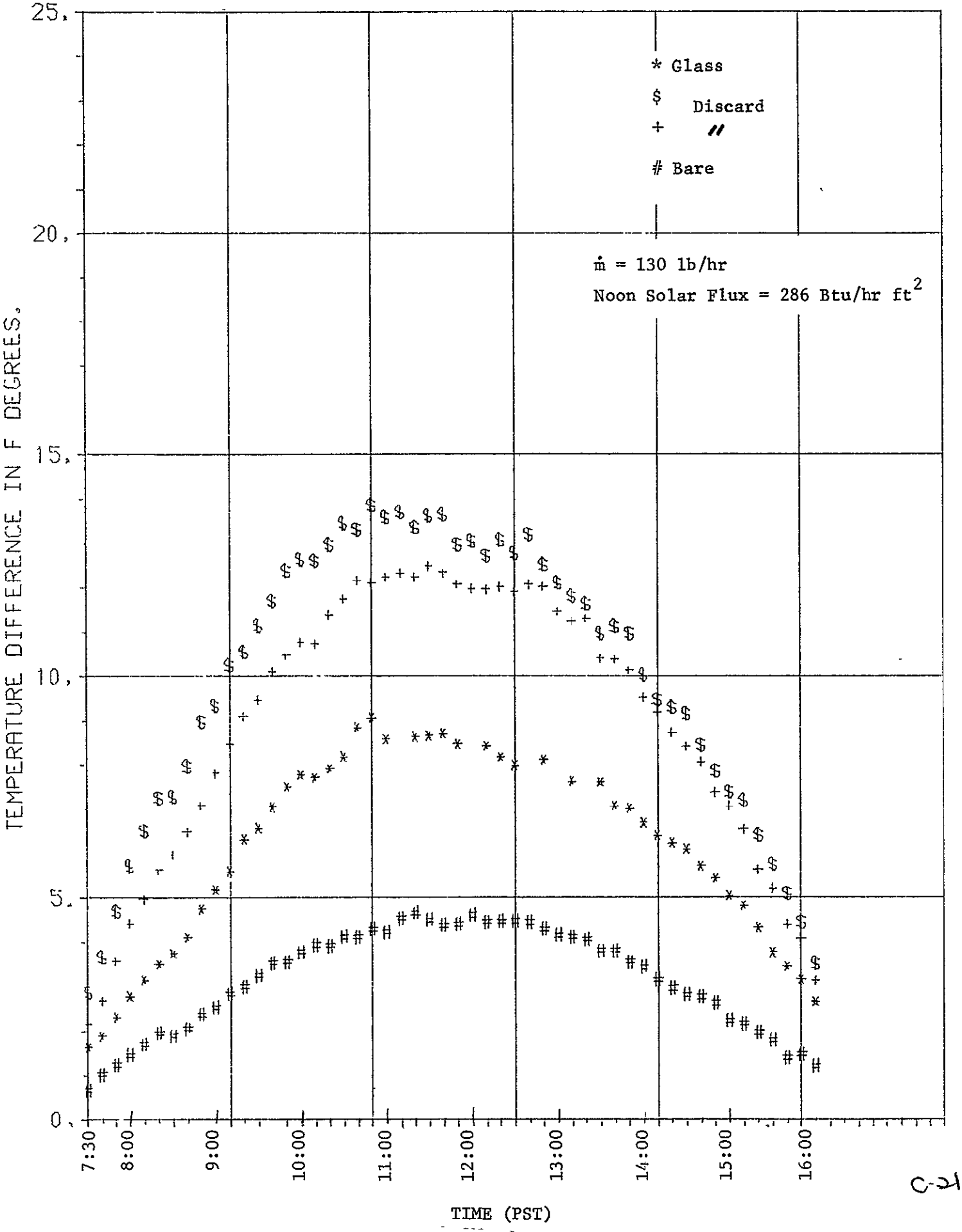

C-21

COMPARISON OF EFFICIENCIES.

AUG. 10, 1977

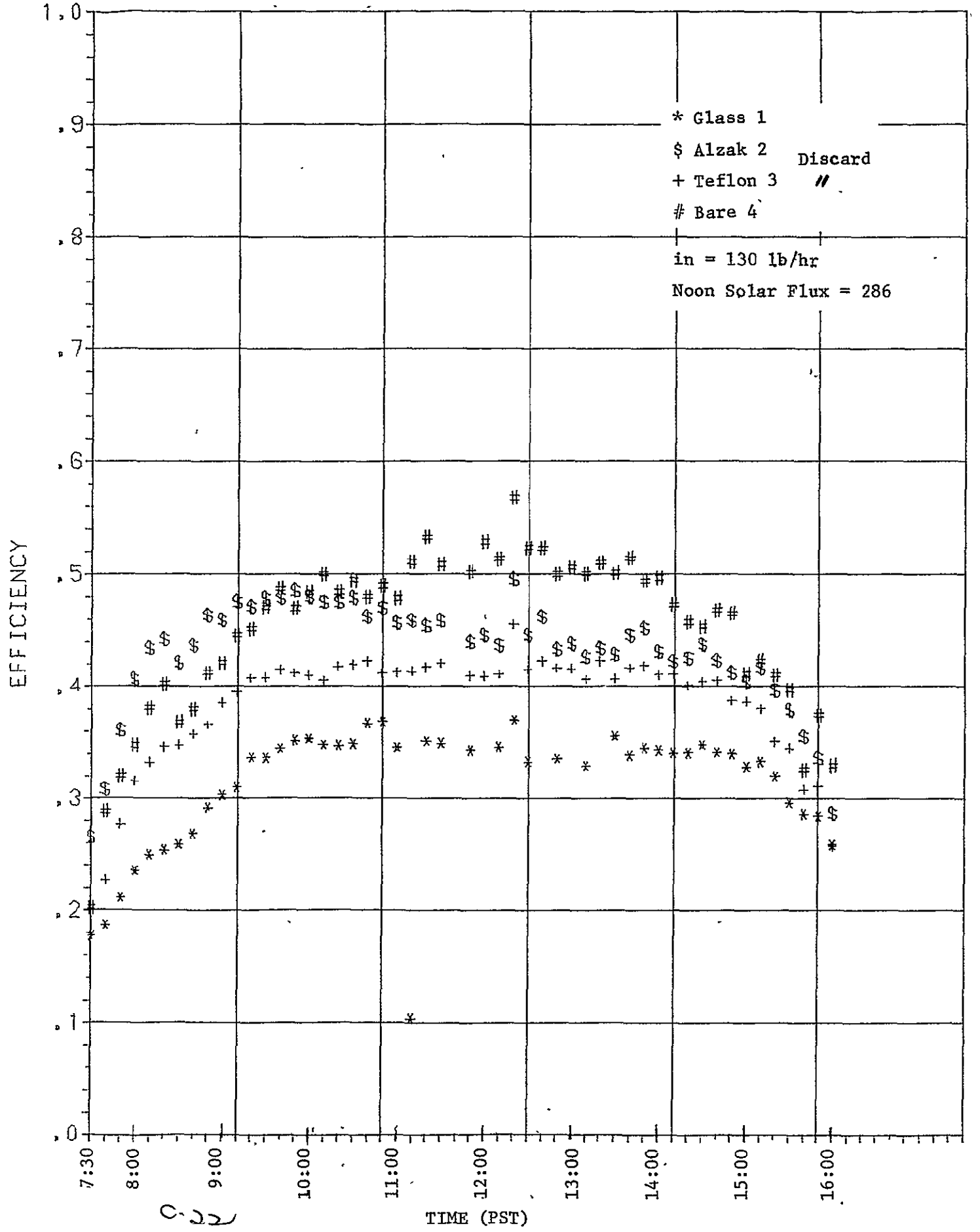

C-22

COMPARISON OF OUTLET TEMPERATURES.

AUG. 10, 1977

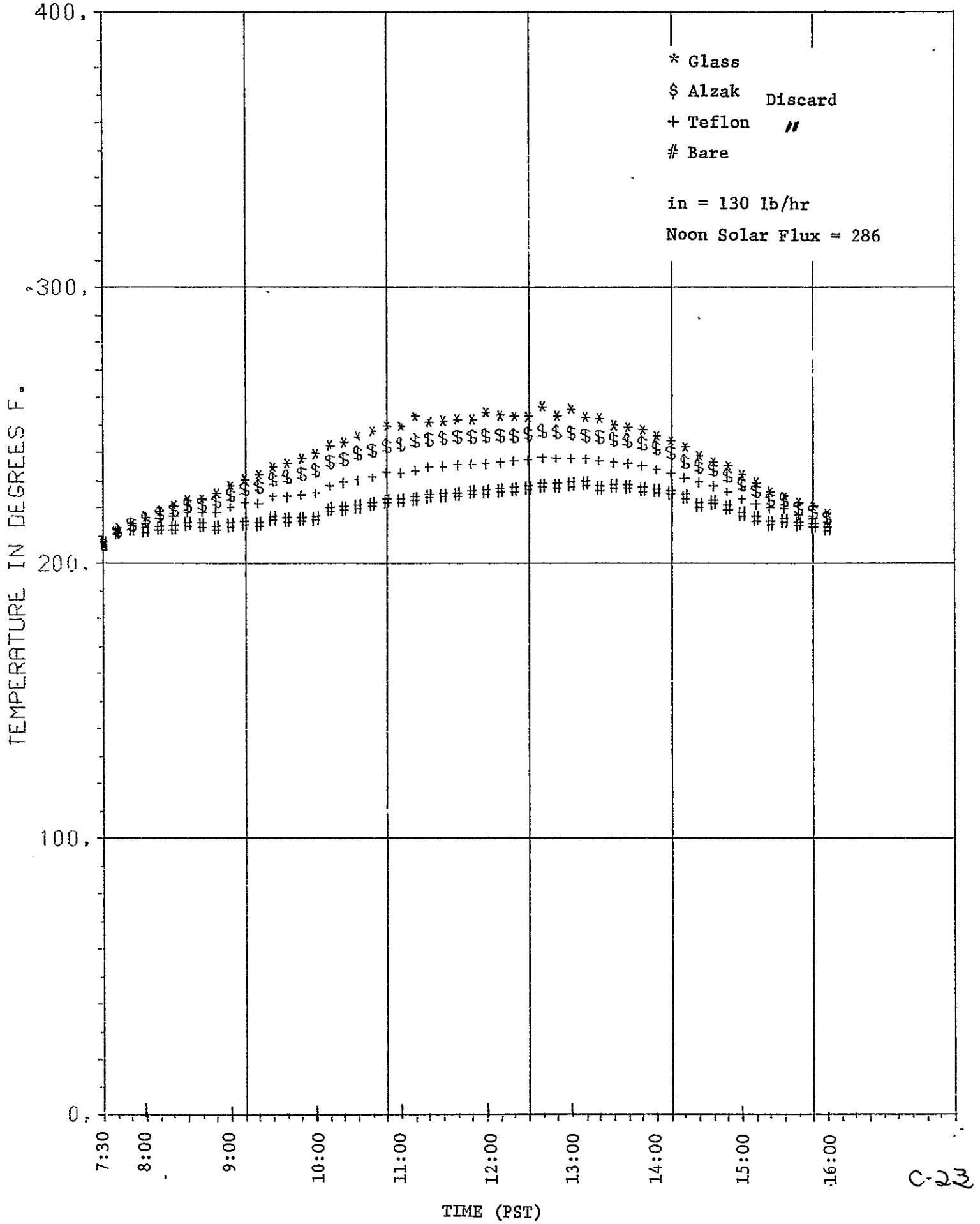

COMPARISON OF OUTLET TEMPERATURES.

AUGUST 11, 1977

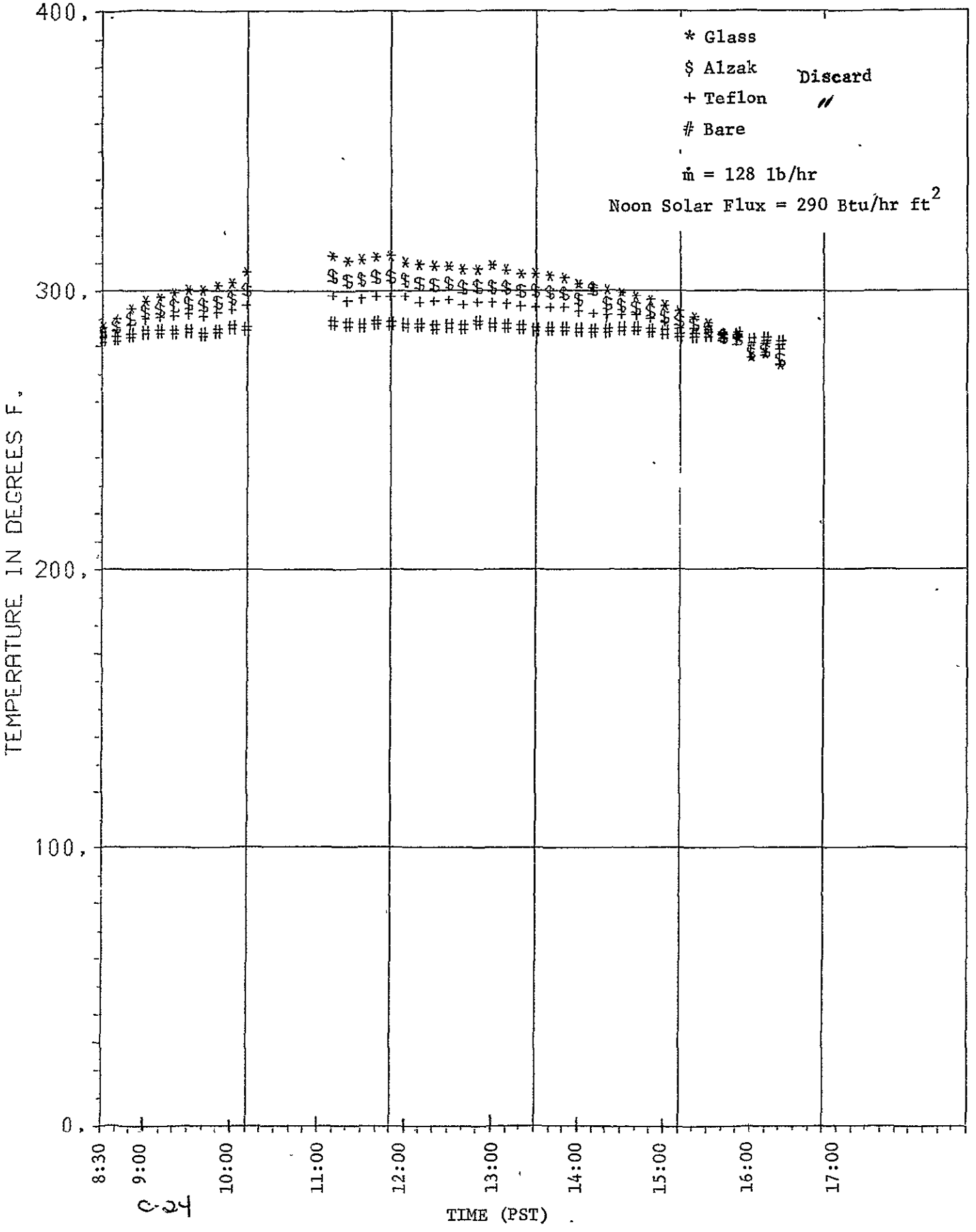

COMPARISON OF EFFICIENCIES.

AUGUST 11, 1977

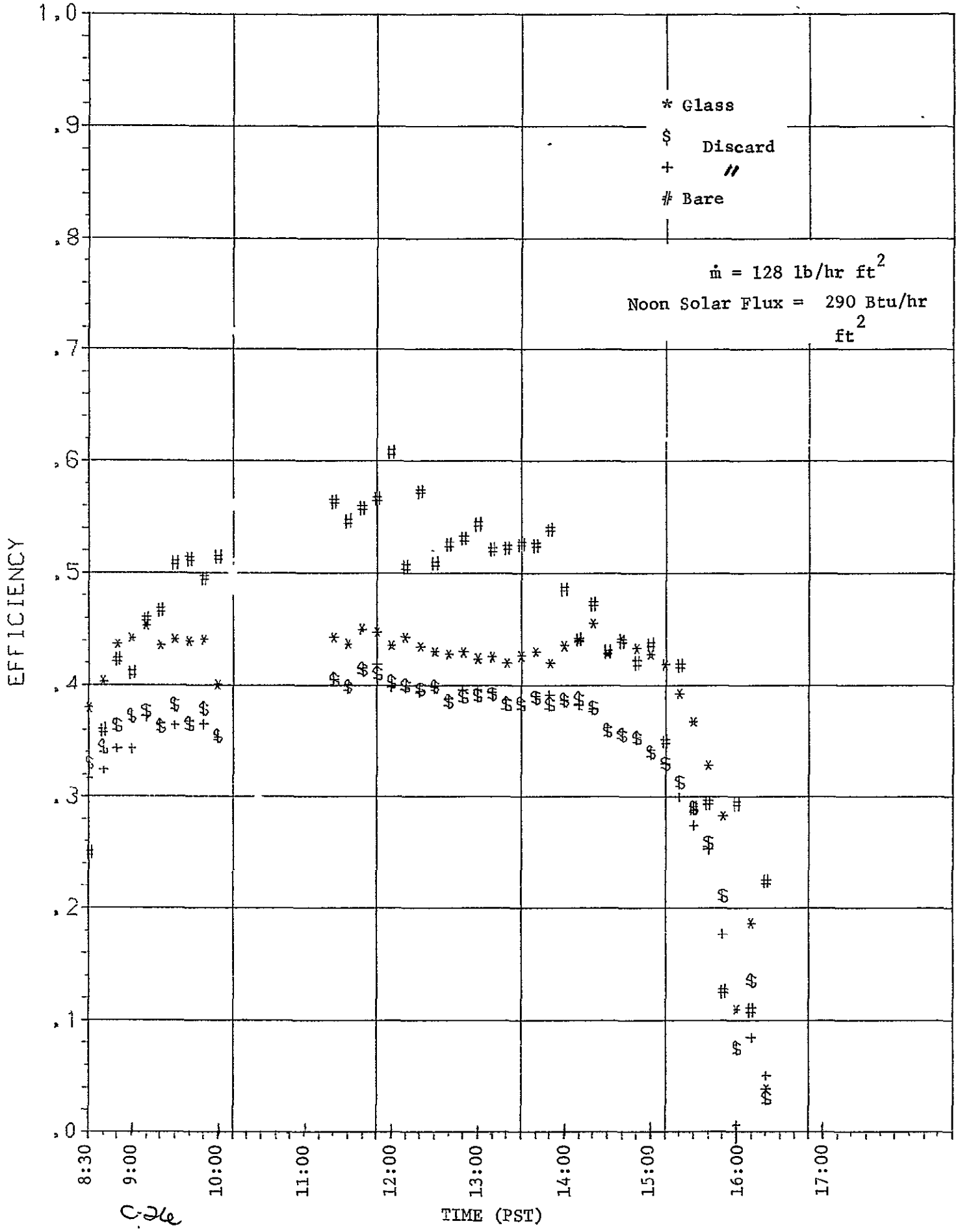

C-26

COMPARISON OF DELTA TS

AUGUST 11, 1977

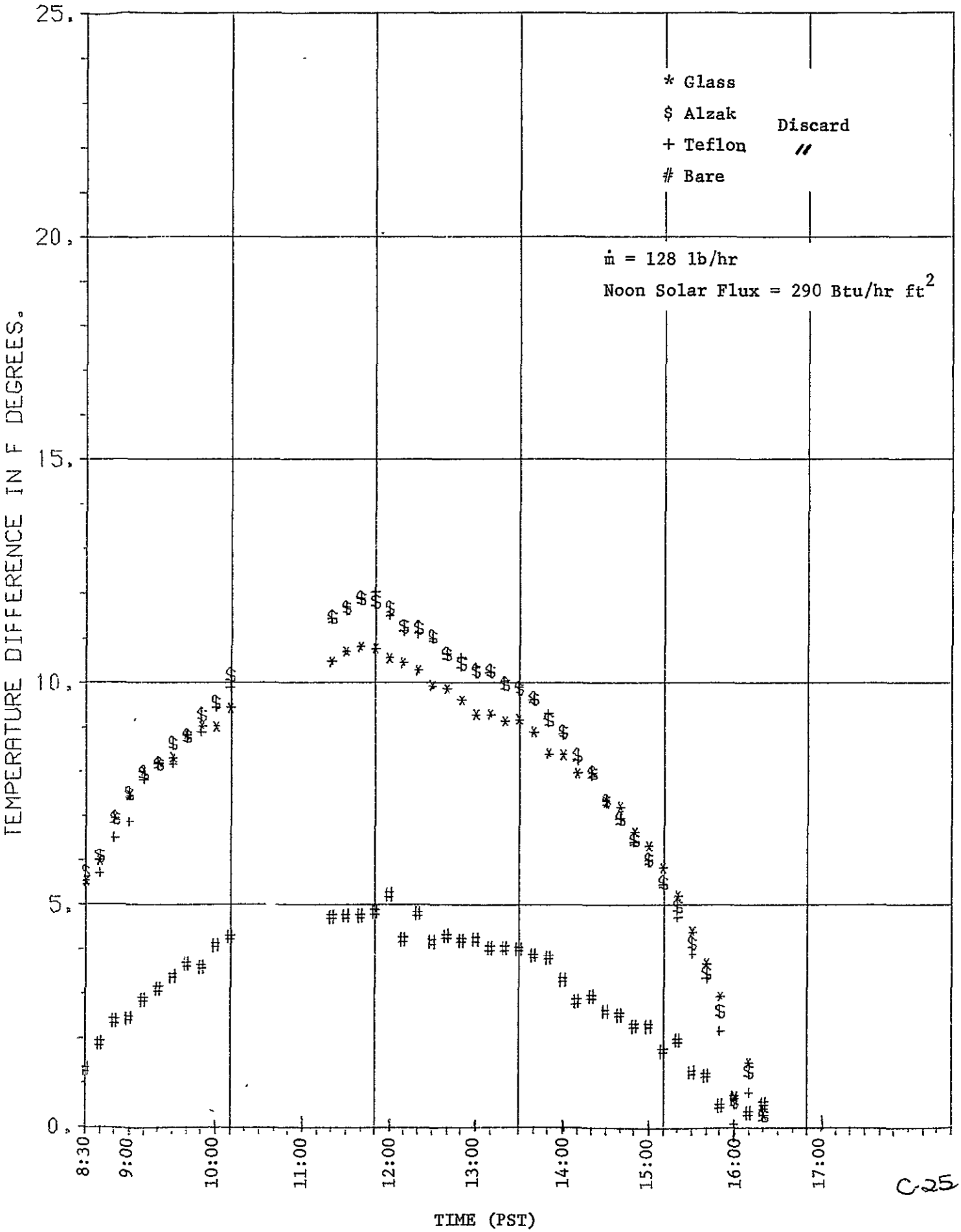

C-25

APPENDIX D

THEORETICAL PERFORMANCE CURVES FOR BURBANK, CALIFORNIA, 1962, PLOTTED BY COMPUTER, FOR YEAR-ROUND OPERATION

The following curves show the daily variation of

TOTAL SOLAR FLUX INCIDENT

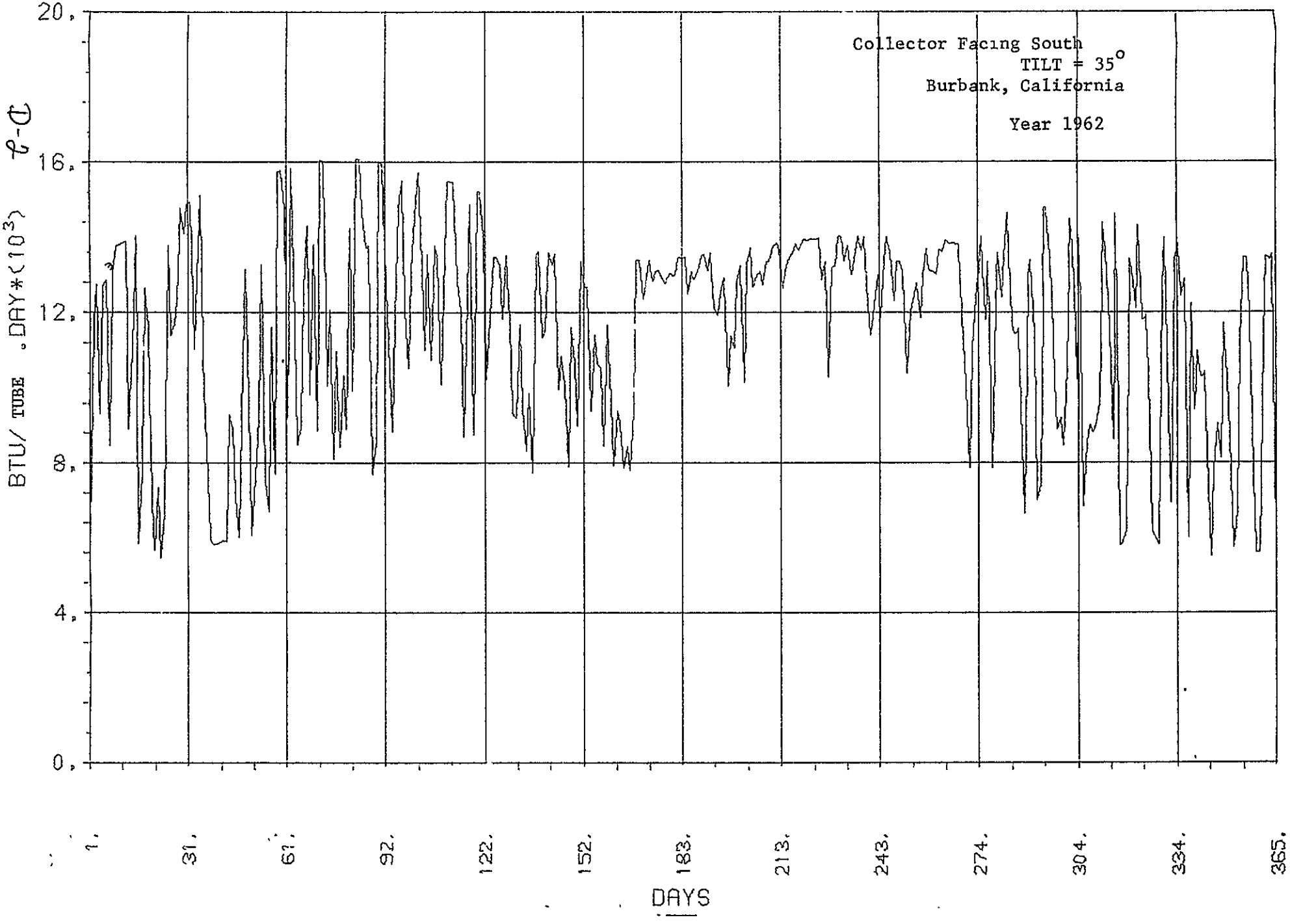

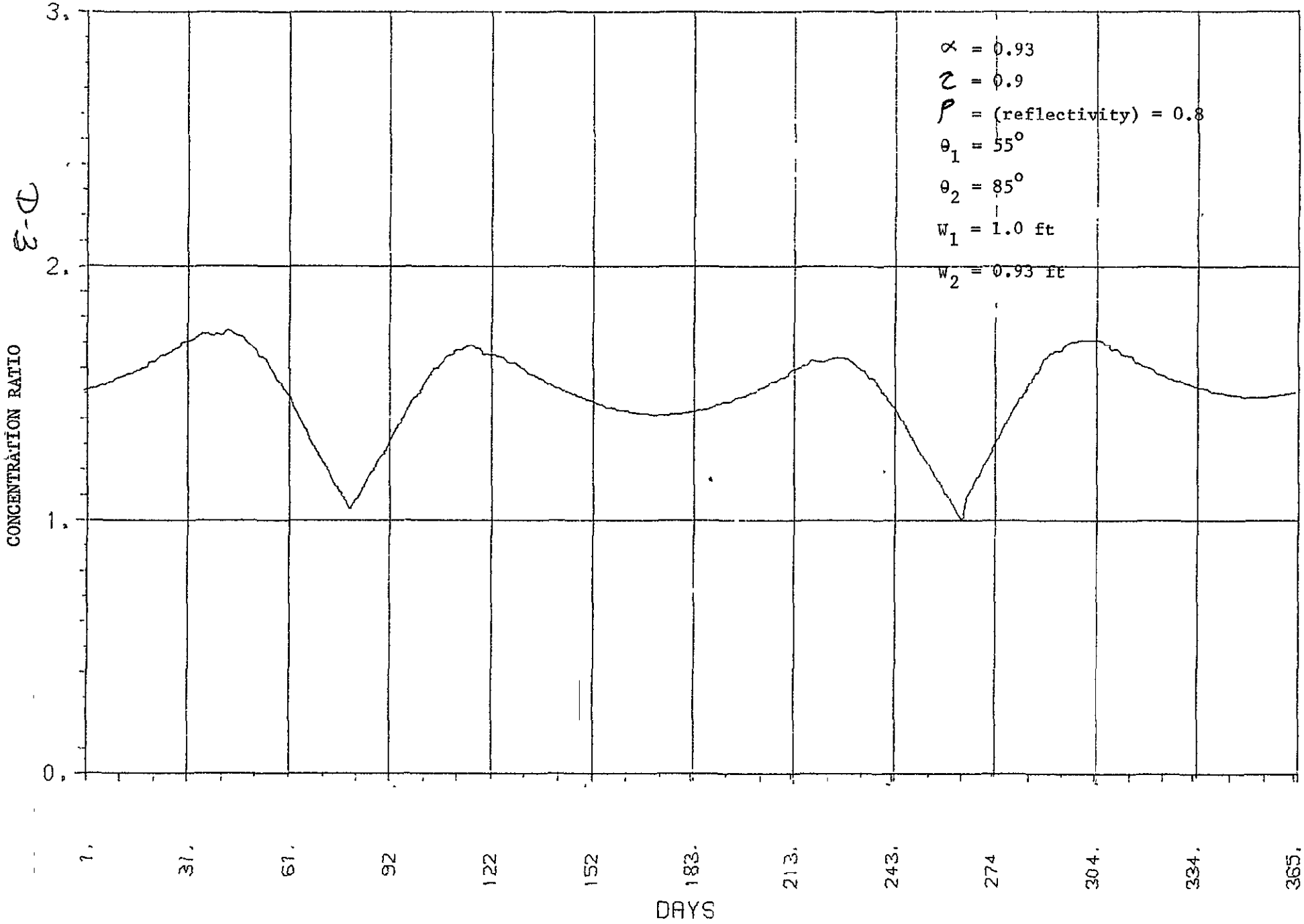
AVERAGE CONCENTRATION RATIO
CR $(\tau\alpha)_e$: Transmission Losses Included
α = 0.93
τ = 0.9
ρ = (reflectivity) = 0.8
θ_1 = 55°
θ_2 = 85°
W_1 = 1.0 ft
W_2 = 0.93 ft
E-C
CONCENTRATION RATIO
3.
2.
1.
0.
1.
31.
61.
92
122
152
183.
213.
243.
274
304.
334.
365.
DAYS

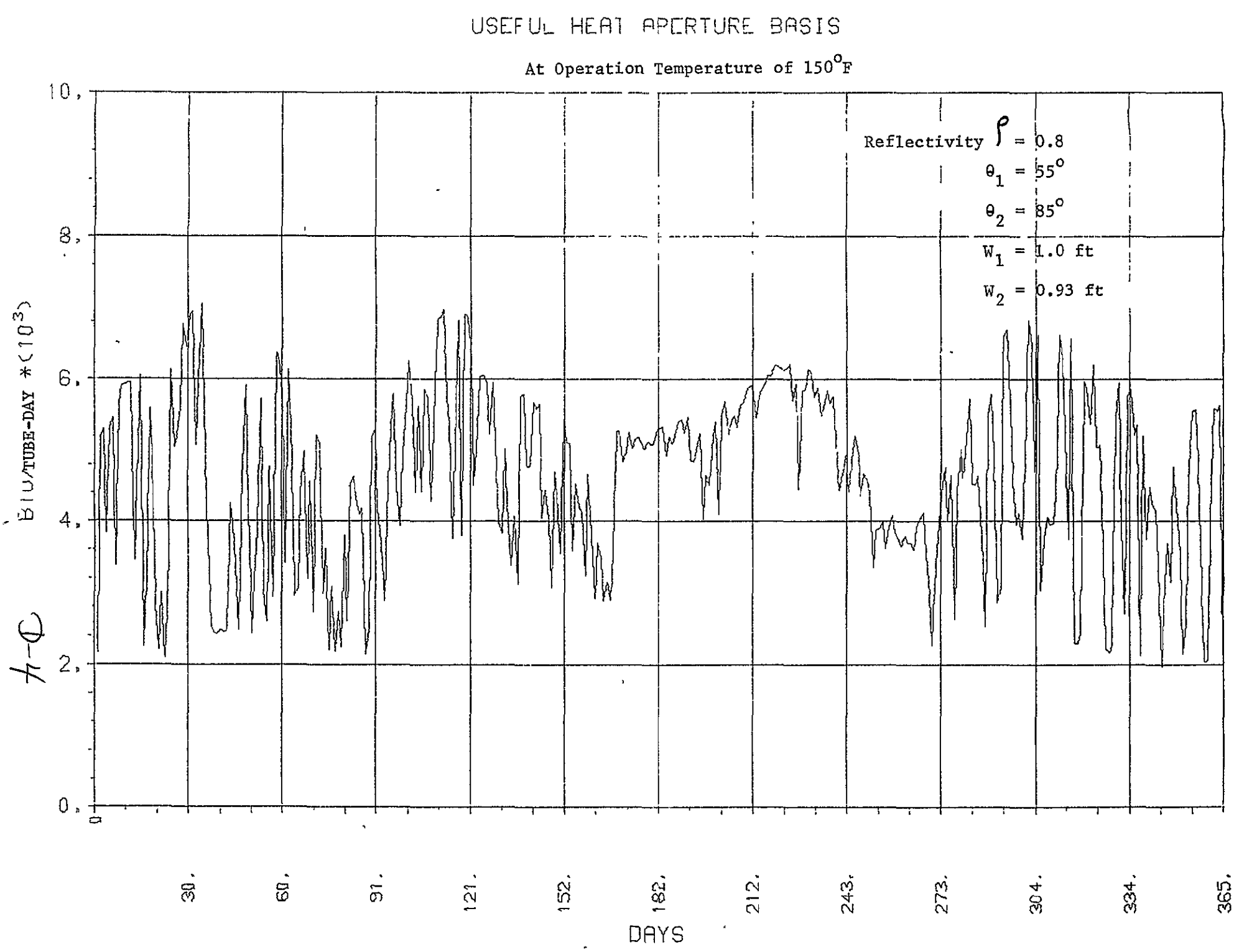
USEFUL HEAT APERTURE BASIS
At Operation Temperature of 150°F
Reflectivity ρ = 0.8
θ1 = 55°
θ2 = 85°
W1 = 1.0 ft
W2 = 0.93 ft
BTU/TUBE-DAY *(10^3)
10.
8.
6.
4.
2.
0.
0
30.
60.
91.
121.
152.
182.
212.
243.
273.
304.
334.
365.
DAYS

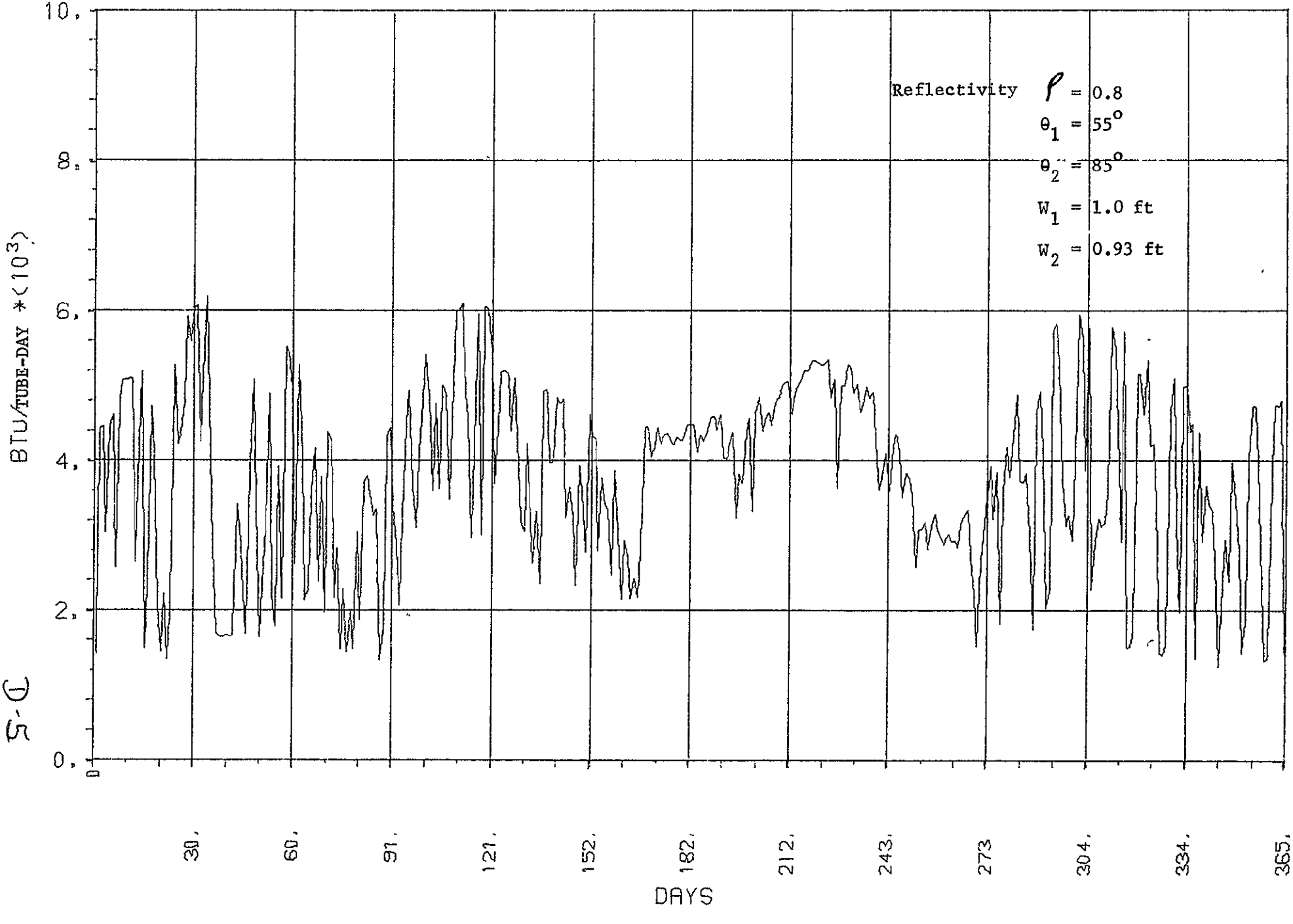
USEFUL HEAT APERTURE BASIS
At Operation Temperature of 250°F
Reflectivity ρ = 0.8
θ1 = 55°
θ2 = 85°
W1 = 1.0 ft
W2 = 0.93 ft
BTU/TUBE-DAY *(10^3)
10.
8.
6.
4.
2.
0.
0
30.
60.
91.
121.
152.
182.
212.
243.
273
304.
334.
365.
DAYS

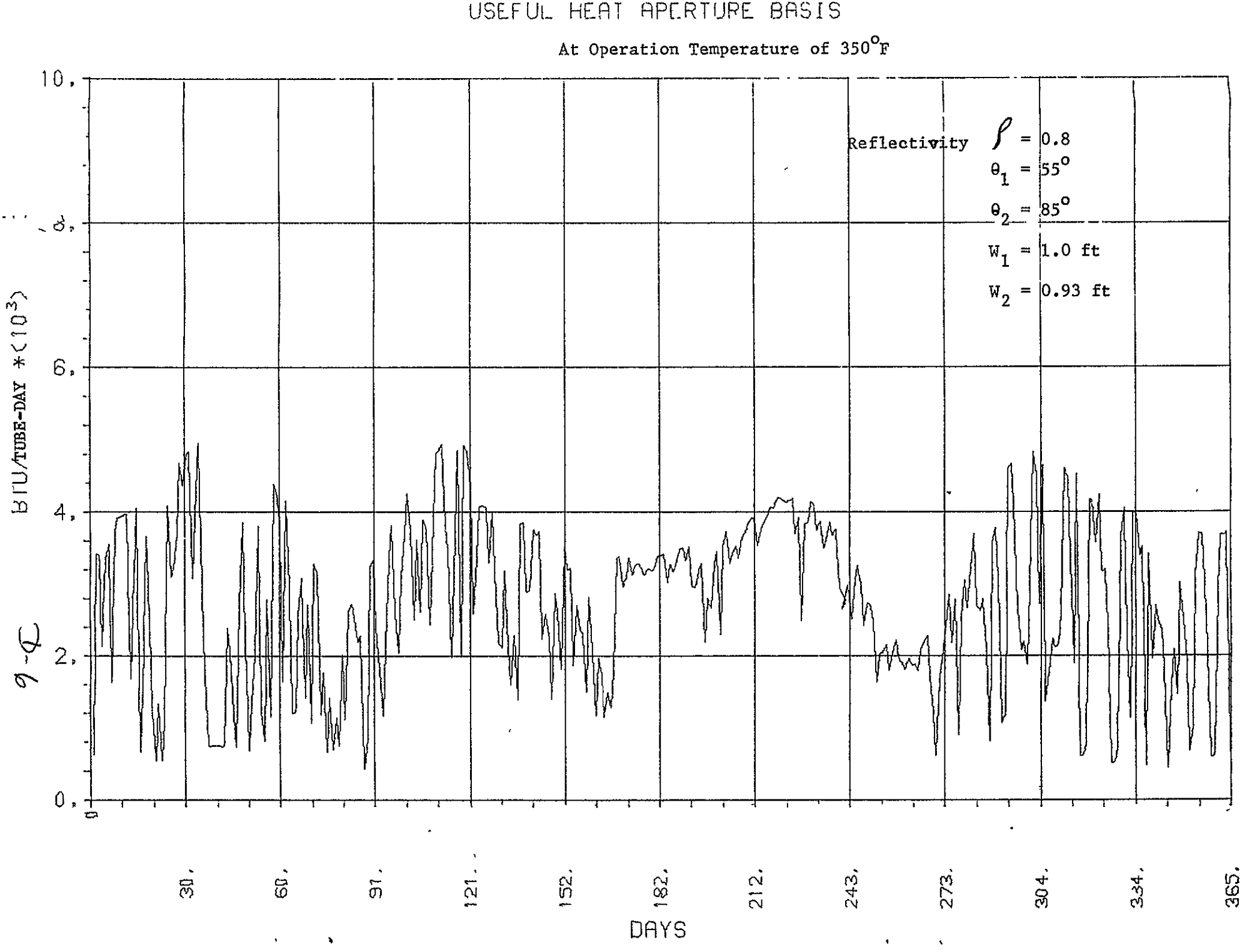
USEFUL HEAT APERTURE BASIS
At Operation Temperature of 350°F
Reflectivity ρ = 0.8
θ1 = 55°
θ2 = 85°
W1 = 1.0 ft
W2 = 0.93 ft
BTU/TUBE-DAY *(10^3)
q-c
10.
8.
6.
4.
2.
0.
0
30.
60.
91.
121.
152.
182.
212.
243.
273.
304.
334.
365.
DAYS

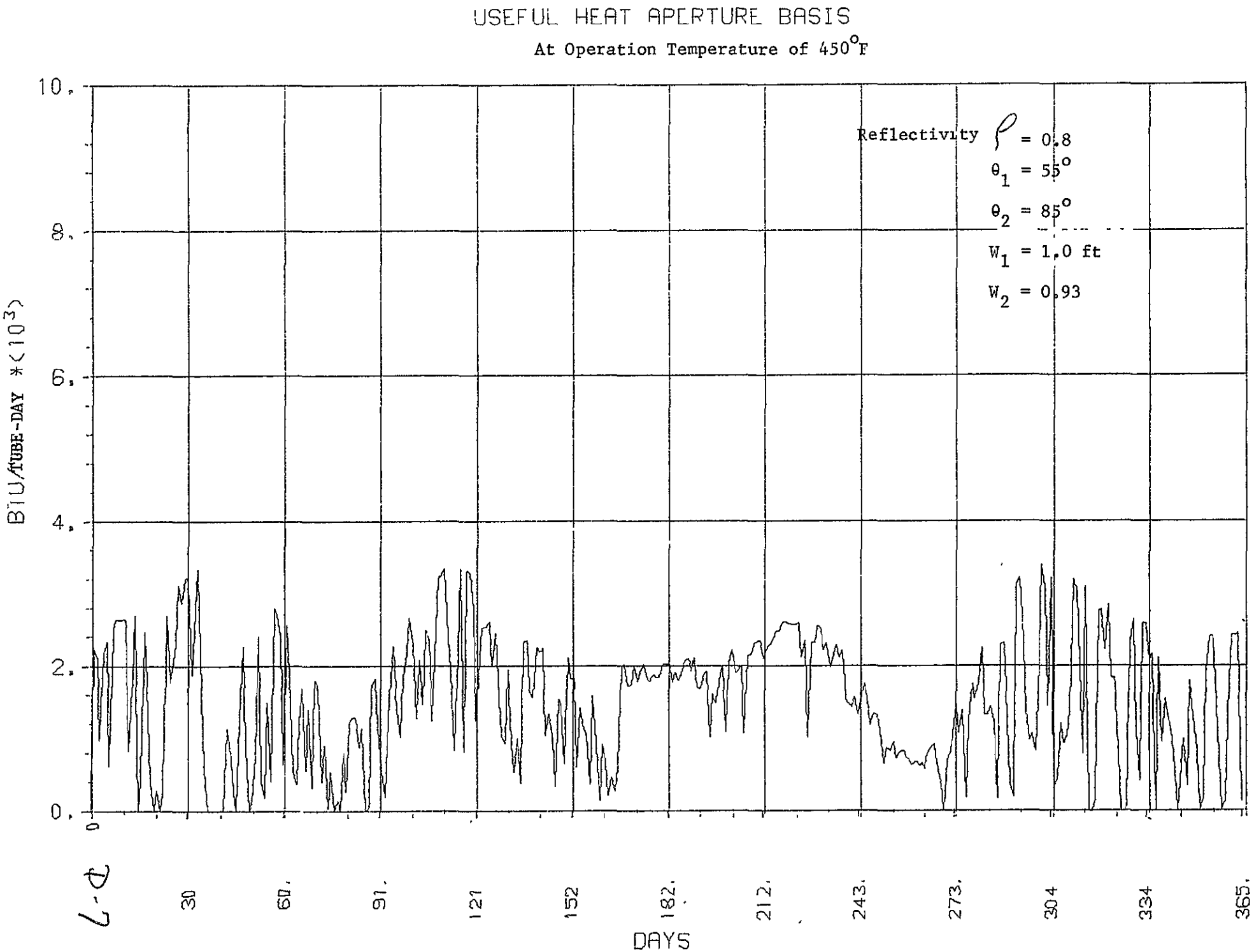
USEFUL HEAT APERTURE BASIS
At Operation Temperature of 450°F
Reflectivity ρ = 0.8
θ1 = 55°
θ2 = 85°
W1 = 1.0 ft
W2 = 0.93
BTU/TUBE-DAY *(10^3)
10.
8.
6.
4.
2.
0.
0
30
60.
91.
121
152
182.
212.
243.
273.
304
334
365.
DAYS

OVERALL COLLECTOR EFFICIENCY

At Operation Temperature of 150°F

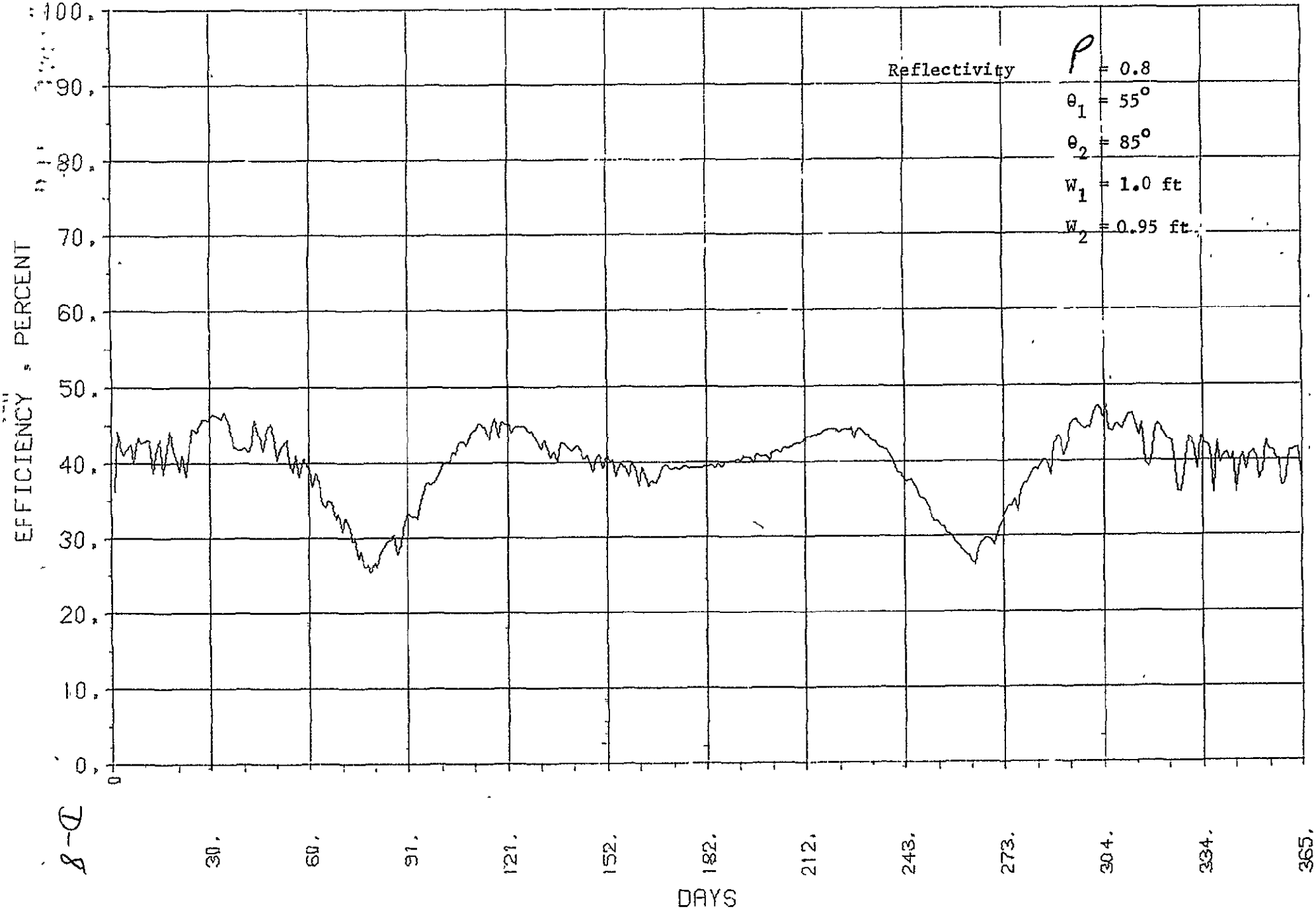

8-T

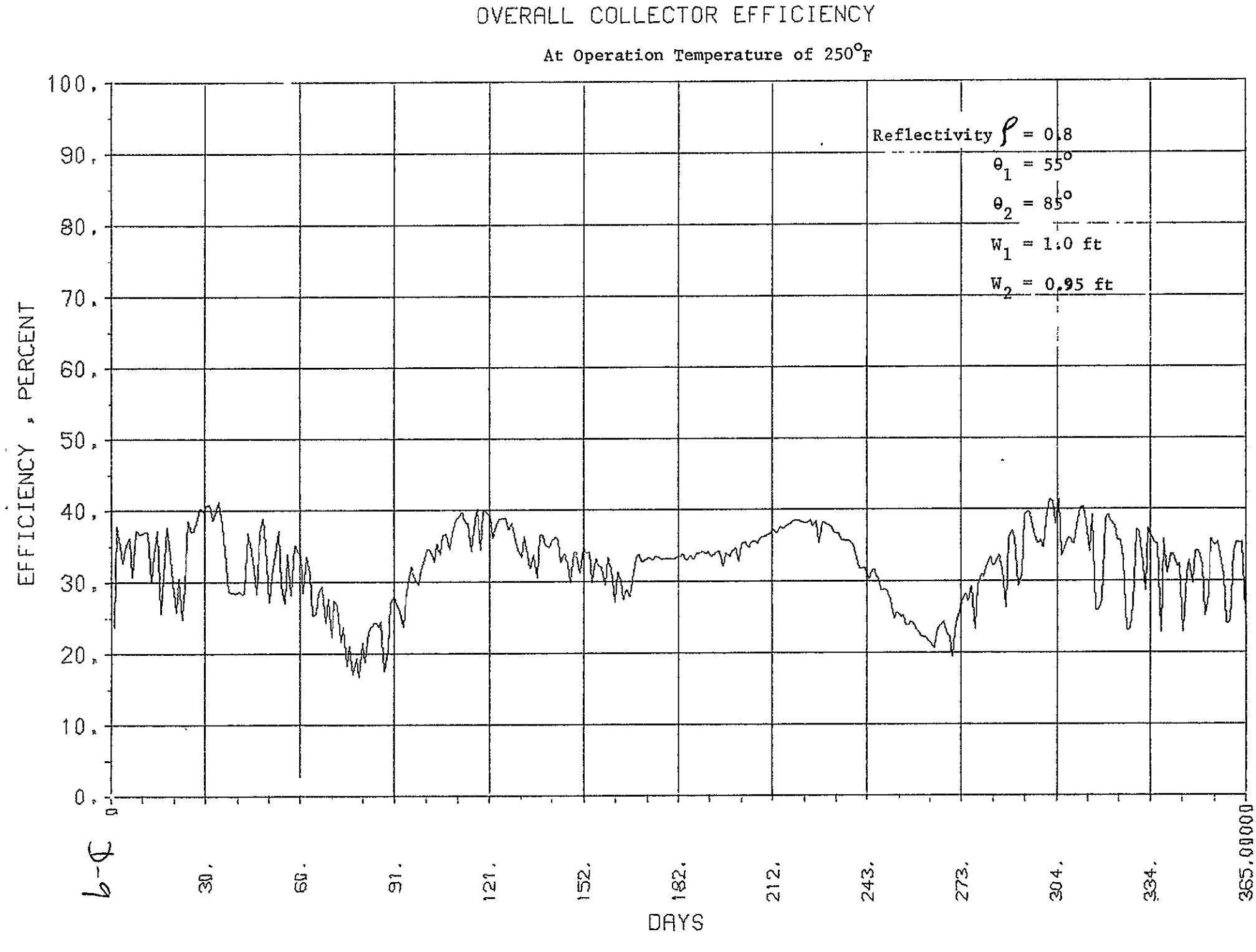
OVERALL COLLECTOR EFFICIENCY
At Operation Temperature of 250°F
Reflectivity ρ = 0.8
θ1 = 55°
θ2 = 85°
W1 = 1.0 ft
W2 = 0.95 ft
EFFICIENCY , PERCENT
100.
90.
80.
70.
60.
50.
40.
30.
20.
10.
0.
0.
30.
60.
91.
121.
152.
182.
212.
243.
273.
304.
334.
365.00000
DAYS

OVERALL COLLECTOR EFFICIENCY

At Operation Temperature of 350°F

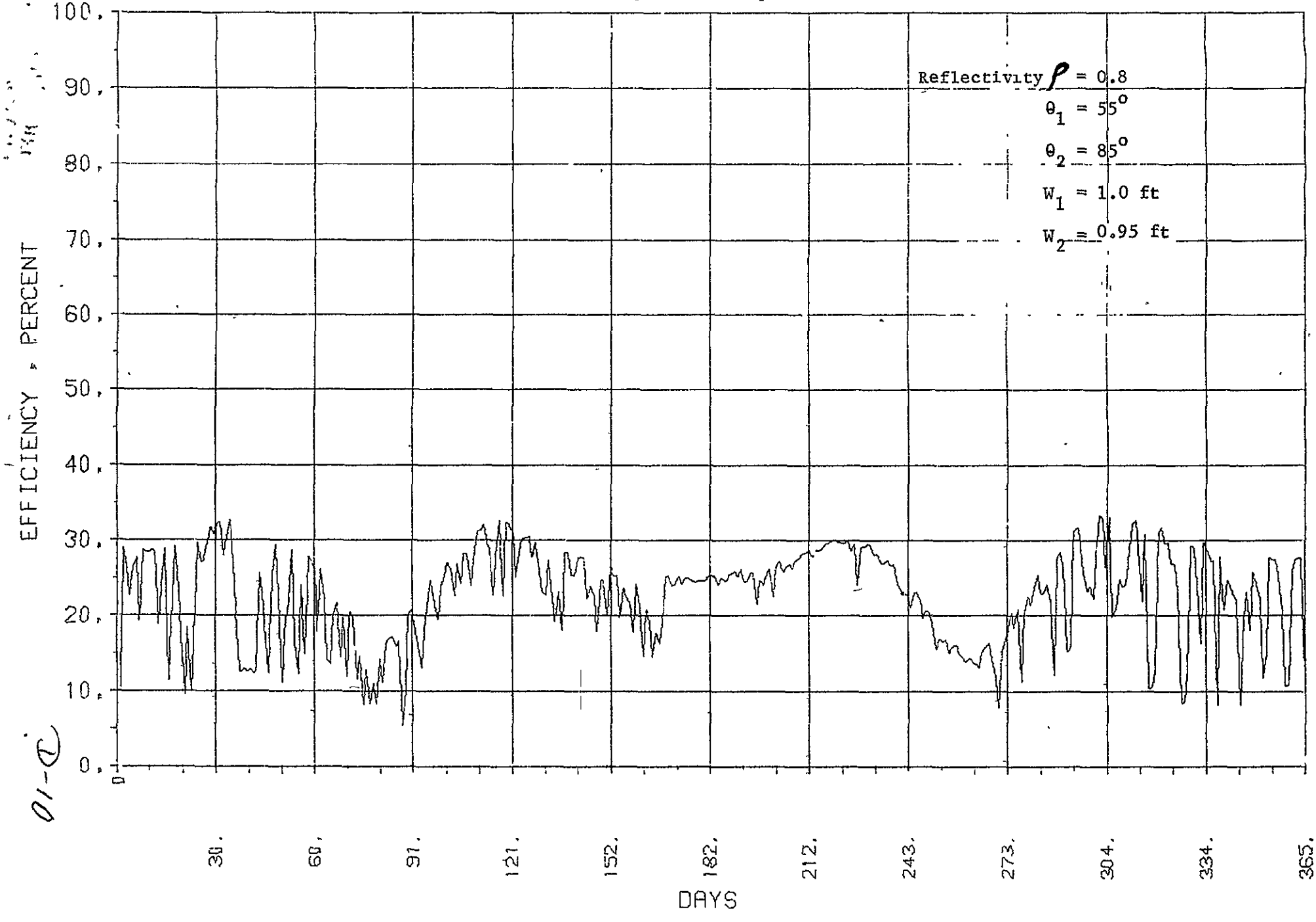

01-C

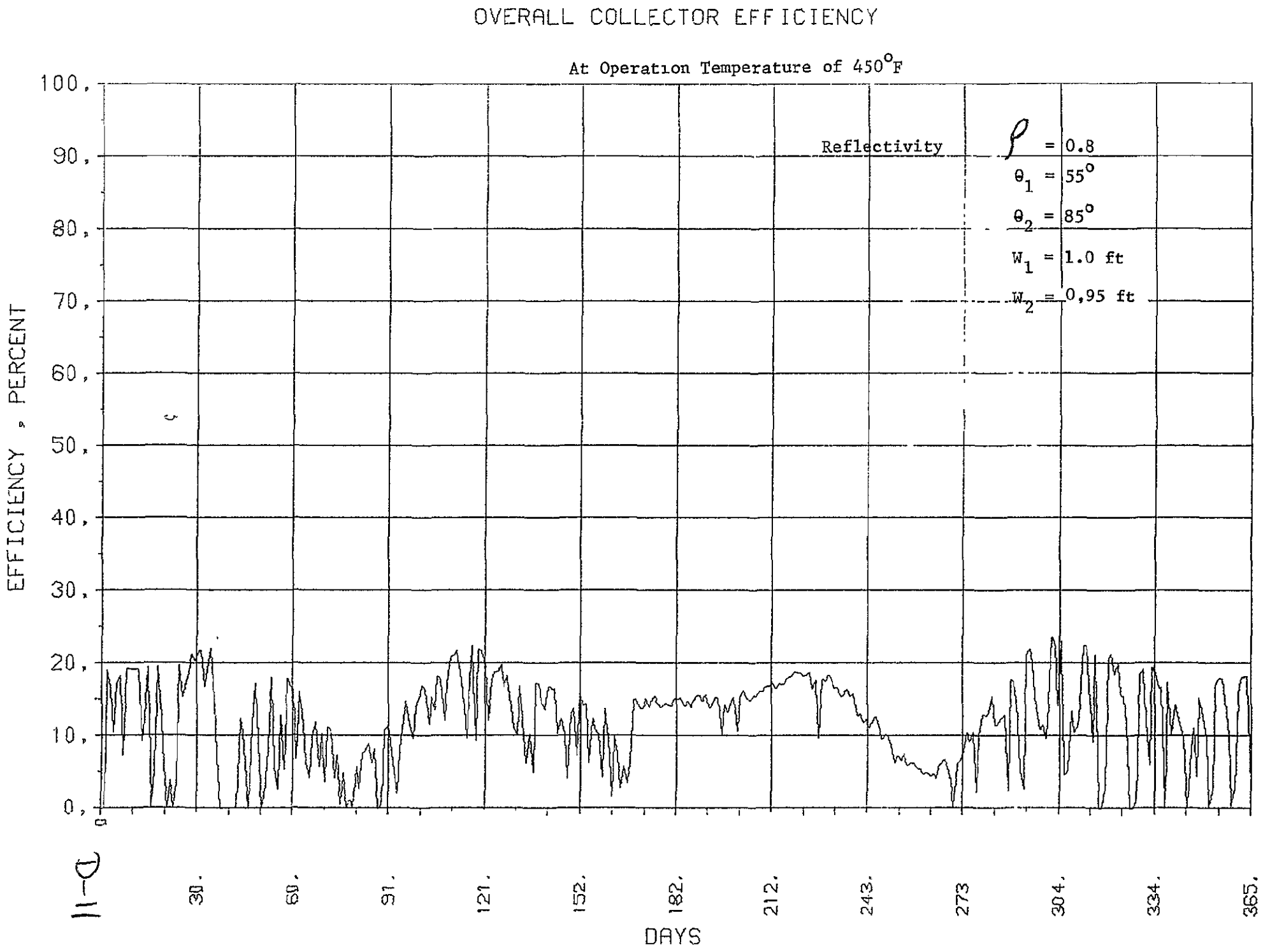
OVERALL COLLECTOR EFFICIENCY
At Operation Temperature of 450°F
Reflectivity ρ = 0.8
θ1 = 55°
θ2 = 85°
W1 = 1.0 ft
W2 = 0,95 ft
EFFICIENCY , PERCENT
100.
90.
80.
70.
60.
50.
40.
30.
20.
10.
0.
0
30.
60.
91.
121.
152.
182.
212.
243.
273
304.
334.
365.
DAYS

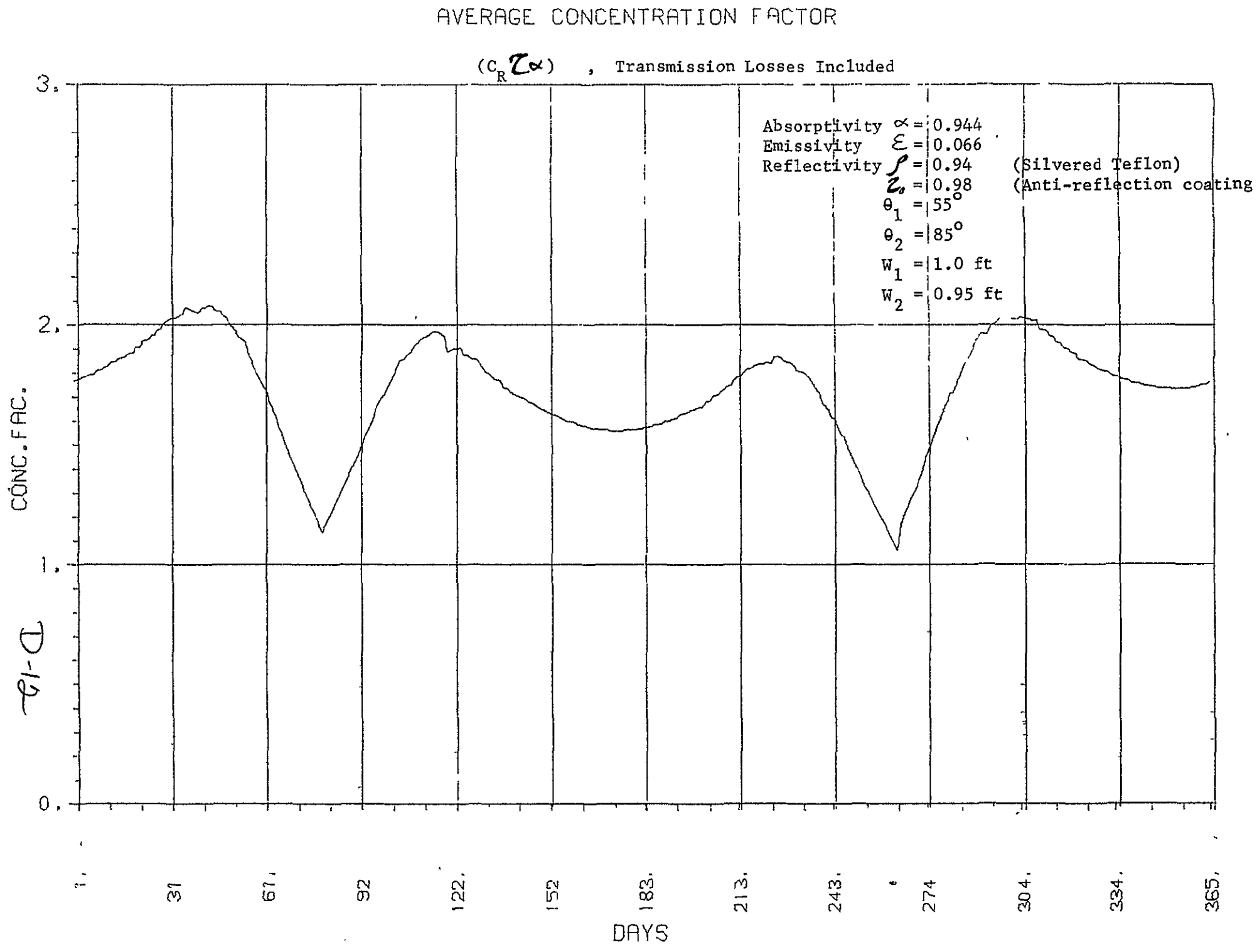
AVERAGE CONCENTRATION FACTOR
($C_R \tau\alpha$) , Transmission Losses Included
Absorptivity α = 0.944
Emissivity ε = 0.066
Reflectivity ρ = 0.94 (Silvered Teflon)
τ_o = 0.98 (Anti-reflection coating
θ_1 = 55°
θ_2 = 85°
W_1 = 1.0 ft
W_2 = 0.95 ft
CONC. FAC.
$\tau\alpha$
3.
2.
1.
0.
1.
31
61.
92
122.
152
183.
213.
243.
274
304.
334.
365.
DAYS

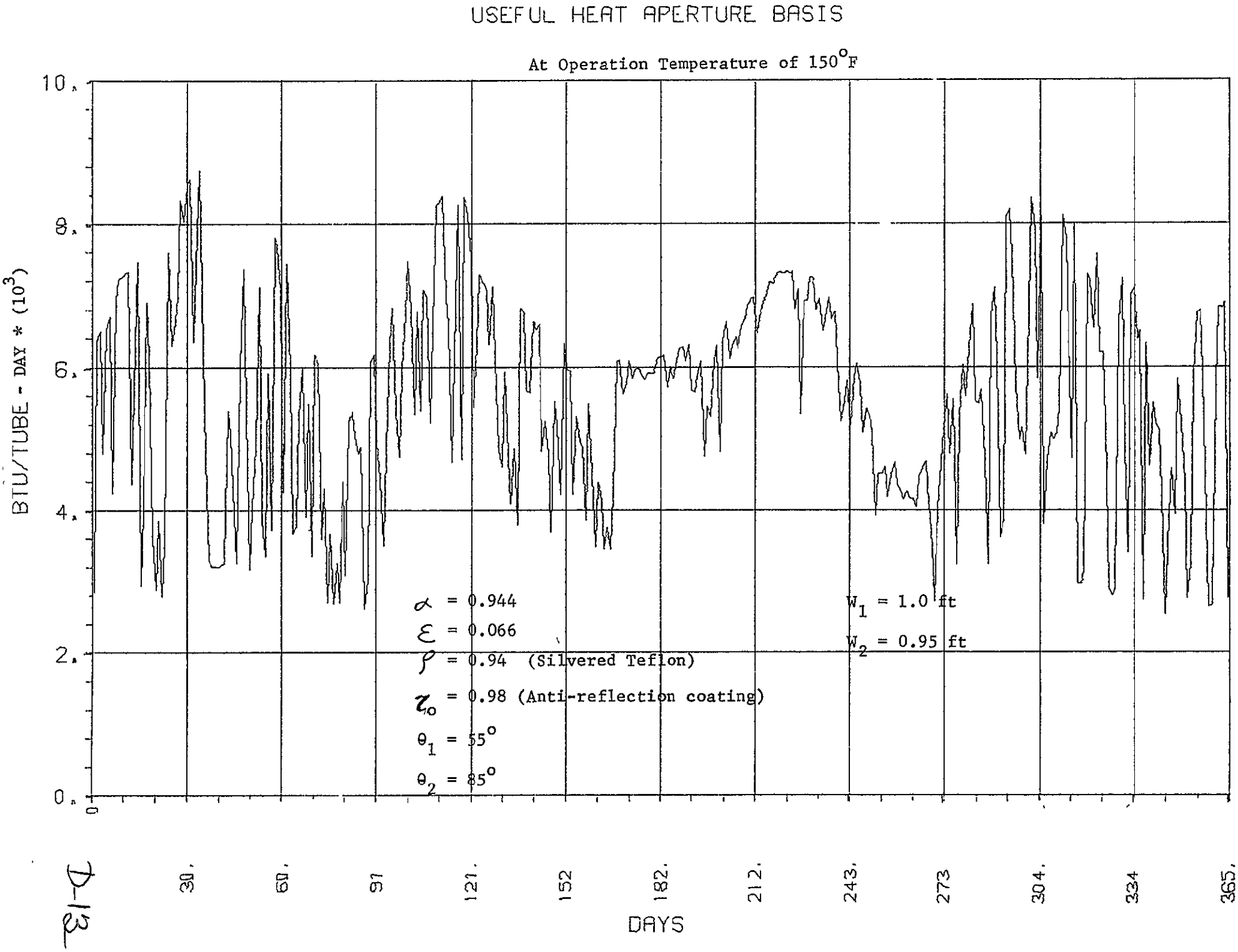
USEFUL HEAT APERTURE BASIS
At Operation Temperature of 150°F
BTU/TUBE - DAY * (10^3)
10.
8.
6.
4.
2.
0.
0
30.
60.
91
121.
152
182.
212.
243.
273
304.
334
365.
DAYS
α = 0.944
ε = 0.066
ρ = 0.94 (Silvered Teflon)
τ_o = 0.98 (Anti-reflection coating)
θ_1 = 55°
θ_2 = 85°
W_1 = 1.0 ft
W_2 = 0.95 ft

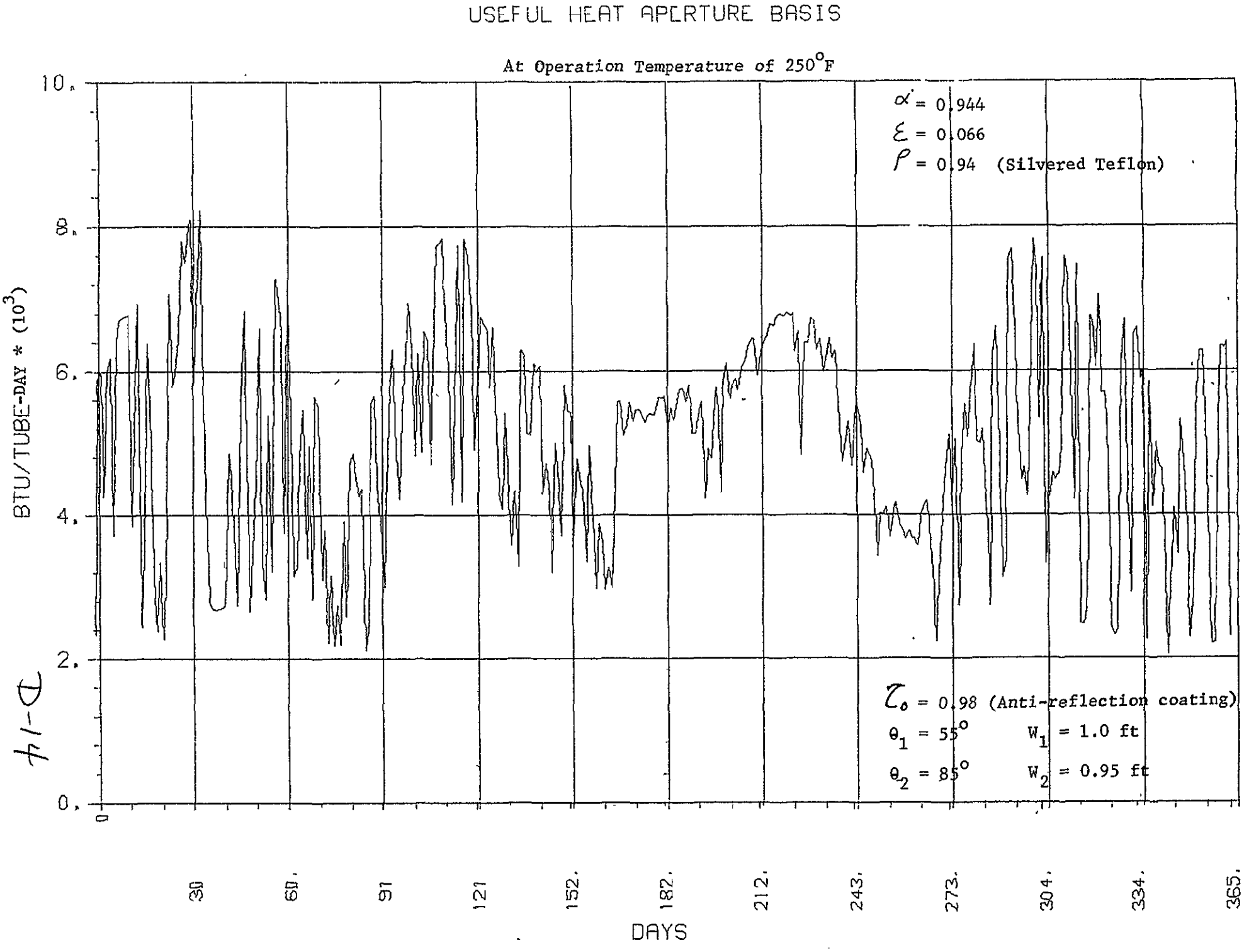
USEFUL HEAT APERTURE BASIS
At Operation Temperature of 250°F
α = 0.944
ε = 0.066
ρ = 0.94 (Silvered Teflon)
τ_o = 0.98 (Anti-reflection coating)
θ_1 = 55°
W_1 = 1.0 ft
θ_2 = 85°
W_2 = 0.95 ft
BTU/TUBE-DAY * (10^3)
$\eta_{1-\alpha}$
10.
8.
6.
4.
2.
0.
0
30
60.
91
121
152.
182.
212.
243.
273.
304.
334.
365.
DAYS

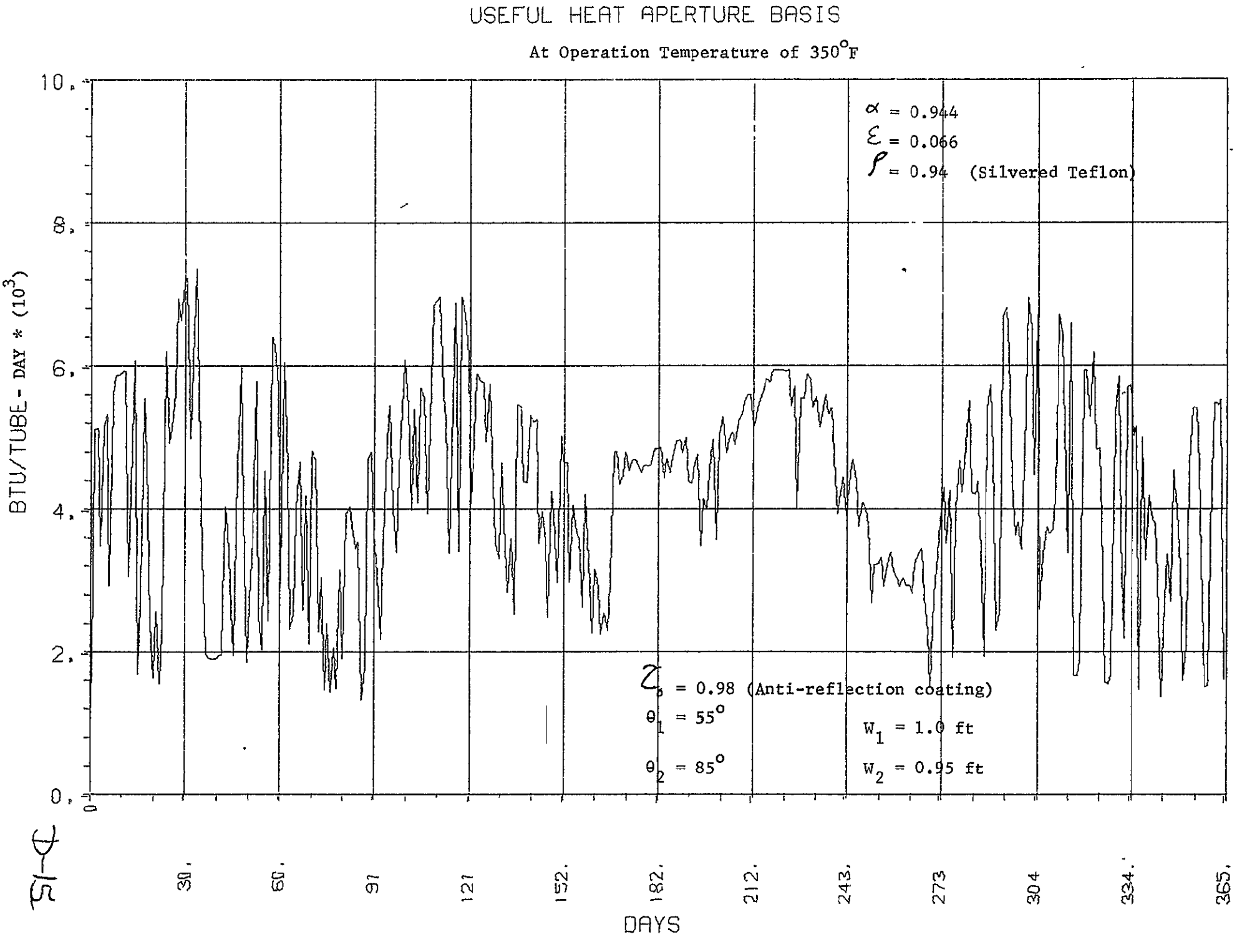
USEFUL HEAT APERTURE BASIS
At Operation Temperature of 350°F
α = 0.944
ε = 0.066
ρ = 0.94 (Silvered Teflon)
τ = 0.98 (Anti-reflection coating)
θ1 = 55°
θ2 = 85°
W1 = 1.0 ft
W2 = 0.95 ft
BTU/TUBE - DAY * (10³)
10.
8.
6.
4.
2.
0.
0
30.
60.
91
121
152.
182.
212.
243.
273
304
334.
365.
DAYS

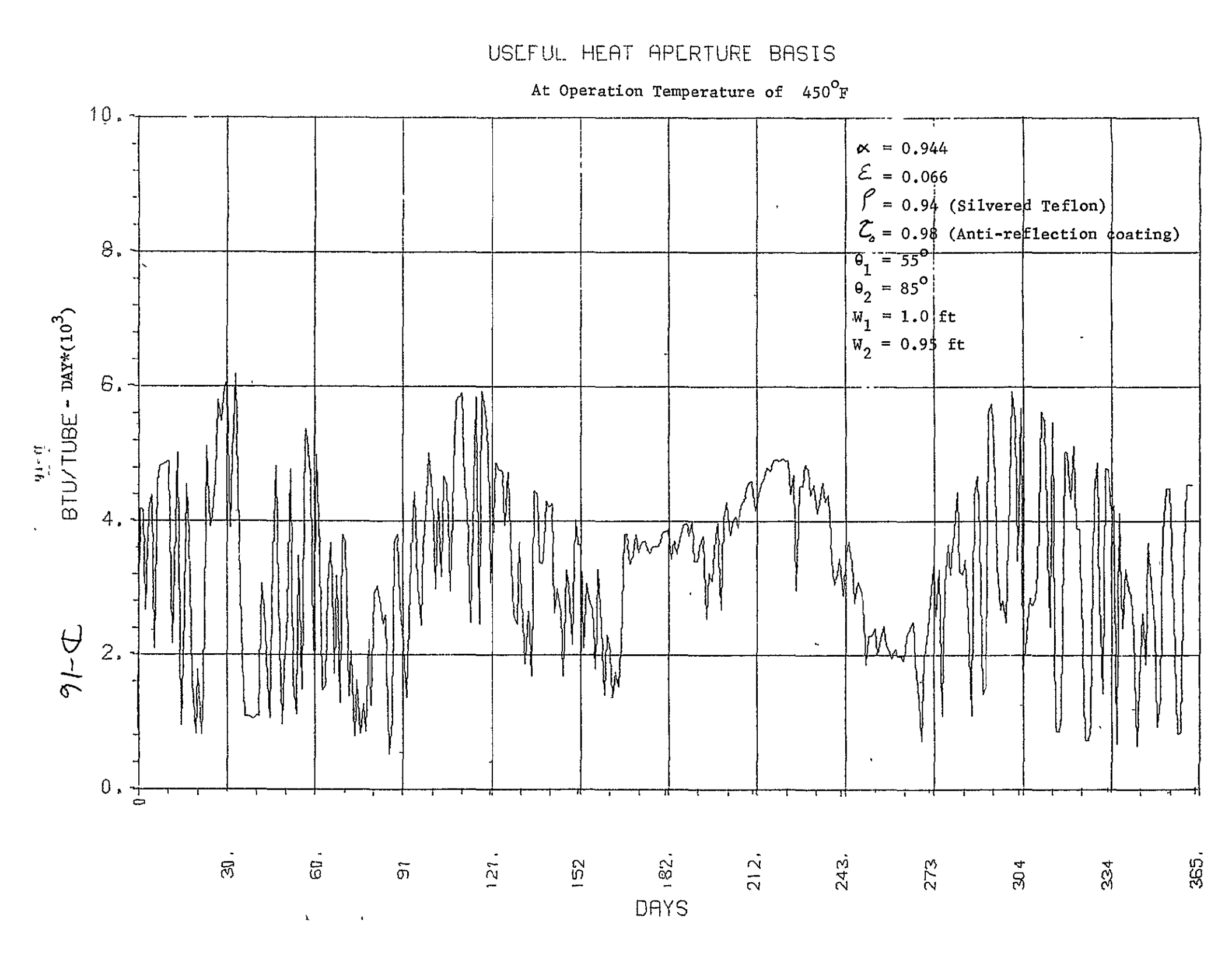
USEFUL HEAT APERTURE BASIS
At Operation Temperature of 450°F
α = 0.944
ε = 0.066
ρ = 0.94 (Silvered Teflon)
τ = 0.98 (Anti-reflection coating)
θ1 = 55°
θ2 = 85°
W1 = 1.0 ft
W2 = 0.95 ft
BTU/TUBE - DAY*(10^3)
10.
8.
6.
4.
2.
0.
0
30.
60.
91
121.
152
182.
212.
243.
273
304
334
365.
DAYS

OVERALL COLLECTOR EFFICIENCY

At Operation Temperature of 150°F

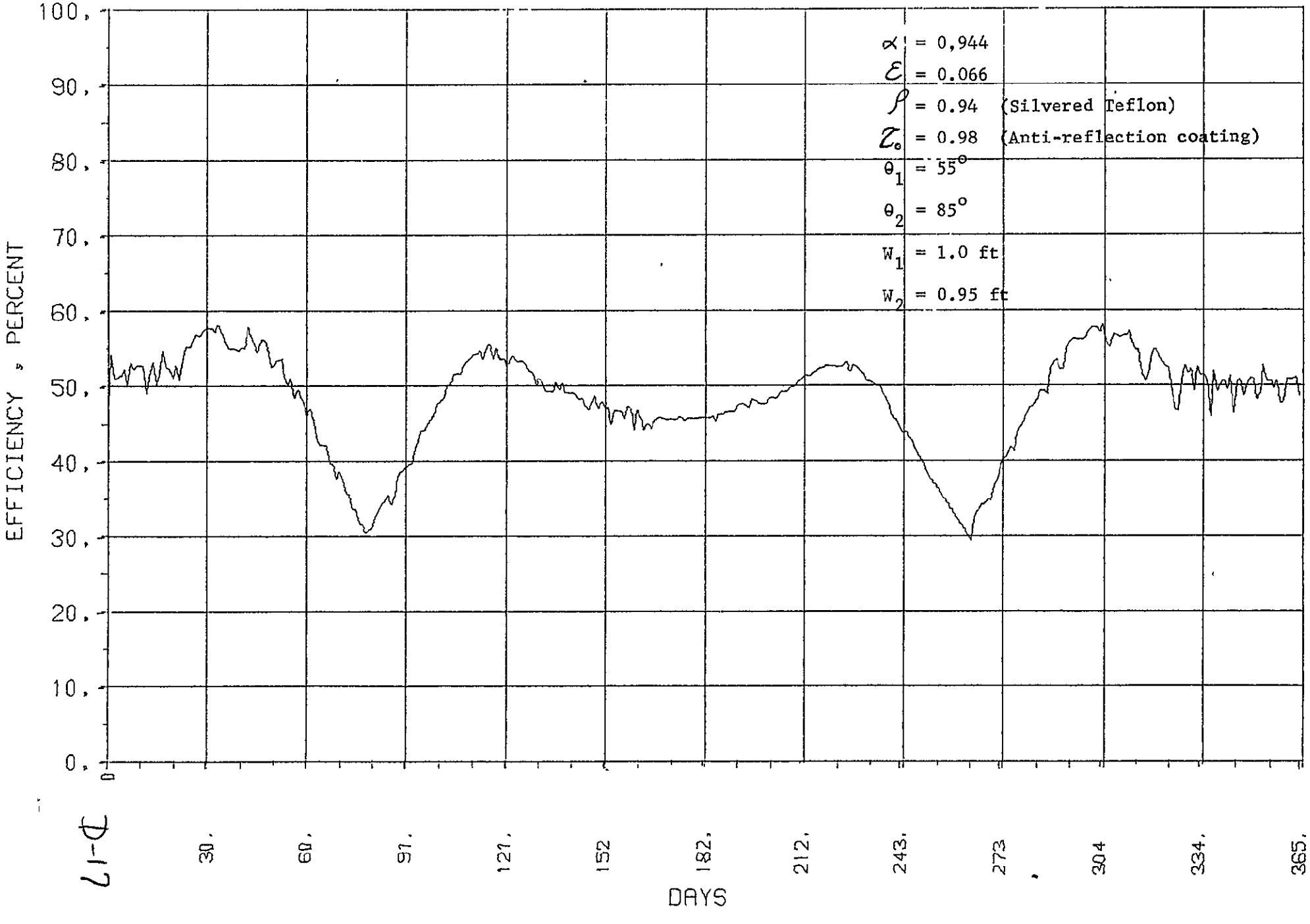

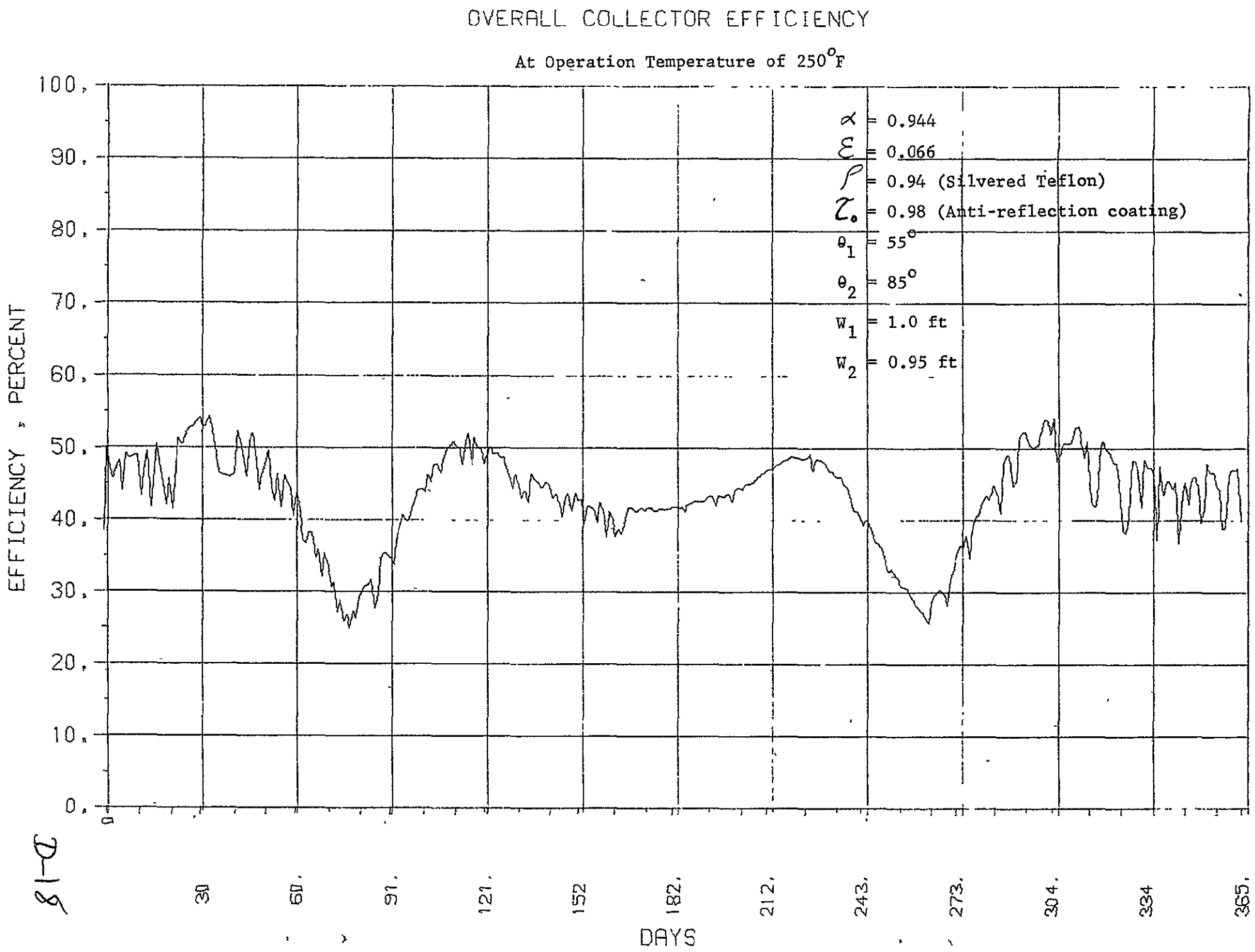
OVERALL COLLECTOR EFFICIENCY
At Operation Temperature of 250°F
α = 0.944
ε = 0.066
ρ = 0.94 (Silvered Teflon)
τ₀ = 0.98 (Anti-reflection coating)
θ1 = 55°
θ2 = 85°
W1 = 1.0 ft
W2 = 0.95 ft
EFFICIENCY , PERCENT
100.
90.
80.
70.
60.
50.
40.
30.
20.
10.
0.
0
30
60.
91.
121.
152
182.
212.
243.
273.
304.
334
365.
DAYS

B-18

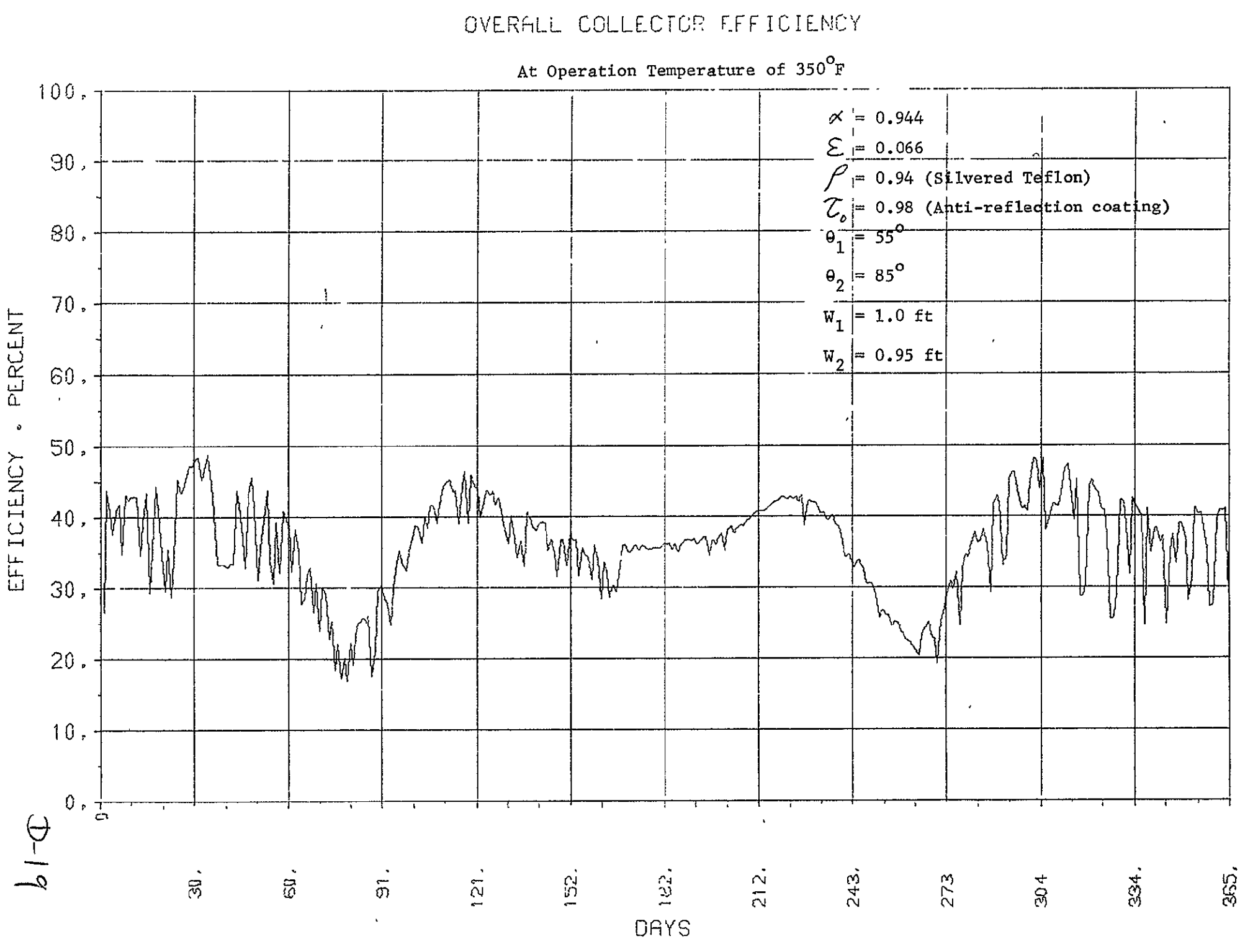
OVERALL COLLECTOR EFFICIENCY
At Operation Temperature of 350°F
α = 0.944
ε = 0.066
ρ = 0.94 (Silvered Teflon)
τ₀ = 0.98 (Anti-reflection coating)
θ₁ = 55°
θ₂ = 85°
W₁ = 1.0 ft
W₂ = 0.95 ft
EFFICIENCY , PERCENT
100.
90.
80.
70.
60.
50.
40.
30.
20.
10.
0.
0
30.
60.
91.
121.
152.
182.
212.
243.
273
304
334.
365.
DAYS

b1-C

OVERALL COLLECTOR EFFICIENCY

At Operation Temperature of 450°F

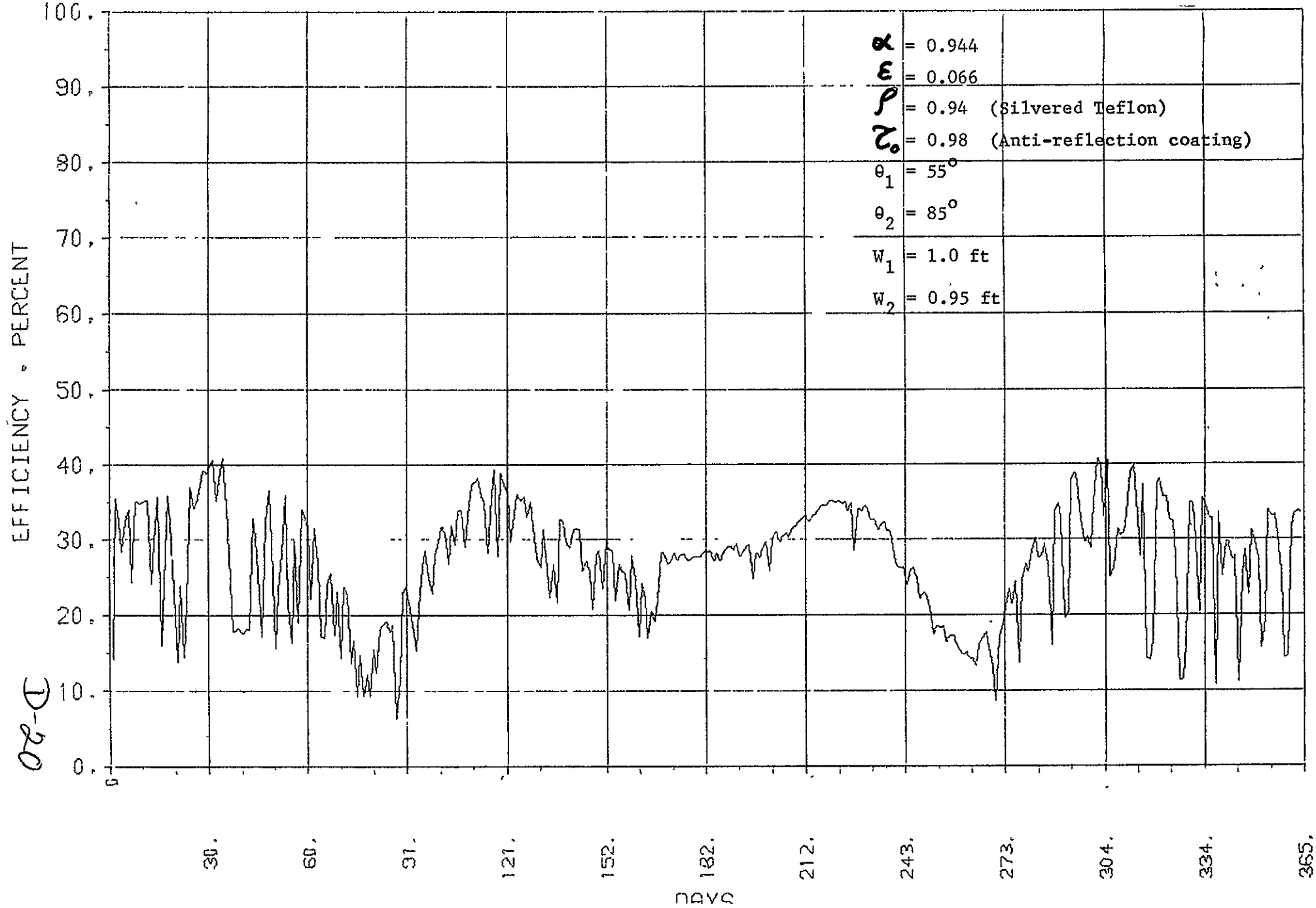

Oz-1

APPENDIX E

VEE-TROUGH/VACUUM TUBE COLLECTOR COST PREDICTIONS

Neither a firm cost nor a formal cost estimate of the evaucated tube receiver is available from the industry. A preliminary cost estimate is, however, attempted to give an idea of the probable tube cost, which is the most important item of the cost of the total collector.

The evacuated tube consists of the following:

Pyrex tube.

Copper absorber plate.

Selective coating on the absorber.

Glass to metal seals.

Clips.

Cost estimates of these components are given based on the material cost data in the published literature and personal communications with the tube manufacturer. The letter, however, implies no commitment from the companies' viewpoint.

Pyrex tubes are arranged to form a collector module of reasonable size. Tube lengths are taken as 8ft. and diameter is varied. The concentration ratio is taken as 3, which turns out to be an optimum for the vee-trough design.

Figure E-1 illustrates the configuration of the tubes and reflectors. The module length is about 17 ft; the width is taken to be 6 ft. for easy access to tubes and reflectors. Each tube has a net absorber length of 7 ft.

Present suggested net prices of pyrex tubes purchased at large quantities are listed in Table E-1. Future cost of the glass tube component of the evacuated collector has to be at least this level or lower. In fact, the evacuated tube fabrication will be most probably done at the factory where no transportation and packaging costs exist and glass breakage is minimal.

Table E-2 gives the breakdown of the cost of the tubular receiver ready to be assembled onto the module. Glass tubes can be arranged on the module such that approximately a 6 x 17 ft. module is obtained. The number of tubes required for such a module as well as frame, manifold and assembly costs (without reflectors) is given in Table E-3.

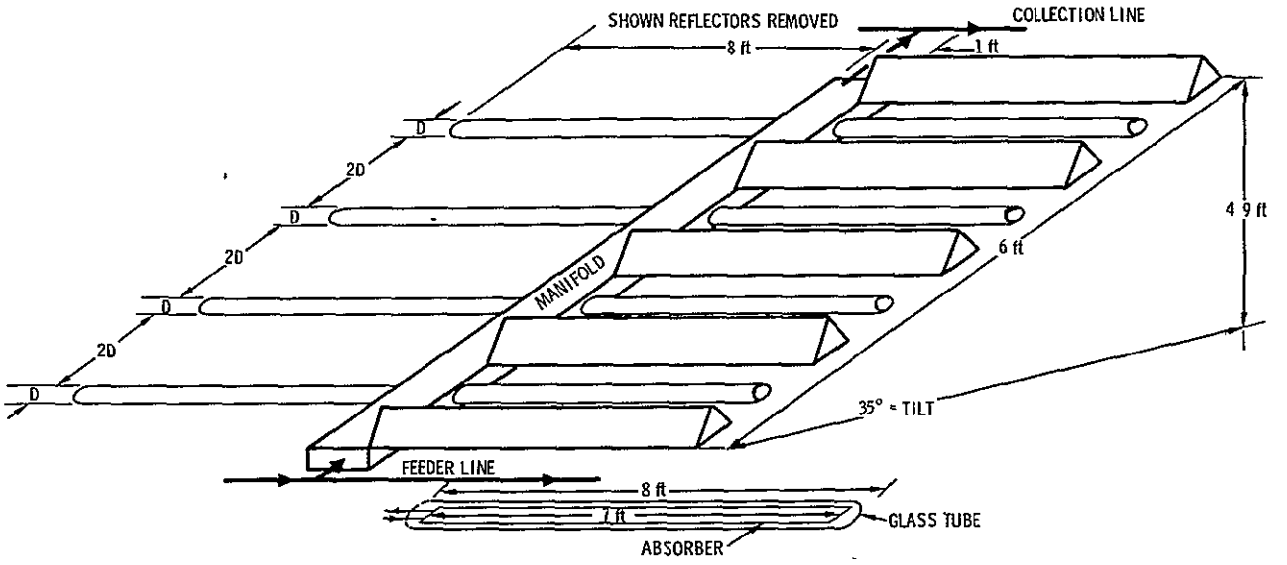

Figure E-1. Vee-Trough/Vacuum Tube Collector Module Configuration

Table E-1. Glass Tube Cost (Data from Corning Glass)

Item	Tube Diameter, in.					
	2	3	4	5	6	7
Tube cost (Pyrex) standard wall						
CGW code	234510	234750	234000	234340	234370	234230
Tube weight, lb/ft	0.46	0.81	1.12	1.73	2.26	2.89
Tube number per case	13	4	4	4	2	2
Tube length, ft	4	4	4	4	4	4
Tube projected area, ft^2	8.66	4	5.33	6.66	4	4.66
Cost per case (600 cases or more)	38.25	22.36	30.96	48.16	30.96	43.93
Tube cost, $\$/ft^2$ (projected area basis)	4.41	5.59	7.57	7.23	7.74	9.42
Tube cost (8 ft long) each	5.9	11.2	20.1	24.1	30.9	47.1

Table E-2. Evacuated Tubular Receiver Cost Estimate

Item	Tube Diameter, in.					
	2	3	4	5	6	7
Tube cost, $/ft^2	4.41	5.59	7.57	7.23	7.74	9.42
Tube projected area, ft^2	1.33	2.0	2.66	3.34	4.0	4.66
Absorber plate area, ft^2	0.88	1.46	2.04	2.63	3.20	3.78
Subtotal tube cost, $	5.9	11.2	20.1	24.1	30.9	47.1
Absorber cost:						
Plate @ 1$/ft^2	0.9	1.5	2.0	2.6	3.2	3.8
Coating @ 0.5$/ft^2	0.5	0.7	1.0	1.3	1.6	1.9
U tube + welding, $ + clips	5.0	5.0	5.0	6.0	6.0	6.0
Glass-metal seals, $	10.0	10.0	10.0	12.0	14.0	16.0
Total tube cost, $	22.3	28.4	40.2	46.0	55.7	74.8
$/ft^2 (absorber area)	25.9	19.5	19.7	17.5	17.4	19.8
$/ft^2 (projected tube area basis)	16.7	14.2	15.1	13.8	13.9	16.1

Table E-3. Vee Trough Concentrator Plus Evacuated Tube Receiver Collector Module Cost

Item	Tube Diameter, in					
	2	3	4	5	6	7
Evacuated Tube Assembly						
Number of tubes per module	24	16	12	10	8	8
Module size, ft	(6X17)	(6X17)	(6X17)	(6.25X17)	(6X17)	(7X17)
Collection area, ft^2 (including reflectors)	84	84	84	87 5	84	98
Glass tube projected area, ft^2	32	32	32	33 4	32	37 3
Tube cost (each), $	22 3	28 4	40 2	46 0	55 7	74 8
Subtotal table cost, $	535	454 4	482 4	460	445	598
Tube assembly costs, $ @ 5$ each	120 0	30 0	60 0	50 0	40 0	40 0
Manifold cost @ 20$/tube	480 0	320 0	240 0	200 0	100 0	100 0
Clamps @ 1 0/tube misc per tube	24 0	16.0	12 0	10 0	8 0	8 0
Misc per tube ($5 0) (insulation, bolts, etc)	120 0	80 0	60 0	50 0	40 0	40 0
Total assembled tube cost, $	1279	950	854 4	770	693	846
Tube Plus Reflector Assembly						
Tube assembly, $	1279	950	855	770	693	846
Reflectors area @ 2 0 ft^2/ft^2 aperture or (6 0 ft^2/ft tube) . ft^2 8 ft length .	96	96	96	100 2	96	112
Reflector metal thickness, in	0 012	0 015	0 020	0 025	0 032	0.040
Reflector cost factor (0 020 in) unity	0 8	0 9	1 0	1 1	1 2	1 4
Reflector metal cost ($/$ft^2$)						
@1 0 $/$ft^2$ unity	0 8	0 9	1 0	1 1	1 2	1 4
@ 0 5$/$ft^2$ unity	0 4	0 45	0 5	0 55	0 6	0 73
Reflector Δ section bottom piece (0 040 in'), $ $ ordinary aluminum (area = 1/2 reflector)	24	24	24	25	24	28
Riveting @ 5$ per Δ section, $ (N + 1) Reflectors on both sides	130	90	70	60	50	50
Finished Δ sections						
Bottoms, $	154	114	94	85	74	78
Sides @ 1 0 $/$ft^2$	77	87	96	110	115	156
Combination	231	201	190	195	189	234
Combination @ 0 5 $/$ft^2$	154	114	94	85	74	78
	35 5	43 5	48	55	57 5	78
	189 5	167 5	142	140	131 5	156
Summary						
Tube + frame cost, $	1279	950	855	770	693	846
Vee troughs @ 1.0 $/$ft^2$ unity	231	201	190	195	189	234
Total module test, $	1510	1151	1046	965	882	1080
Absorber area	21 0	23 3	24 5	26 2	25 6	30 3
Aperture area	84	84	84	87 5	84	98
Collector cost $/$ft^2$ absorber	71.9	49 4	42 7	36 8	34 4	35 6
Collector cost aperture area, $/$m^2$	18.0	13 7	12 45	11 02	10 5	11 02
If vee troughs are tube @ 0 5 $/$ft^2$	1279	950	855	770	693	846
	189 5	157 5	142	140	131 5	156
Total module cost, $	1468 5	1107 5	997	910	824 5	1002
$/$ft^2$ absorber	69 2	47 5	40 7	34 7	32 2	33 1
$/$ft^2$ aperture	17 5	13 2	11 7	10 4	9 81	10 2
$/$m^2$ aperture	188 3	142	125 9	111 9	105 8	109 8